2010-06-03

Co– and Post–Translational N–Linked Glycosylation of Cardiac Potassium Channel Subunits: A Dissertation

Tuba Bas
University of Massachusetts Medical School

CO– AND POST–TRANSLATIONAL N–LINKED GLYCOSYLATION OF CARDIAC POTASSIUM CHANNEL SUBUNITS

A Dissertation Presented

by

TÛBA BAŞ

Submitted to the Faculty of the University of Massachusetts Graduate School of Biomedical Sciences, Worcester in partial fulfillment of the requirements for the degree of

DOCTOR OF PHILOSOPHY

June, 03 2010

Interdisciplinary Graduate Program

CO– AND POST–TRANSLATIONAL N–LINKED GLYCOSYLATION OF CARDIAC POTASSIUM CHANNEL SUBUNITS

A Dissertation Presented
By

TÛBA BAŞ

The signatures of the Dissertation Defense Committee signifies completion and approval as to style and content of the Dissertation

_____
William R. Kobertz, Thesis Advisor

_____
Reid Gilmore, Member of Committee

_____
Anthony Carruthers, Member of Committee

_____
Daniel Hebert, Outside Member of Committee

The signature of the Chair of the Committee signifies that the written dissertation meets the requirements of the Dissertation Committee

_____
Kendall Knight, Chair of Committee

The signature of the Dean of the Graduate School of Biomedical Sciences signifies that the student has met all graduation requirements of the school.

_____
Anthony Carruthers
Dean of the Graduate School of Biomedical Sciences
Interdisciplinary Graduate Program
June, 03 2010

DEDICATIONS

I dedicate this thesis work to my husband, Volkan Çetin for his constant emotional support on this though journey and my parents Azize Baş and Mehmet Baş for their love, patience and support.

ACKNOWLEDGEMENTS

I would like to thank my advisor, Professor William R. Kobertz for his constant support and encouragement through out this work. Bill has been an exceptional mentor and a great friend. His patience, analytical thinking and open-mindedness are just some of the many virtues I will follow throughout my scientific career. Bill, your enthusiasm and optimism about science made me fall in love with biochemistry again and again. You made me appreciate negative results and taught me how to channel dead-end looking projects into exciting paths. Most importantly, thanks for letting me be myself! You gave me my freedom and yet watched at a very close distance; any time I needed help, you were there for me. As I always say: you are the best, boss!

I would like to thank Professor Reid Gilmore for his very much appreciated advice, support and guidance. I was so lucky and so honored to work with such a great scientists.

I would like to thank my first mentor, Professor Craig C. Mello. Craig, your scientific enthusiasim and your dedication to genetics was so contagious; I immediately got infected as I stepped into your lab. It took me 4 years to realize traditional genetics was not the best match to my personality. Looking back, I have no regrets to start my carreer as a geneticist. I learned so much from you and I got the right scientific perspective that made me very well equipped for my future scientific carreer. It was a pleasure working with you and an honor to be part of your scientific team!

I would like to thank Proffessor Kendall Knight for his support during my big transitions. Thanks for believing in me and supporting me!

I would like to thank Dean of Graduate School of Biomedical Sciences, Prof Anthony Carruthers and his team for transforming GSBS program to excellence and creating a great scientific community for students.

I would like to thank my committee members Anthony Carruthers, Reid Gilmore, and my chair Kendall Knight for making everything as beneficial and as enjoyable for me. I can safely say that I had the best committee! Thank you all!

I would like to thank my outside committee member, Daniel Hebert, for being a part of this work.

I would like to thank all past and present Kobertz lab members, Steven Gage, Kshama Chandrasekhar, Yuan Gao, Heidi Hafemann, Anatoli Lvov, ZhengMao Hua, Karen Mruk, Kristina Gonzalez, Jessica Rocheleau and Trevor Morin. You all made Kobertz Lab, a wonderful environment to work. You were great as lab mates, friends and colleagues. I especially want to thank Kshama Chandrasekhar, Yuan Gao and Anatoli Lvov for being wonderful collaborators; it has been a great joy working with you. Steven Gage, I have a lot to thank you. You have been a great classmate, a great colleague and an excellent friend.

I would like to thank Steven Gage, Mary Chau and Volkan Çetin for editing this manuscript. Thanks so much!

I would like to thank all the members of the Mello lab (2001-2005). I had some of the best days of my life with you. Soyoung Kim, Takao Ishidate, Lisa Medusia and

Kuniaki Nakamura were not only great friends; they were excellent collegues and mentors. I especially would like to thank Soyoung Kim for her constant support and love throughout these years.

I would like to thank the Gilmore and Zamore labs for letting me use their equipment.

THESIS ABSTRACT

KCNE1 (E1) peptide is the founding member of the KCNE family (1-5), which is a class of type I transmembrane β-subunits. KCNE1 peptides assemble with and modulate the gating, ion conducting properties and pharmacology of a variety of voltage-gated K^+ channel α-subunits, including KCNQ1 (Q1). Mutations that interfere with the function of either E1 and/or Q1 and disrupt the assembly and trafficking of KCNE1-KCNQ1 channel complexes give rise to diseases such as Romano-Ward (RW) and Jervell Lange Nielsen Syndrome (JLNS), two different forms of Long QT Syndrome (LQTS).

Using enzymatic deglycosylation assays, immunofluorescence techniques and quantitative cell surface labeling, we showed that KCNE1 peptides are retained in the early stages of the secretory pathway as immaturely N-linked glycosylated proteins. KCNE1 co-assembly with KCNQ1 leads to E1 progression through the secretory pathway and glycan maturation, resulting in cell surface expression.

N-linked glycosylation of some membrane proteins is critical for proper folding, co-assembly and subsequent trafficking through the biosynthetic pathway. Previous studies have shown that genetic mutations that disrupt one of the two N-linked glycosylation sites on KCNE family members lead to LQTS (T7I, KCNE1 and T8A, KCNE2) (Schulze-Bahr et al., 1997; Sesti et al., 2000a; Park et al., 2003). Having confirmed that KCNE1 proteins acquire N-linked glycans, we examined the kinetics and efficiency of N-linked glycan addition to KCNE1. We showed that KCNE1 has two distinct N-linked glycosylation sites. The N-terminal sequon is a traditional co-

translational site. The internal sequon (which is only ~ 20 residues away from the N-terminal sequon) acquires N-linked glycans primarily after protein synthesis (post-translationally). Surprisingly, mutations that prevent N-glycosylation at the co-translational site also reduce the glycosylation efficiency of post-translational glycosylation at the internal sequon, resulting in a large population of unglycosylated KCNE1 peptides that are retained in the early stages of the secretory pathway and do not reach the cell surface with their cognate K^+ channel. We showed that KCNE1 post-translational N-glycosylation in the endoplasmic reticulum is a cellular mechanism that ensures E1 proteins acquire the maximal number of glycans needed for proper channel assembly and trafficking. Our findings provide a new biogenic mechanism for human disease by showing that the JLNS mutation, T7I, not only inhibits glycosylation of the N-terminal sequon, but also indirectly prevents the glycosylation of the internal sequon, giving rise to a large population of assembly incompetent hypoglycosylated KCNE1 peptides.

To further investigate the two N-linked glycosylation sites on KCNE1, we generated structure-function deletion scans of KCNE1 and performed positional glycosylation scanning mutagenesis. We examined the glycosylation pattern of glycosylation mutants in an effort to define the glycosylation window important for proper KCNE1 assembly and trafficking. Our findings suggested a nine amino acid periodicity to serve as a desirable glycosylation site and a better substrate for N-glycosylation.

Appendix II shows work on the characterization of the C-terminally HA-tagged KCNE1 protein, which was used throughout the experiments presented in Chapter II, Chapter III and Chapter IV. Analysis of the C-terminally HA-tagged KCNE1 protein revealed that in heterologous expression systems KCNE1 had an internal translational start site, a methionine at position 27. A proteolytic cleavage site was also identified at the arginine cluster spanning residues 32 through 38 bearing the two known Long QT mutations (R32H and R36H) (Splawski et al., 2000; Napolitano et al., 2005).

My work in Professor Craig C. Mello's lab during the first four years of my graduate study is presented in Appendix I. The highly conserved Wnt/Wingless glycoproteins regulate many aspects of animal development. Wnt signaling specifies endoderm fate by controlling the fate of EMS blastomere daughters in 4-cell stage *Caenorhabditis elegans* embryos. A suppressor genetic screen was performed using two temperature sensitive alleles of *mom-2*/Wnt to identify additional regulators of the Wnt/Wingless signaling pathway during *C. elegans* endoderm specification. Five intragenic suppressors and three extragenic suppressors of *mom-2*/Wnt embryonic lethality were identified. We cloned *ifg-1*, eIF4G homologue, as one of the extragenic suppressors suggesting an intriguing connection between the Wnt signaling pathway and the translational machinery.

TABLE OF CONTENTS

LIST OF TABLES

LIST OF FIGURES

LIST OF ABBREVIATIONS

α-subunit	Pore-forming subunit
β-subunit	Accessory subunit
C-terminal, C-terminus	Carboxy-terminal, carboxy-terminus
C. elegans	*Caenorhabditis elegans*
eIF4G	Human eukaryotic translation initiation factor 4G
EKG	Electrocardiogram
ER	Endoplasmic reticulum
ERAD	ER associated protein degradation
HA	Hemagglutinin A
hERG	Voltage-gated potassium channel, subfamily H (eag-related)
I_{Ks}	Delayed rectifying cardiac potassium current
ifg-1	Initiation factor 4G (eIF4G) family member
JLNS	Jervell and Lange-Nielsen syndrome
K^+	Potassium (ion)
K_v channel	Voltage-gated potassium channel
KCNE1, MinK, IsK, E1	Voltage-gated potassium channel subfamily E member 1
KCNE2-5, MiRP1-4, E2-5	Voltage-gated potassium channel subfamily E member 2-5
KCNQ1, KvLQT1, Kv7.1, Q1	Voltage-gated potassium channel, KQT-like subfamily, member 1
KCNQ2-5, Kv7.2-5	Voltage-gated potassium channel, KQT-like subfamily, member 2-5
LQT(S)	Long QT syndrome
mom-2	more mesoderm
N-glycosylation	Asparagine-linked glycosylation (N-linked glycosylation)
N-terminal, N-terminus	Amino-terminal
O-glycosylation	Threonine- or serine-linked glycosylation
PKC	Protein kinase C
RWS	Romano-Ward syndrome
S1-6	Voltage-gated potassium channel transmembrane helix 1-6
TEVC	Two-electrode voltage clamp
TM	Transmembrane domain
WT	Wild-type
Wnt	Wg (wingless) and Int

PREFACE

In Chapter II, C-terminally HA-tagged KCNE1 protein was used to examine intracellular localization of KCNE1 peptides in the whole cell immunofluorescence studies. I constructed and characterized the C-terminally HA-tagged KCNE1 protein (Appendix II). Kshama Chandrasekhar conducted the biochemistry and immunofluorescence experiments and showed that KCNE1 subunits require co-assembly with K^+ channels for efficient trafficking and cell surface expression. The work presented in Chapter II has been published in a peer-reviewed journal.

In Chapter III, Kshama Chandrasekhar provided the preliminary observations for the work presented and is credited with the second authorship. Dr. Anatoli Lvov is credited authorship for the electrophysiology experiments. Yuan Gao is credited authorship for the proteosomal inhibitor experiment. Professor Reid Gilmore has been our guide on glycosylation work. I characterized KCNE1 N-glycosylation through extensive biochemical analysis and described a novel mechanism for the biogenesis of Long QT syndrome. The experimental work has been written up as a manuscript for publication.

In Chapter IV, I performed structure-function deletion scans and positional glycosylation mutagenesis to elucidate the differential behavior of the two N-linked glycosylation sites on KCNE1. Yuan Gao provided the immunoblot for a glycosylation mutant and she will be pursuing this project.

In Appendix I, I present my work in Mello Lab. I performed suppressor screens of mom-2/Wnt and I was able to isolate both intragenic and extragenic suppressors. Dr Takao Ishidate helped me with conducting the suppressor screens. Dr Soyoung Kim pursued and completed the project with the help of Rita Sharma and Dr Masaki Shirayama. Dr Soyoung Kim and I will be co-authors in the soon to be published work. The experimental work has been written up as a manuscript for publication.

In Appendix II, I characterized the C-terminally HA-tagged KCNE1. Trevor Morin, Steven Gage and Jessica Rocheleau helped with electrophysiology experiments.

References:

Chapter II:

Chandrasekhar, K. D., Bas, T., and Kobertz, W. R. 2006. KCNE1 subunits require co-assembly with K^+ channels for efficient trafficking and cell surface expression. *J Biol Chem*. 281: 40015-40023.

Chapter III:

Bas, T., Chandrasekhar, K. D., Lvov, A., Gao, Y., Gilmore, R., and Kobertz, W. R. 2010. Post-translational N-Glycosylation of type I transmembrane KCNE1 peptides: Implications for disease. *Manuscript in Preparation*.

Appendix I:

Kim S *****, **Bas T ***, Ishidate T, Sharma R, Shirayama M, and Mello CC. (*** equal contribution**). Screening for suppressors of mom-2 embryonic lethality: A connection between the Wnt signaling pathway and the translational machinery in C. Elegans. *Manuscript in preparation*.

CHAPTER I

INTRODUCTION

Part I: Voltage-gated potassium channels

Historia:

The plasma membrane is a biological barrier that confines the interior of the cell from the outside environment. Cells can exhibit a voltage difference across their plasma membrane through the selective separation of ions and creating an electrochemical gradient. This voltage difference, also known as membrane potential, is important for proper functioning of the cell (Alberts et al., 2002; Hunte and Richers, 2008). Membrane potential is also essential for signal transmission between different parts of a cell in electrically excitable cells, such as neurons. The membrane potential is held at a relatively stable value called the resting potential, which stays in -40 to -90 mV range for most cell types. The membrane potential arises from the interaction of ion pumps and ion channels embedded in the membrane (Hille, 2001; Levitan and Kaczmarek, 2002).

Ion pumps are transmembrane proteins that are able to move ions across the plasma membrane against their concentration gradient. In contrast, ion channels are membrane-embedded proteins that allow the passive diffusion of ions down their electrochemical gradient; therefore they establish the voltage gradient across the plasma

membrane (Hille, 2001). Other than this very fundamental function, ion channels have additional physiological roles and if they fail to function properly they can cause a broad range of diseases known as channellopathies (Hubner and Jentsch, 2002; Marban, 2002).

Generally, ion channels are composed of several proteins that assemble, creating a water-filled pore through the plane of the membrane. This water-filled pore allows ions to diffuse passively and often selectively depending on the type of the channel (Ackerman and Clapham, 1997; Hille, 2001). Thus, one way to classify channels is according to the ions that they permeate: namely, chloride channels; sodium channels; calcium channels; proton channels; non-selective cation channels and potassium channels.

Potassium channels are found in most cell types in practically all living organisms. Beside this central role in maintaining the membrane potential, potassium channels have many other functions, from shaping the action potentials to regulating cellular processes like hormone secretion (Ackerman and Clapham, 1997; Hille, 2001; Levitan and Kaczmarek, 2002). Therefore, their malfunction can lead to diseases like diabetes and even in some cases life threatening cardiac arrhythmias (Lehmann-Horn and Jurkat-Rott, 1999).

There are four major classes of potassium channels: calcium activated potassium channels, inwardly rectifying potassium channels, tandem pore-domain potassium channels and voltage-gated potassium channels. Calcium activated potassium channels open in response to the presence of intracellular calcium ions and voltage changes. Inwardly rectifying potassium channels pass positive charges (current) more easily in the

inward direction (into the cell) at negative membrane potentials and do not allow potassium efflux at positive membrane potentials; unlike other potassium channels where potassium currents are preferentially carried outward at depolarized membrane potentials. Tandem pore-domain potassium channels are also known as two-pore-domain potassium channels. They are responsible for baseline or leak currents. Voltage-gated potassium channels open and close in response to the changes in membrane voltage (Hille, 2001).

Voltage-gated potassium channels:

Voltage-gated potassium channels are composed of four transmembrane subunits which can form either homo- or heterotetramers. These subunits, also known as α-subunits, are arranged around a central conducting pore, Figure 1.1***A***. Each α-subunit has 6 transmembrane domains (S1-S6) with both amino and carboxy termini facing the cytoplasm. The narrowest part of the pore is formed by a loop between S5 and S6 and it is called the selectivity filter (Doyle et al., 1998; Zhou et al., 2001; Williamson et al., 2003; Miloshevsky and Jordan, 2008). Selectivity and high conductance rates are crucial factors for the biological function of the channels and voltage-gated potassium channels are indeed highly selective with the ions they permeate. In addition, ion transport rates are close to the aqueous diffusion limit (Hille, 2001).

Voltage-gated potassium channels are expressed in both non-excitable and excitable cells. Excitable cells are cell types capable of changing their membrane

A

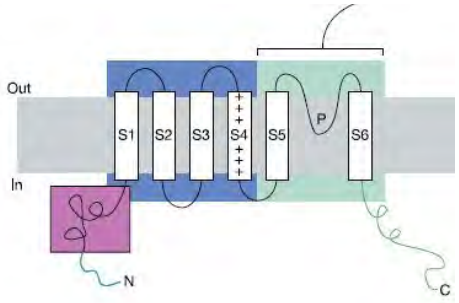

B

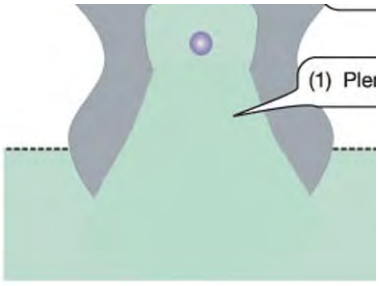

Figure 1.1: (***A)*** **The K^+ channel family transmembrane architecture**. Top left: Four similar 6-transmembrane subunits (S1-S6) surround a central pore (P), forming a voltage-gated potassium channel. Both N- terminus (purple) and C- terminus (green) are facing the cytoplasm. S4 region bears positive charges and serves as the voltage sensor (S1-S4, blue). S5 and S6 form the pore region (light green). Tetramerization domain (purple) is in the N-terminus. Top right: The prototype for the pore forming domain of bacterial KcsA K^+ channel with only two transmembrane helices (homologous to S5 and S6). Dark green is the interior of the protein, grey is the water exposed surface. The four spheres represent the four K^+ ion binding sites. The water-filled ~~"c~~avity" resides between the selectivity filter and bundle crossing. ***B***. **Structural requirements of K^+ channel ion permeation**. Left: Diagram of an open K^+ channel based on the crystal structure of the MthK channel (Jiang et al., 2002b). Intracellular vestibule is wide-open. Pore helix dipoles are highlighted. Right: A view derived from the high resolution structure of the KcsA channel (Zhou et al., 2001). A narrower (probably closed) access to a water-filled cavity in the middle of the membrane protein is shown. Purple sphere, a trapped K^+ ion; green spheres are eight water molecules; red spheres, backbone oxygens of the selectivity filter; and orange spheres, side chain oxygen atoms (Yellen, 2002).

potentials, and include neurons and cardiomyoctes. The canonical change in membrane potential is an action potential. An action potential is a transient change in the voltage across the cell membrane. During an action potential a cascade of events commences, resulting in signal transmission within the cell, Figure 1.2 (Kleber and Rudy, 2004). During the final steps of the action potential voltage-gated potassium channels are the main players that bring the membrane potential to its resting level. Every α-subunit possesses a voltage sensor with multiple charged amino acids on the S4 transmembrane helix (Figure 1.1***A***). Charge repulsion within this region is responsible for sensing the changes in membrane potential (Gandhi and Isacoff, 2002). The time required for voltage-gated potassium channels to bring the depolarized membrane potential from positive to its resting state, a process known as hyperpolarization, is determined by the voltage sensitivity and gating kinetics. During hyperpolarization, voltage-gated potassium channels are activated by positive voltage and this results in the outward flow of potassium ions to reduce the positive charge inside the cell and terminate (or prevent) excitation. In some cases channels can begin opening within milliseconds. An open channel can pass millions of ions per second making it a high throughput and highly selective system (Morais-Cabral et al., 2001; Levitan and Kaczmarek, 2002; Yellen, 2002).

The merits of this highly efficient system come from its architectural features that were provided by the crystal structures of the pores of two different bacterial potassium channels, KcsA and MthK Figure 1.1***B*** (MacKinnon et al., 1998; Morais Cabral et al., 1998; Long et al., 2005). Stabilization of potassium ions are achieved in two ways: First,

Depolarizing Currents

Cardiac Action Potential

Repolarizing Currents

Figure 1.2: ***Top***: **The major ion channels and an electrogenic transporter in cardiac cells**. K^+ channels (green) mediate K^+ efflux from the cell; Na^+ influx is achieved through Na^+ channels (purple) and Ca^{2+} influx through Ca^{2+} channels (yellow). The Na^+/Ca^{2+} exchanger (red) transports three Na^+ ions for each Ca^{2+} ion across the plasma membrane. ***Bottom***: **Ionic currents and genes underlying the cardiac action potential**. The top three currents are: I_{Na}, $I_{Ca,L}$ and $I_{Na/Ca}$ are depolarizing currents shown as functions of time, followed by their corresponding genes. Underneath the depolarizing currents is a ventricular action potential. Repolarizing currents and their corresponding genes are presented below the action potential (Marban, 2002).

part of the permeation pathway is broad enough to accommodate a large amount of water to stabilize the potassium ion. Second, electrostatic influence of helix dipoles stabilizes the cations near the entrance to the narrow selectivity filter within the center of the lipid bilayer Figure 1.1***B***. In addition, the selectivity filter of the potassium channel mimics the water structure around a potassium ion making it more like a custom made polar oxygen cage for potassium ions, enhancing selectivity. Finally, potassium ions pass through with simultaneous occupancy by multiple ions in the selectivity filter Figure 1.1***B***. This creates electrostatic repulsion between the adjacent potassium ions helping the rapid permeation and allowing high transport rates (Doyle et al., 1998; Zhou et al., 2001; Yellen, 2002).

There is an enormous variety in voltage-gated potassium channels. They are encoded by at least 40 different genes in mammals. Alternative splicing, posttranslational modifications and heteromultimerization increase this variety (Wulff et al., 2009). The α-subunits of voltage-gated potassium channels have been grouped into 12 classes labeled Kvα1-12 according to the sequence homology of the transmembrane domain (Gutman et al., 2005). Other than this broad nomenclature, many subfamilies of voltage-gated potassium channels have been discovered exhibiting typical structural features including voltage sensor, toxin binding sites, and a single ion-conducting pore (Hille, 2001). Also, voltage-gated potassium channels enhance channel diversity further through the association with auxiliary subunits, known as β-subunits. β-subunits do not conduct current on their own; instead they modulate the activity of voltage-gated potassium channels via changing the kinetic properties, regulation, pharmacology, and

structure of the channel (Isom et al., 1994; Adelman, 1995; Catterall, 1995; Trimmer, 1998; Pongs et al., 1999; Deutsch, 2002; Hanlon and Wallace, 2002; Yellen, 2002).

The KQT-like channels, also known as the KCNQ family, encode voltage-gated potassium channels with unusual features. Unlike the other voltage-gated six transmembrane helix channels, KQT-like channels do not have an N-terminal tetramerization domain (Deutsch, 2002). Accordingly, they depend on the interactions with accessory subunits. They also form heterotetramers with other members of the family. Initially, these channels were cloned in a genetic screen searching for the proteins involved in cardiac arrhythmia (Wang et al., 1996). There are five members of the KCNQ family known to date, namely KCNQ1-5. KCNQ channels are widely distributed in the body and they are expressed in the heart, ear, cochlea, brain, eye, kidney, lung, pancreas, breast, testis, small intestine, colon, rectum and placenta (Robbins, 2001; Gutman et al., 2005).

<u>Part II:</u> KCNQ1: Voltage-gated potassium channel, KQT-like subfamily, member 1

The original name of KCNQ1 was "potassium voltage-gated channel, KQT-like subfamily, member 1". KCNQ1 is the official symbol of the gene. KCNQ1 is a 676 amino acid protein. Like other members of the voltage-gated potassium channel family, KCNQ1 has six transmembrane helices, with both amino- and carboxy-termini facing the

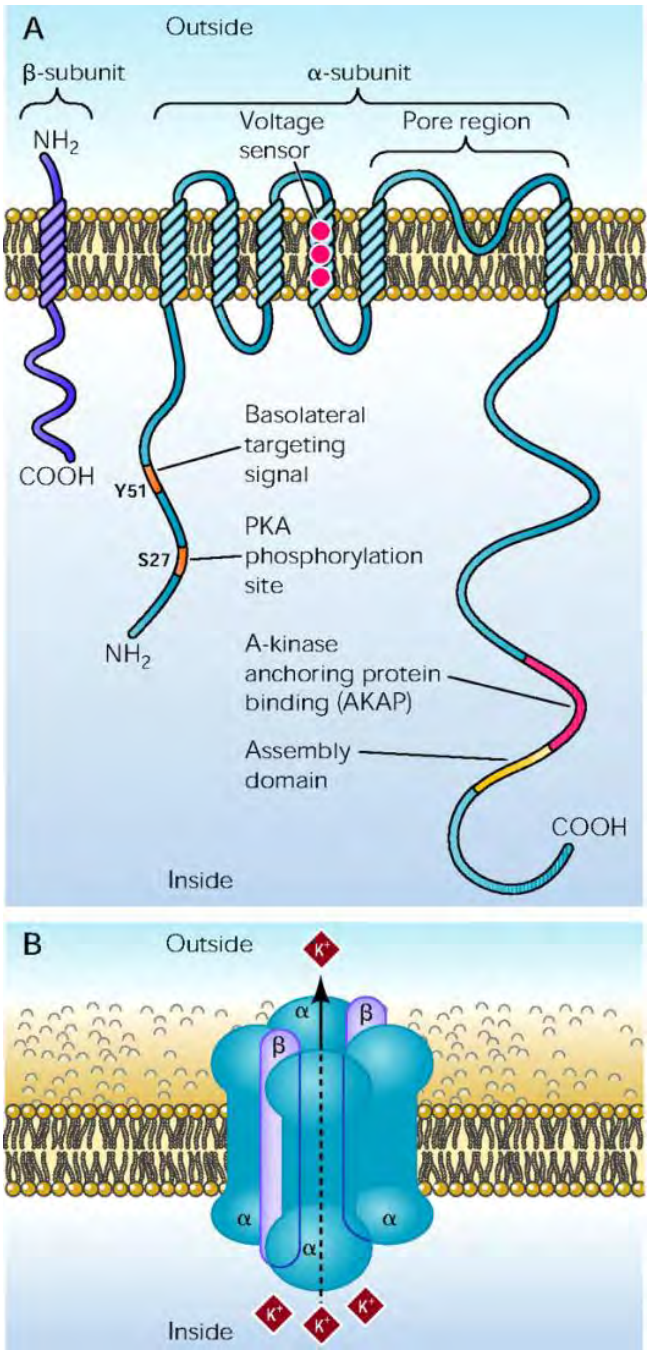
A
Outside
β-subunit
α-subunit
Voltage sensor
Pore region
NH2
COOH
Y51
Basolateral targeting signal
S27
PKA phosphorylation site
NH2
A-kinase anchoring protein binding (AKAP)
Assembly domain
COOH
Inside
B
Outside
K+
α
β
β
α
α
α
K+
K+
K+
Inside

Figure 1.3. ***A***: **Topology of KCNE and KCNQ1 proteins**. Some of the domains important for regulation of the KCNQ1 channel and topology of the KCNE proteins are indicated. All five KCNE proteins have a single transmembrane domain with different lengths of NH_2 and COOH termini. ***B***: **Channel architecture of KCNQ1 α-subunit with KCNE proteins**. Four KCNQ1 α-subunits assemble with two KCNE β-subunits resulting in β-subunit-specific currents (Jespersen et al., 2005; Morin and Kobertz, 2008a).

cytoplasm and a single pore-loop-helix motif Figure 1.3***A*** (Robbins, 2001). KCNQ1 has a relatively short N-terminal domain where it bears a PKA phosphorylation site at S27. KCNQ1 also has a large C-terminal domain where it harbors interaction sites for several cell signaling molecules including two PKC phosphorylation sites at T381 and S399 (Busch et al., 1992; Lo and Numann, 1998; Kurokawa et al., 2003; Chen et al., 2005). KCNQ1 has a potential glycosylation site, N289, at the region connecting the transmembrane domains S5 and S6 (Figure 1.1***A*** and Figure 1.3***A***). Up until very recently, there was no information about the functional significance of this site (Freeman et al., 2000). However, a group showed that changing N289 to a glutamic acid reduced current density by 56% with no further evidence showing its relation to hypo-glycosylation (Zaika et al., 2008).

KCNQ1 proteins are expressed in the inner ear and heart (Panaghie et al., 2006). In the inner ear, these channels are responsible for the transport of potassium ions out of the cells and maintain ionic homeostasis required for normal hearing (Nicolas et al., 2001; Wangemann, 2002). In the heart, they form I_{ks} channels responsible for the slow delayed outwardly-rectifying cardiac potassium current. These currents are essential for the rhythmicity of the heart (Bendahhou et al., 2005; Lundquist et al., 2005). Also, the KCNQ1 protein is involved in transport of molecules across cell membranes in the kidney, lung, stomach and intestine (Lehmann-Horn and Jurkat-Rott, 1999; Jespersen et al., 2005). The currents arising from homotetrameric KCNQ1 channels in over expression systems do not match any observed physiological potassium currents. KCNQ1 channel shows rapid activation and a large degree of inactivation. In order to

present the physiologically observed gating properties KCNQ1 channels require co-assembly with KCNE peptides (Melman et al., 2002b).

Part III: KCNE Family - A family of voltage-gated potassium channel β-subunits

The KCNE family members function as ancillary subunits (β-subunits) of voltage-gated potassium channels. These proteins control the surface expression, voltage dependence, ion selectivity, unitary conductance, gating kinetics, and pharmacology of several channels (Abbott and Goldstein, 1998; Trimmer, 1998; Pongs et al., 1999). The hallmark of the KCNE family of peptides is that they assemble with and modulate KCNQ1 channels in heterologous expression systems (McCrossan and Abbott, 2004). Until now, there are 5 known members of the KCNE family: KCNE1 (MinK/IsK), KCNE2 (MiRP1), KCNE3 (MiRP2), KCNE4 (MiRP3) and KCNE5 (KCNE1L) (Takumi et al., 1988; Abbott and Goldstein, 1998; McCrossan and Abbott, 2004). These small glycoproteins (100 to 170 amino acids) are type I transmembrane peptides; they have a single transmembrane domain where the N-terminus is facing outside and the C-terminal is facing the inside of the cell (Figure 1.3***A*** and Figure 1.4***A***). All KCNE peptides have at least one N-linked glycosylation site located within the first 30 amino acids of the N-terminus (Figure 1.4***A***). The C-terminal and transmembrane domains of KCNE peptides are mainly α-helical and interact with KCNQ1 in a bipartite manner, dramatically modulating the channel complex function (Mercer et al., 1997; Gage and Kobertz, 2004; Rocheleau et al., 2006; Chen and Goldstein, 2007; Liu et al., 2007).

A

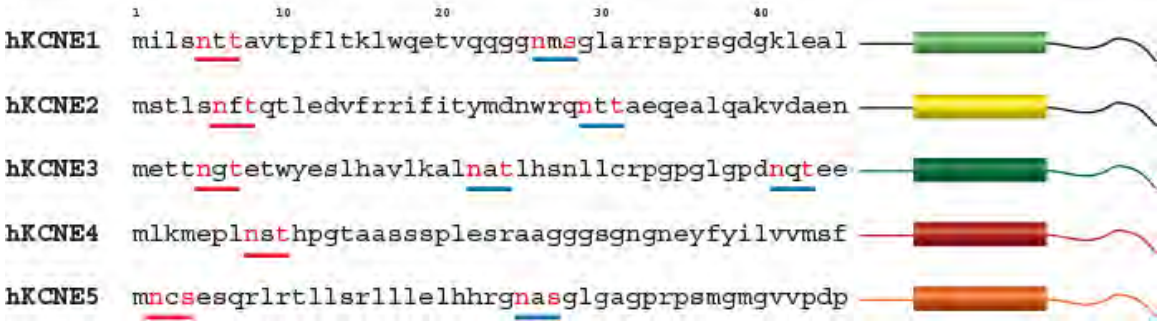
1
10
20
30
40
hKCNE1 milsnttavtpfltklwqetvqqggnmsglarrsprsgdgkleal
hKCNE2 mstlsnftqtledvfrrifitymdnwrqnttaeqealqakvdaen
hKCNE3 mettngtetwyeslhavlkalnatlhsnllcrpgpglgpdnqtee
hKCNE4 mlkmeplnsthpgtaasssplesraagggsgngneyfyilvvmsf
hKCNE5 mncsesqrlrtllsrlllelhhrgnasglgagprpsmgmgvvpdp

B

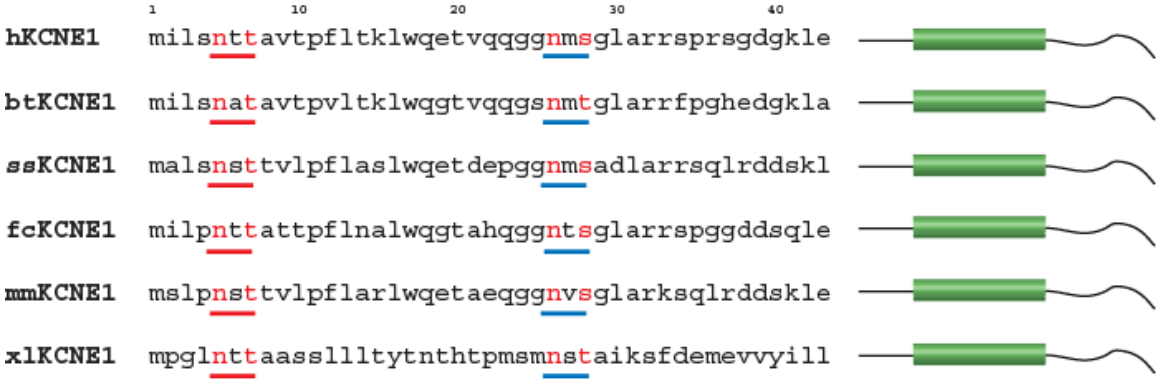
1
10
20
30
40
hKCNE1 milsnttavtpfltklwqetvqqggnmsglarrsprsgdgkle
btKCNE1 milsnatavtpvltklwqgtvqqgsnmtglarrfpghedgkla
ssKCNE1 malsnsttvlpflaslwqetdepggnmsadlarrsqlrddskl
fcKCNE1 milpnttattpflnalwqgtahqggntsglarrspggddsqle
mmKCNE1 mslpnsttvlpflarlwqetaeqggnvsglarksqlrddskle
xlKCNE1 mpglnttaasslllltytnthtpmsmnstaiksfdemevvyill

Figure 1.4: (***A)***. **The N-terminal glycosylation site is conserved among KCNE family members (1-5).** The first glycosylation site is underlined red and the internal glycosylation sites are underlined blue. Asparagines (n) and serines (s) or threonines (t) are in red. Cylinders denote transmambrane domains. (***B)*** **Sequence alignment of KCNE1 N-terminus**. The two N-linked glycosylation sites on KCNE1 are conserved among species. h: human, bt: bos taurus (cattle), ss: sus scrofa (pig); fc: felis catus (domastic cat), mm: mus muculus (house mouse), xl: xenopus laevis (African clawed frog).

All known KCNEs are expressed in the heart; KCNE2-5 in CNS; KCNE2-4 in kidney and lung; KCNE2-3 in stomach; KCNE1 in inner ear; KCNE3 in small intestine, colon, skeletal muscle (Abbott and Goldstein, 2001). The wide distribution of KCNE peptides in the body shows their diverse roles from controlling the excitability of the heart and CNS, to facilitating potassium recycling in the gastrointestinal tract, to modulating vascular tone in blood vessels (McCrossan and Abbott, 2004). Recently, it has been shown that all KCNEs are expressed in the immune system (Sole and Felipe, 2010). Mutations in KCNE genes can lead to acquired and/or congenital diseases of cardiac muscle, skeletal muscle and inner ear (Abbott and Goldstein, 2001; McCrossan and Abbott, 2004).

KCNE peptides are highly promiscuous regulatory subunits. Each has been shown to interact with several different voltage-gated potassium channel α-subunits such as Kv2.1, Kv3.1, Kv3.2, Kv4.2K, KCNQ1 (Kv7.1), HERG (Kv11.1) (Sanguinetti et al., 1996; McDonald et al., 1997; Melman et al., 2001; Zhang et al., 2001; Finley et al., 2002; Ohya et al., 2002a; Lewis et al., 2004; McCrossan and Abbott, 2004; Gordon et al., 2006; Um and McDonald, 2007). Also, some KCNEs assemble with the same α-subunit in a tissue specific manner. One example would be assembly with α-subunit KCNQ1. KCNQ1-KCNE complexes have known roles in physiological processes including cardiac repolarization through I_{ks} current (KCNE1) (Barhanin et al., 1996; Sanguinetti et al., 1996), acid-secretion in the gut (KCNE2), K^+ homeostasis in the lung and colon (KCNE3), maintaining ion equilibrium in inner ear (KCNE1) (Marban, 2002; Wangemann, 2002), and possibly regulation and diversification of I_{ks} (KCNE4 and

KCNE5) (Angelo et al., 2002; Grunnet et al., 2002; Bendahhou et al., 2005; Lundquist et al., 2005).

<u>Part IV:</u> KCNE1: Voltage-gated potassium channel, Isk-related family, member 1

The official name of KCNE1 gene is "potassium voltage-gated channel, Isk-related family, member 1". KCNE1 is the gene's official symbol. KCNE1, the founding member of KCNE family, is a type I transmembrane protein. KCNE1 is a 129 amino acid glycoprotein. It has two N-linked glycosylation sites in the extracellular N-terminal side, N5 and N26 (Figure 1.4***A*** and Figure 1.4***B***). There is no high resolution crystal structure of KCNE1. Serial perturbation studies of KCNE1 suggest that the C-terminal domain of KCNE1 is mainly α-helical (Rocheleau et al., 2006; Chen and Goldstein, 2007; Liu et al., 2007). In addition, fourier transform infrared (FTIR) and circular dichrosim (CD) spectroscopy studies show that the transmembrane domain of KCNE1 forms an α-helical conformation in lipid or detergent environments, which is consistent with biochemical perturbation scans (Mercer et al., 1997; Rocheleau et al., 2006; Chen and Goldstein, 2007).

KCNE1 has been shown to form complexes with Kv3.1, Kv3.2, Kv4.3, HERG K^+ channels (McDonald et al., 1997; Bianchi et al., 1999; Deschenes and Tomaselli, 2002; Lewis et al., 2004). KCNE1 subunits also associate with KCNQ1 α-subunits in a tissue specific manner and modify channel gating, ion selectivity, single-channel conductance,

pharmacology (channel's sensitivity to small molecule activators and inhibitors) and regulation (Barhanin et al., 1996; Sanguinetti et al., 1996; Abbott and Goldstein, 1998).

KCNE1 is widely expressed in mammalian tissues. It is expressed in heart cardiac muscle (Zhang et al., 2001; Finley et al., 2002); in smooth muscle and epithelia in the stomach (Ohya et al., 2002a; Ohya et al., 2002b), kidney, uterine endometrium, submandibular duct (Sugimoto et al., 1990), inner ear (Sakagami et al., 1991; Nicolas et al., 2001). In addition, KCNE1 mRNA is found in the small intestine, lung, leukocytes, testis and ovaries (Chouabe et al., 1997); pancreas (Demolombe et al., 2001), uterus (Folander et al., 1990) and brain (Ohya et al., 2002b).

Part V: KCNQ1 - KCNE1 channel complex and disease:

Historia:

KCNQ1 was cloned in a genetic study searching for a mutation that is responsible for inherited cardiac arrhythmia (Wang et al., 1996). However, this six transmembrane voltage-gated potassium channel with a classical pore-forming P loop gave rise to rapidly-activating, non-inactivating K^+ current that did not match any known native cardiac myocyte current. When KCNQ1 and KCNE1 were coexpressed in mammalian cells native I_{Ks} channel currents were observed (Figure 1.5***A*** and Figure 1.5***B***) (Barhanin et al., 1996; Sanguinetti et al., 1996; Sesti and Goldstein, 1998).

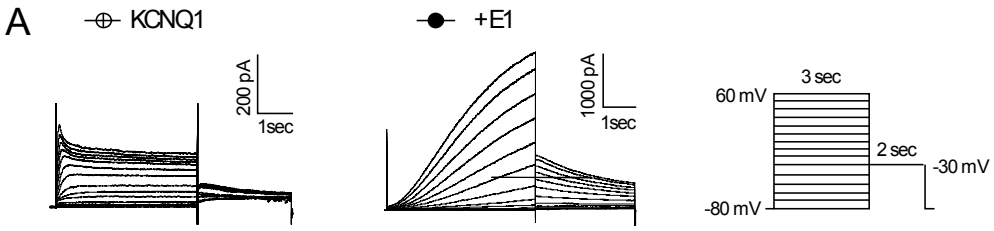
A
KCNQ1
+E1
200 pA
1sec
1000 pA
1sec
3 sec
60 mV
2 sec
-30 mV
-80 mV

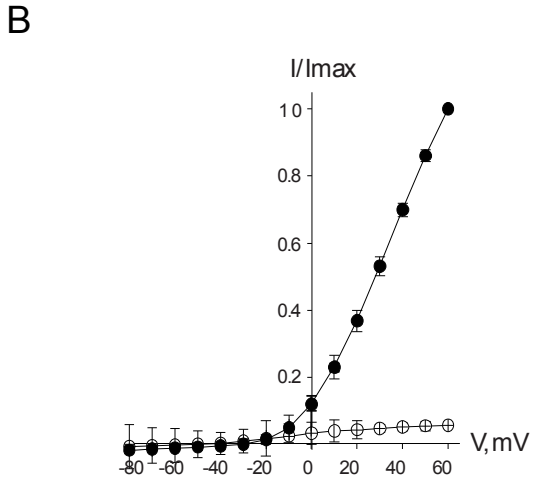
B
I/Imax
1.0
0.8
0.6
0.4
0.2
V, mV
-80
-60
-40
-20
0
20
40
60

Figure 1.5: **Current properties of KCNQ1 channels change when co-expressed with KCNE1**. (***A***) Representative families of I_{Q1} and I_{Ks} traces were recorded from CHO cells. Cells were transfected only with KCNQ1 (KCNQ1) or cotransfected with KCNE1 (+E1). The currents were evoked by 3-s depolarization prepulses from a holding potential of -80 mV in 10-mV increments at an interpulse interval of 30 s to test voltages -70 to +60 mV. To monitor the tail currents the depolarization prepulses were followed by repolarization to -30 mV for 2 s. (***B)*** Relative mean peak currents (I/Imax) were normalized to the maximal I_{Ks} (Q1/E1) and plotted as a function of the prepulse voltage (V). n = 3 – 5, mean ± S.E.M. Figure 1.5 was kindly generated by Dr Anatoli Lvov.

The I_{Ks} channel currents have slower activation rates, slower deactivation rates compared to KCNQ1 channel currents. KCNE1 modulates KCNQ1 channel by changing the unitary conductance (Romey et al., 1997; Sesti and Goldstein, 1998); effecting the channel gating by slowing activation and deactivation and decreasing the voltage sensitivity (Barhanin et al., 1996; Sanguinetti et al., 1996; Sesti and Goldstein, 1998); changing ion selectivity by selecting more effectively against Cs^+ and NH_4^+ ions (Sesti and Goldstein, 1998); modifying the pharmacology by influencing the block or activation by some drugs such as Class III anti-arrhythmic agents, mefenamic acid and DIDS (4,4-diisothiocyanato-stilbene-2,2'disulphonate) (Busch et al., 1997; Abitbol et al., 1999; Lerche et al., 2007).

A tethered blocker strategy allowed the assessment of the number and composition of KCNE subunits assembling with KCNQ1 α-subunits (Morin and Kobertz, 2008b). The stoichiometry of the KCNQ1-KCNE1 complex is shown to be 4:2 (Figure 1.3***B***) (Morin and Kobertz, 2008a). Though the KCNQ1-KCNE1 protein-protein interaction is a controversial topic, one model suggests that KCNE1 subunits are intimately associated with the channel pore; therefore they are positioned close to the residues forming the conduction pathway (Melman et al., 2004; Jespersen et al., 2005). All KCNE peptides share a conserved 20 amino acid stretch in the cytoplasmic domain neighboring the transmembrane domain. For KCNE1 this region is required for KCNQ1 channel modulation (Takumi et al., 1991; Tapper and George, 2000). Also, it has been shown that a triplet of amino acids located in the transmembrane domain is essential for current modulation (Melman et al., 2001). In addition, the specificity of the β-subunit

(KCNE1, T58 and KCNE3, V72) is dictated by a single residue within this triplet (Melman et al., 2002a). Structure-function studies defined the minimal KCNE1 segment required for proper function. The deletion of residues 10-39 had no noticeable effect; yet residues between 4-25 and 4-39 were crucial for proper KCNE1 function. Further truncation studies involving the C-terminus showed that the minimal functional KCNE1 spanned residues 1-9 and 40-94 including the transmembrane domain (Takumi et al., 1991; Abbott and Goldstein, 1998; Tapper and George, 2000).

KCNQ1-KCNE1 channel complex and disease:

KCNE1 co-assembles with KCNQ1 K^+ channels in some epithelial tissues and the heart. In epithelia KCNQ1/KCNE1 channels take part in transepithelial transport by recycling potassium across the basolateral membrane, maintaining the resting potential and regulating Cl^- secretion and/or Na^+ absorption (Figure 1.6) (Jespersen et al., 2005). In murine tracheal epithelial cells, KCNE1 plays a role in regulatory volume decrease response (Grahammer et al., 2001). In kidney, KCNE1 and KCNQ1 are found in the proximal tubule and the distal tubule of the nephron (Demolombe et al., 2001). Though the function of KCNQ1/KCNE1 channel in kidney epithelia is not clear, the KCNE1 knockout mice suffer from renal problems such as hypokalemia, volume depletions, urinary and fecal salt wasting (Vallon et al., 2001; Attali, 2002).

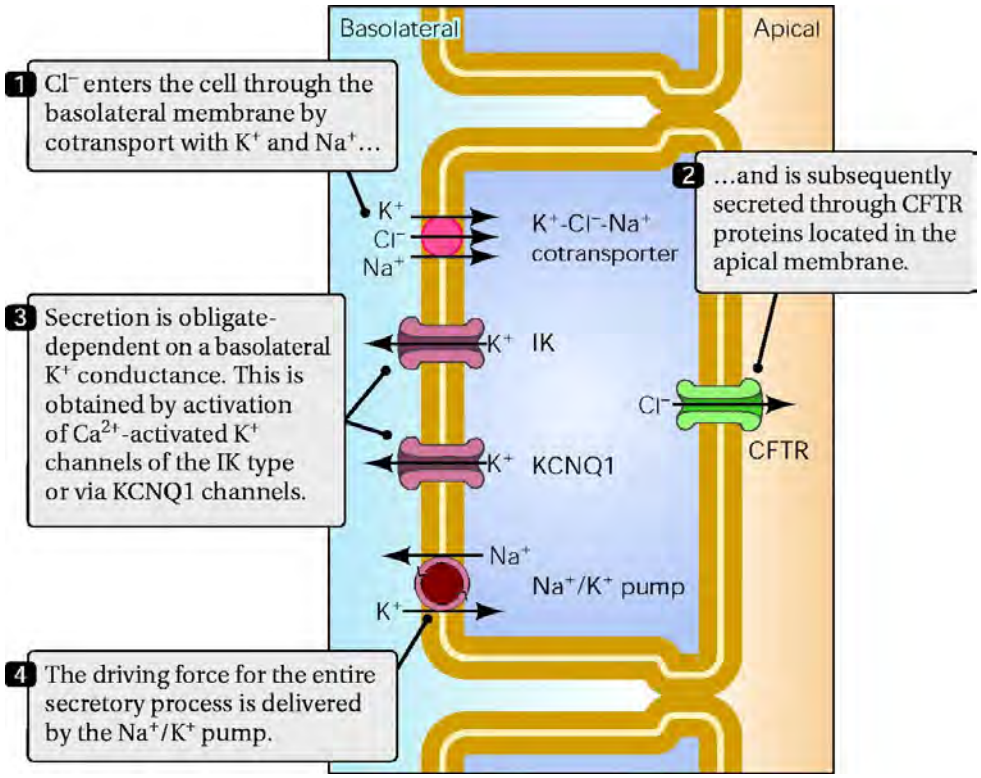

Figure 1.6: **The role of KCNQ1 channels in epithelial function**. In a prototype secretory epithelial cell, KCNQ1 channels are essential for recycling potassium across the basolateral membrane for transepithelial secretion of the chloride ions and maintaining ionic homeostasis (Jespersen et al., 2005).

In epithelial cells from the inner ear, KCNQ1 channels are coexpressed with KCNE1 in the apical membranes of the marginal cells of the stria vascularis and vestibular dark cells (Nicolas et al., 2001; Wangemann, 2002). In the inner ear, endolymph is the fluid that fills the membranous labyrinth enclosed by the heterogenous epithelium. The major salt in endolymph is KCl and potassium ion (K^+) is the major charge carrier for the sensory transduction (Figure 1.7). KCNQ1/KCNE1 channels are responsible for K^+ release into endolymph and for the formation of endolymph in the cochlear and vestibular labyrinth, which is essential for hearing (Vetter et al., 1996; Tyson et al., 1997; Marban, 2002). Mice that lack either KCNE1 or KCNQ1 after postnatal day 3 have collapsed endolypmhatic space due to lack of potassium secretion from strial marginal cells and vestibular dark cells (Vetter et al., 1996). In vestibular dark cells of KCNE1 null mutant mice, KCNQ1 remains in the cytoplasm rather than being trafficked to the apical membrane (Nicolas et al., 2001). Therefore, KCNE1 may be necessary for KCNQ1 trafficking, suggesting a posttranslational interaction between KCNE1 and KCNQ1 (Wangemann, 2002). Patients with Jervell and Lange-Nielsen syndrome who lack either KCNE1 or KCNQ1 suffer from sensorineural deafness that is due to the collapsed endolymphatic space (Neyroud et al., 1997; Schulze-Bahr et al., 1997).

In heart KCNQ1/KCNE1 channels give rise to cardiac I_{Ks} currents (Figure 1.2 and Figure 1.5). I_{Ks} current is the slowly activating component of the cardiac delayed repolarization (Barhanin et al., 1996; Sanguinetti et al., 1996). These currents activate and deactivate very slowly. I_{Ks} channels (KCNQ1/KCNE1 channels) are in part

Figure 1.7: **Potassium recycling in the inner ear**. The high K^+ concentration and positive potential of endolymph of the scala media is maintained through the inconcert function of ion channels and ion pumps. Bottom right shows the model for K^+ secretion from the stria vascularis. A basolateral Na^+/K^+-ATPase pumps K^+ in and Na^+ out of the marginal cells and creates a gradient to drive Cl^- into the cell in a co-transport process. K^+ is then secreted apically by KCNQ1/KCNE1 K^+ channels, allowing a net secretion into the endolymph in spite of its high K^+ concentration. Chloride is recycled through basolateral Cl^- channels. Bottom left is the the diagram of an outer hair cell. Potassium enters through apical mechanosensitive channels and leaves the cell through KCNQ4 K^+ channels present in the basal membrane. Then, K^+ is recycled back to the stria vascularis through supporting cells and fibrocytes of the spiral ligament for another round of secretion (Jentsch, 2000).

responsible for the duration of the action potential in cardiac muscle, which can be followed by the time interval between the Q and T peaks on an electrocardiogram (ECG/EKG). Genetic mutations in either E1 or Q1 give rise to delayed repolarization of the heart following a heartbeat, which can be reflected as the prolongation of the Q-T interval (Figure 1.8***A*** and Figure 1.8***B***). This irregularity might lead to *torsade de pointes* (a form of arrhythmic heartbeat that originates from the ventricles) that may cause palpitations, fainting, seizures and sudden death due to ventricular fibrillation. Inherited diseases of the cardiac rhythm are Romano-Ward, a form of autosomal dominant long-QT syndrome (LQTS) and **J**ervell-**L**ange-**N**ielsen **S**yndrome (JLNS), the inherited autosomal recessive LQTS accompanied with congenital deafness (Figure 1.8***C***) (Splawski et al., 2000; Tyson et al., 2000).

There are over 90 KCNQ1 and 10 KCNE1 mutations that can cause Long-QT Syndrome including mutations in the following frequencies: missense mutations, splice-site mutations, nonsense mutations, in-frame deletions and frameshift mutations (Splawski et al., 2000). For KCNQ1, most mutations reside in intracellular and transmembrane domains followed by the pore region (Splawski et al., 2000; Napolitano et al., 2005). For KCNE1, mutations are located in the intracellular domain followed by the transmembrane and the extracellular domains (Schulze-Bahr et al., 1997; Splawski et al., 2000). KCNQ1 and KCNE1 mutations can interfere directly with function, regulation, assembly and/or trafficking and lead to prolonged action potentials and long-QT syndrome (Keating and Sanguinetti, 2001; Dahimene et al., 2006).

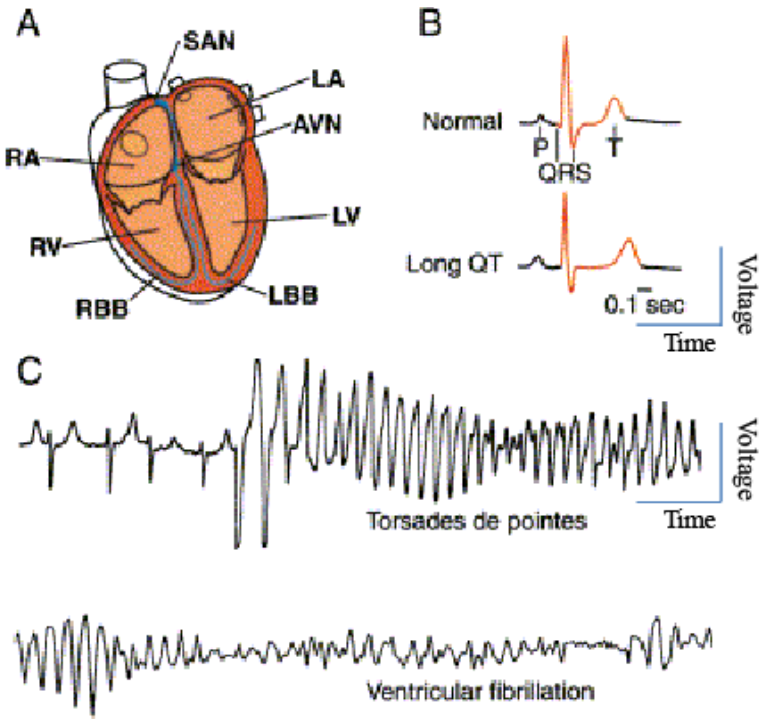

Figure 1.8: A healthy heart vs an unhealthy heart. (***A)***. A schematic representation of a four-chambered heart (RA:right atrium, LA:left atrium, RV:right ventricle, LV:left ventricle). Specialized cells act as a pacemaker (the sino-atrial node, SAN). Conducting tissues are the atrio-ventricular node (AVN) and the right and left bundle branches (RBB, LBB). (***B)*** Normal electrocardiogram (ECG) and an ECG with QT interval prolongation. The P wave shows atrial depolarization, QRS complex reflects ventricular depolarization and the T wave represents ventricular repolarization. A normal QT interval takes about 0.40 s. Abnormal cardiac repolarization gives rise to QT interval prolongation. (***C***) ECG showing a normal sinus rhythm turning into torsades de pointes ventricular tachycardia and ventricular fibrillation (Keating and Sanguinetti, 2001) .

Part VI: Post-translational modifications of proteins

Historia:

Gene expression starts with transcription of DNA into RNA. The transcript encoding for a protein is a messenger RNA (mRNA). During protein synthesis, also known as translation, mRNA is decoded into canonically 20 different amino acids to produce an amino acid chain (the list of endogenous amino acids has been extended to 22 through the recent addition of selenocysteine and pyrrolysine (Hao et al., 2002)). In every gene, a nucleotide triplet code of the DNA encodes an amino acid that is added to the growing polypeptide chain. Translation is followed by protein folding where the nascent polypeptide chain folds into its characteristic and functional three-dimensional structure (Rossmann and Argos, 1981).

After translation most proteins go through a variety of chemical modifications known as post-translational modifications (PTMs). These covalent changes follow the translation of mRNA nucleotide sequences into amino acid based protein sequences at the ribosome (Wold, 1981). Posttranslational modifications alter the function of proteins by changing their activity, trafficking and localization, turnover and interactions with other proteins. These modifications increase proteome diversity through covalent modifications of the side chains of amino acids and peptide linkages. About 5 % of the human genome is dedicated to expanding diversity by encoding the necessary enzymes needed for posttranslational modifications (Walsh, 2006). An enzyme particular for a

certain posttranslational modification shows a great deal of promiscuity for its substrates. This increases the number of modified proteins. The enzymes are also the ultimate decision makers for the type of amino acid side chains modified and the type of covalent chemical modifications introduced.

There are more than 200 kinds of posttranslational modifications of proteins. These modifications can be divided into two major classes: The first one is the covalent addition of one or more groups on a protein; the second one is the hydrolytic cleavage of one or more peptide bonds. In the first group, through the catalytic activity of enzymes groups like phosphoryl, acetyl, or glycosyl are covalently attached to the amino acid side chains of proteins. In the second group, enzymes known as proteases (protein hydrolyses) catalyze the cleavage of the peptide bonds. There are hundreds of enzymes encoded in the human genome that take part in these modifications. A single protein can have several of these posttranslational modifications through the enzyme selectivity for the correct region and sequence on the modified side chains. This is done with great precision, allowing large numbers of combinations and increasing the proteome diversity.

Posttranslational modifications empower proteins in many ways. Introducing negative charges can change the conformation of the microenvironment of the protein. This might effect the overall conformation of the protein in ways unimaginable without posttranslational modifications (Johnson and Lewis, 2001). For example, phosphorylation of two sites might end up creating docking sites for partner proteins that can specifically recognize the tetrahedral phosphate dianionic side chains. Posttranslational modifications may also enhance the catalytic capacity of the modified

proteins. Conversion of inactive apo forms of proteins to holo forms by covalent modifications like protein lipoylation, biotinylation and phosphopantetheinylation increases the catalytic efficiency of the protein considerably. Finally, posttranslational modifications such as ubiquitylation, acylation, glycosyl phosphatidylinositol (GPI) anchoring, farnesylation/ geranylgeranylation, and glycosylation all guide trafficking and subcellular localization of the proteins.

The posttranslational modifications can be examined under eight major categories: protein phosphorylation by protein kinases, sulfuryl transfers, protein methylation, protein N-acetylation, protein lipidation, ubiquitination, proteolytic post-translational modification of proteins and protein glycosylation. Some of the posttranslational modifications are mentioned in detail to provide sufficient background for the upcoming Data Chapters and Appendix II.

Protein phosphorylation by protein kinases: Phosphorylation, like other posttranslational modifications, changes the function of the target protein. The changes effect the protein's association with other proteins, enzyme activity and/or location. Protein kinases are the enzymes that catalyze the transfer of the γ-PO_3^{2-} group from ATP onto the nucleophilic –OH group of the amino acid side chain of serine/threonine or tyrosine. A little more than 500 protein kinases are encoded in the human genome (Manning et al., 2002) and more than 30% of all human proteins are substrates for protein kinases (Cohen, 2000). Overall phoshorylation plays an important role in the regulation of the majority of the cellular pathways, mainly in signal transduction (Cohen, 2002).

Proteolytic Post-translational Modification of Proteins: Proteases are the enzymes that catalyze the hydrolysis of peptide bonds of select target proteins and can modify their activity (Walsh, 2006). This posttranslational modification of the protein can be biosynthetic (activation and/or inhibition of the substrate) or degradative. Controlled proteolysis plays many roles in cellular processes; defense responses like antigen processing, programmed cell death, shedding of cell surface proteins; developmental processes like the proteolytic action of sperm enzymes penetrating into an egg; and signaling pathways like the Notch signaling are some of the many cellular processes that are triggered by proteolytic processing (Thornberry and Lazebnik, 1998; Ye and Fortini, 2000; Walsh, 2006).

The hydrolytic cleavage of the peptide bond is thermodynamically favored (K_{eq} is about 10^5) under physiological conditions. Therefore, proteolysis is an irreversible posttranslational modification that is tightly controlled spatially and temporally. Failure of proper regulation leads to apoptotic cell death intracellularly and tissue destruction extracellularly.

Proproteins are synthesized as the inactive precursors of proteins and undergo proteolytic post-translational modifications for proper function. Proproteins that are synthesized in one compartment are transported to another compartment for activation, where they undergo proteolytic processing by a specific protease. The mechanism of proteolytic cleavage depends on the substrate, location and the protease. There are more than 11,000 proteases among species and most of them are highly specific for their substrates. Proteases can be classified according to their site of action (attacking amino

terminus, carboxy terminus or inter peptide bonds of substrates) or by their catalytic mechanism. According to the catalytic mechanism classification there are four major categories: aspartic acid proteases, metallo proteases, cysteine proteases, serine proteases (Puente et al., 2003).

One major group of serine proteases is the proprotein convertase (PC) family. They are calcium dependent serine endoproteases with conserved signal peptides, pro-regions, catalytic and P-domains. Their C-terminal regions play a role in subcellular routing. Proprotein convertases are activated by the autocatalytic cleavage of the N-terminal propeptide followed by the release of prodomain and proper folding for their enzymatic activity. They assist protein maturation through proteolytic cleavage as proteins pass through the secretory pathway.

Proprotein convertases cleave at multibasic recognition sites with the general motif (K/R)-$(X)_n$-(K/R) ↓ , where X is any amino acid except Cys, and n = 0, 2, 4, or 6. There are seven proprotein convertases known to date, namely: PC1/3, PC2, Furin, PACE4, PC4, PC5/6, and PC7 (Nakayama, 1997; Seidah and Chretien, 1999). It is predicted that still many unidentified proteases participate in the proteolytic cleavage of proteins (Zhou et al., 1999). Hopefully, their discovery will reveal the underlying reasons for many unexplained proteolytic cleavages.

Among proprotein convertases, Furin is the best understood. Furin is expressed in the trans-Golgi network, endosomal secretory compartments and plasma membrane. After the intramolecular cleavage of prodomain, furin exits the endoplasmic reticulum (ER). When furin reaches the trans-Golgi network (TGN) the calcium-enriched, acidic

pH conditions lead to a second cleavage that releases the prodomain and activates the enzyme (Anderson et al., 1997; Thomas, 2002).

Proprotein convertases are ubiquitously expressed in many tissues such as gut, liver, kidney, brain and neuroendocrine system. Among many of their physiological roles, malfunctioning of the proprotein convertases leads to disease states such as cancer, diabetes, lipid disorders, obesity, atherosclerosis, infectious diseases and neurodegenerative diseases (Scamuffa et al., 2006). Proprotein convertases have a variety of functions and show promise as therapeutic targets (Seidah and Chretien, 1999).

Part VII: N-linked Glycosylation of Proteins

Historia:

Protein glycosylation is the covalent attachment of mono-, oligo-, or polysaccharides to proteins, forming glycoconjugates called glycoproteins. The sugar containing portion of a glycoprotein is made up of complex heteropolymers known as glycans. Glycans are composed of monosaccharides with related chemical structure like hexoses that include glucose (Glc), mannose (Man), galactose (Gal), N-acetylglucosamine (GlcNAc), N-acetylgalactosamine (GalNAc) in the D configuration and other modified forms of simple hexoses like glucuronic acid (GlcA), xylose (Xyl), fucose (Fuc) and sialic acids like N-acetylneuraminic acid (NeuAc). These monomers

form oligo- or polysaccharides through glycosidic linkages. A glycosidic linkage is formed when a monosaccharide at the hemiacetal of the ring conformation reacts with a hydroxyl group of another monosaccharide. Glycosidic bond formation is an energetically unfavorable process and the free energy required is generated by coupling the reaction to the energetically favorable hydrolysis of nucleotide triphosphate and with the help of glycosyltransferases (GTFs). A glycosyltransferase is specific for the nucleotide sugar donor and the acceptor. Both making and breaking of glycosidic linkages are parts of the glycosylation process. Glycosidases catalyse the hydrolysis of glycosidic linkages and this reaction is energetically favorable. Glycosidases are also specific for glycosidic linkages involving a particular sugar. To date there is no established structure-function relationship for glycan addition to proteins. Glycans are assembled without any template and they do not have a unique folded structure (Taylor and Drickamer, 2006).

Glycans modify the structure and function of membrane proteins and secreted proteins. In eukaryotes, the majority of proteins that are synthesized in the rough endoplasmic reticulum are glycosylated. Also, certain glycans are added to proteins in the cytoplasm and nucleus. For some proteins, these carbohydrate side chains are essential for proper folding, and with some secreted glycoproteins they enhance protein stability. In addition to these structural roles, glycans serve as tags in glycoprotein trafficking, target glycoproteins to the appropriate luminal compartments and play a part in a series of quality-control checks. They also modulate protein-protein interactions and

protect against proteolysis. Glycosylation of some membrane proteins can be essential for cell-cell adhesion.

1–2% of the total number of human genes encode oligosaccharyltransferases, glycosyltransferases, glycosidases, lectins, and many other proteins directly involved in glycan assembly (Kikuchi and Narimatsu, 2006; Narimatsu, 2006). To date over 40 human congenital diseases have been associated with glycogene mutations and many more remain to be discovered (Schachter and Freeze, 2009). Inherited diseases related to glycan biosynthesis are quite heterogeneous. Patients with carbohydrate-deficient glycoprotein syndromes (CDGS), leukocyte adhesion deficiency syndrome II (LAD II), congenital dyserythropoietic anemia type II (HEMPAS), galactosemia, and abnormalities in proteoglycan synthesis suffer from malfunction of multiple organ systems (Varki et al., 2009). In cancer cells, glycosylation is altered and these changes are used as markers for tumor progression (Dall'olio, 1996).

There are three classes of glycosylation: **C**-linked glycosylation where glycans are attached to a **carbon** on a tryptophan side chain; **O**-linked glycosylation - glycans are attached to the hydroxy **oxygen** of serine, threonine, tyrosine, hydroxylysine or hydroxyproline side chains; **N**-linked glycosylation where glycans are attached to the **nitrogen** of asparagine (and very rarely to the nitrogen of arginine side chains). ***C-linked glycosylation (C-mannosylation)***: The C-1 atom of a single mannose residue is added in an α-linkage to the C-2 atom of the indole ring of tryptophan at specific sites in proteins (Furmanek and Hofsteenge, 2000). Potentially there are over 335 mammalian proteins that are C-mannosylated (Krieg et al., 1998). Though C-mannosylation is a highly

common protein modification, not much is known about its function. ***O-linked glycosylation***: O-glycosylation occurs in the Golgi apparatus. The hydroxyl side chain of serine and threonine residues of proteins serve as nucleophiles to form a sugar-O-protein bond. In higher eukaryotes the donors for O-linked proteins are sugar nucleotides like UDP-Gal, UDP-GalNAc, GDP-Fuc, UDP-Glc, UDP-GlcNAc (Ten Hagen et al., 2003). O-linked glycan addition is catalyzed by a family of glycosyltransferases. There are two major groups of proteins that are heavily O-glycosylated: mucins and proteogylcans. Mucins are large proteins that hold water. They are present at the surfaces of the digestive and genital tracts and respiratory system (Taylor and Drickamer, 2006). Proteoglycans like mucins are heavily O-glycosylated proteins. Proteoglycans give strength to the extracellular matrix and they serve as co-receptors for growth factors on the plasma membrane (Taylor and Drickamer, 2006). O-linked glycans provide resistance to thermal change, protect from proteolytic attack; assist protein sorting and function as ligands for receptors (Ten Hagen et al., 2003).

N-linked glycosylation of Proteins:

N-linked glycosylation is a form of co-translational and a series of post-translational modifications. In eukaryotes N-Glycosylation starts with the addition of a 14-sugar precursor to the asparagine residue in the protein as the growing nascent polypeptide chain comes out of the translocon (Figure 1.9 and Figure 1.10). In the

human genome, more than half of all the proteins are N-glycosylated (Apweiler et al., 1999).

Much of the N-linked glycosylation machinery is conserved in eukaryotes. N-glycosylation has an assembly pathway and a processing pathway. Three cellular compartments are involved in N-glycan addition and maturation: the cytosol, the endoplasmic reticulum (ER) and the Golgi. In the cytoplasmic face of the ER membrane the precursor glycan donor is made through a complex set of reactions in which the 14 monosaccharide residues (the two GlcNAcs and five mannoses) are put together with the help of membrane enzymes, UDP-GlcNAc and GDP mannose donors. These sugars are assembled on dolichol, a polyisoprenoid lipid carrier, which anchors the growing sugar chain to the ER membrane. Later, this heptasaccharyl-PP-dolichol intermediate is flipped to the ER membrane lumenal side by the Rft1 protein (Helenius et al., 2002). The next seven sugars are added on the lumenal side of the ER membrane. Sugar donors are mannose-P-dolichol and glucose-P-dolichol; the Alg (**A**sparaginyl-**l**inked-**g**lycan) enzymes catalyze the incremental build up of core lipid-linked oligosaccharide, $Glc_3Man_9GlcNAc_2$-PP-dolichol (Burda and Aebi, 1999). The structure of these core glycans are conserved in most eukaryotes (Figure 1.9). High mannose oligosaccharides of the $Glc_3Man_9GlcNAc_2$-PP-dolichol are then transferred onto selected asparagines of the nascent protein as it is translocated into the ER lumen. The transfer is catalyzed through the enzymatic action of the oligosaccharyltransferase (OST) complex that recognizes the consensus glycosylation site (sequon) on the protein.

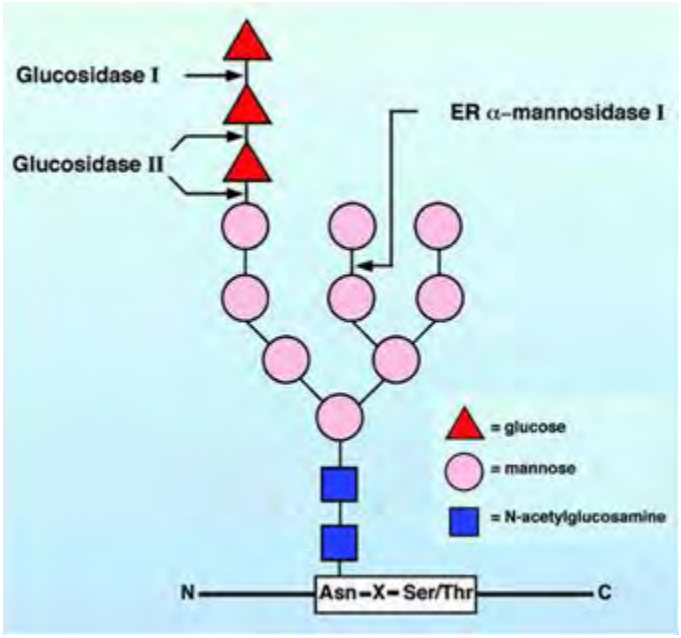

Figure 1.9: **The N-linked core oligosaccharide ($Glc_3Man_9GlcNAc_2$-)**. In the ER, the core oligosaccharides are transferred onto proteins through formation of an N-glycosidic bond with the side chain of an asparagine that is part of the Asn-X-Ser/Thr consensus sequence on the protein. Glucosidases remove the terminal glucose residues and mannosidases remove central terminal mannose residue in the ER. The symbols for the different sugars are indicated on the right (Helenius and Aebi, 2001).

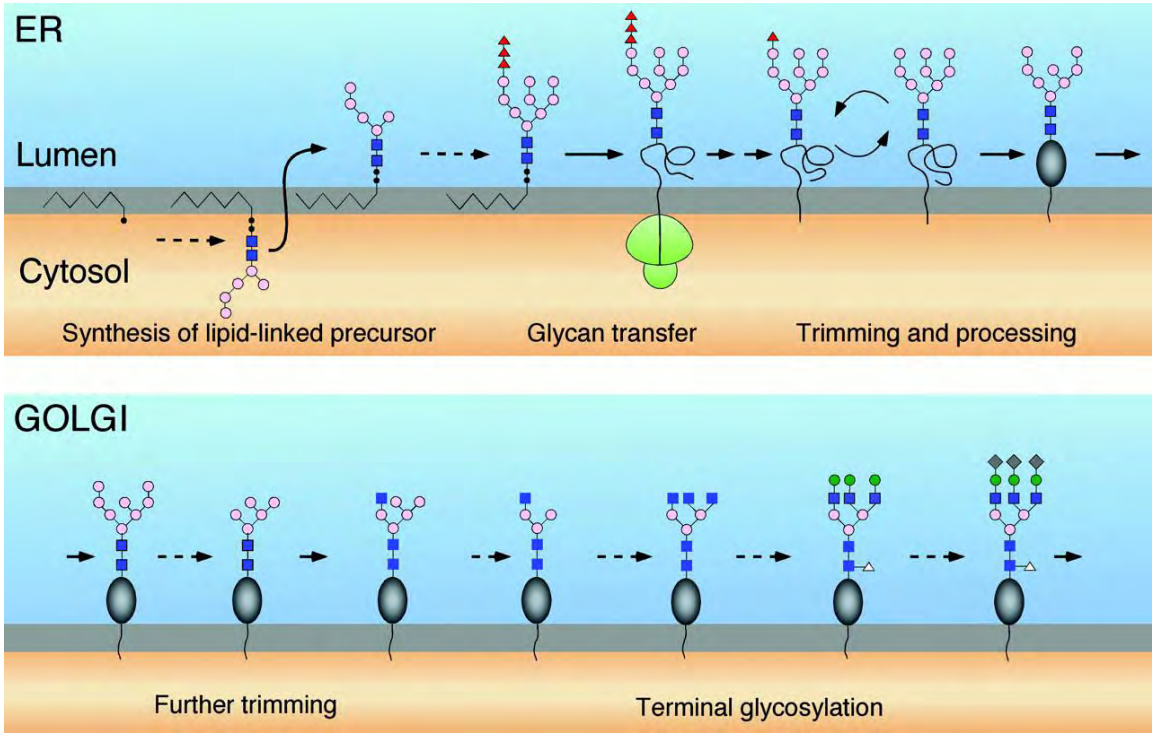
ER
Lumen
Cytosol
Synthesis of lipid-linked precursor
Glycan transfer
Trimming and processing
GOLGI
Further trimming
Terminal glycosylation

Figure 1.10: Synthesis and maturation of N-linked core oligosaccharides in the secretory pathway. Oligosaccharide synthesis starts on the cytosolic surface of the ER membrane. ALG7 catalyzes the addition of GlcNAc-P to Dol-P. Next 6 more sugars are added to this Dol-PP-carrier. After the addition of two N-actetylglucosamines and five mannoses, the oligosaccharides are flipped to the lumenal side of the membrane and four more mannose residues are attached followed by the addition of three glucoses forming the core glycan (Figure 1.9). Oligosaccharyltransferase enzyme complex catalyzes the transfer of the core oligosaccharide complex onto the asparagine residues of the nascent polypeptide chains. After a series of deglucosylation and reglucosylation steps properly folded proteins leave the ER and traffic through the secretory pathway. In the Golgi oligosaccharides undergo further trimming and terminal glycosylation steps. Unlike the ER homogeneous ER glycoforms, Golgi-generated glycoforms are highly diverse (Helenius and Aebi, 2001). The symbols for the different sugars are: red triangle: glucose, pink circle: mannose, blue square: N-Acetylglucosamine, white triangle: fucose, green circle: galactose, black diamond: sialic acid.

Traditionally, N-linked glycosylation was believed to be a cotranslational process. As the nascent peptide chain passes through the translocation channel (Sec61 complex) and enters the lumen of rough endoplasmic reticulum (RER), the OST complex recognizes the sequon, NXT/S (where X can be any amino acid other than proline). Then, OST complex transfers the high mannose oligosaccharides cotranslationally as long as the sequon is 65-75 residues away from the peptidyl-transferase site on the large ribosomal subunit (Chen et al., 1995; Whitley et al., 1996). Recently, posttranslational N-glycosylation of human coagulation factor VII (FVII) was shown in several mammalian cell lines (Bolt et al., 2005).

Mammalian OST is a heteromultimeric complex that is made up of eight proteins. In yeast the OST complex is made up of single copies of the following proteins: Ost1p, Ost2p, Ost3p or Ost6p, Ost4p, Ost5p, Wbp1p, Swp1p, and Stt3p (Kelleher and Gilmore, 2006). Vertebrate, plant, and insect genomes encode two STT3 isoforms: STT3A and STT3B (Kelleher et al., 2003). The STT3 proteins are directly involved in the catalytic activity of the OST complex (Yan and Lennarz, 2002). Recently, it has been demonstrated that STT3A is primarily responsible for the cotranslational glycosylation of the nascent polypeptide chain as it enters to the ER lumen; whereas STT3B is important for both cotranslational glycosylation, and it can mediate posttranslational glycosylation (Ruiz-Canada et al., 2009).

After the transfer of the oligosaccharide core onto the Asn residues, the newly formed glycoprotein is further processed in the ER (Walsh, 2006). ER lumen glucosidases, glucosidase I and glucosidase II, act sequentially to remove the three

terminal glucoses and transfrom the initial N-glycan chain ($Glc_3Man_9GlcNAc_2$- Asn-Protein) to $Man_9GlcNAc_2$-Asn-Protein (Parodi, 2000b). During this hydrolytic trimming process, the intermediate form $GlcMan_9GlcNAc_2$- Asn-Protein serves as a handle for soluble ER protein chaperone, calreticulin and the ER membrane-associated protein chaperone, calnexin. Calreticulin and calnexin act in an ER quality control mechanism and monitor proper protein folding by recognizing the terminal glucose of the oligosaccharide (Parodi, 2000b). At this point the glycoproteins enter a cycle of deglucosylation (glucosidase II) and reglucosylation (UDP-glucose glycoprotein glucosyltransferase) ensuring the proper folding of the glycoproteins during the process (High et al., 2000; Parodi, 2000a; Roth, 2002). During this cycle, hopelessly misfolded proteins are shipped to the cytoplasm and their glycans are removed by protein glycanase N. Next, misfolded proteins are ubiquitinylated and sent to the proteasome for degradation. Meanwhile, properly folded $Man_9GlcNAc_2$-Asn-proteins are passed on to Golgi complex for further processing (Figure 1.10) (High et al., 2000; Trombetta and Parodi, 2003; Walsh, 2006).

In the cis Golgi compartment, hydrolytic trimming of the core glycans continues by mannosidases and $Man_3GlcNAc_2$-(Asn-proteins) is the final dominant oligosaccharide in higher eukaryotes at this stage (Trombetta, 2003). In the medial- and trans-Golgi, trimming ceases and re-building starts. Glycosyltransferases residing in these compartments build the outer branches of the glycans by adding monosaccharides such as N-acetylglucosamines, galactoses, N-acetylgalactosamines, fucoses and sialic acids, producing diverse final products. A glycoprotein can have different compositions of

glycans, known as glycoforms, leading to a heterogeneous population of a single polypeptide. Though the extent of this heterogeneity varies from protein to protein, a glycoprotein with multiple glycosylation sites can have as many as 100 glycoforms, yet only a few of them predominate (Taylor and Drickamer, 2006).

The core glycan assembly and trimming reactions in the ER are highly conserved in higher eukaryotes; and the differences among species are observed in the late stages of glycan chain maturation. There are three main classes of N-linked glycans resulting from the core oligosaccharides, $Glc_3Man_9GlcNAc_2$- (Asn-Protein): high-mannose oligosaccharides, complex oligosaccharides and hybrid oligosaccharides (Taylor and Drickamer, 2006). High-mannose oligosaccharides have many mannose residues in addition to the two N-acetylglucosamines just like the core glycans. Complex oligosaccharides contain many other types of saccharides. Hybrid oligosaccharides are the combination of both. After the initial trimming in the ER, the fate of the core glycan is determined by its accessibility to the glycan modifying enzymes in the Golgi compartments. The more accessible the saccharides are the more modifications they will get; hence they will become more complex.

The functions of N-linked glycosylation can be divided into two broad categories: physico-chemical functions and biological functions. Physico-chemical functions (Shental-Bechor and Levy, 2009) include altering the glycoprotein's electrical charge, mass, size and viscosity in solution; effecting protein solubility; controlling protein folding; stabilizing protein conformation; providing thermal stability and protecting against proteolysis. Biological functions are regulating intracellular trafficking and

localization of glycoproteins; determining the lifetime of glycoproteins in circulation; modifying immunological properties; modulating activity of enzymes and hormones; participating in cell-cell interactions and acting as cells surface receptors for lectins, antibodies and toxins, etc. (Lis and Sharon, 1993).

Disturbances in the assembly or processing of N-glycans lead to diseases that belong to the congenital disorders of glycosylation (CDG). The mutant CDG genes discovered thus far lead to a reduction in the amount of fully assembled Dol-PP-$GlcNAc_2Man_9Glc_3$, causing abnormalities in a large group of glycoproteins (Jaeken and Carchon, 2000). Congenital disorders of glycosylation are multisystem diseases and allele severity effects the patient phenotype immensely. The list of CDGs is growing and some of the known disorders of N-glycan assembly include: CDG-Ia, (phoshomannomutase (PMM) deficiency); CDG-Ib (phoshomannose isomerase deficiency); CDG-Ic (glucosyltransferase I deficiency); CDG-1d (mannosetransferase VI deficiency); CDG-Ie (dolichol-phosphate-mannose synthase-1 deficiency); CDG-If. CDG-1a, CDG-1c, CDG-1d, CDG-1e are all neurological diseases. CDG-Ib is a hepatic-intestinal disease. CDG-If results in developmental problems and neurological defects. Disorders of N-glycan processing include: CDG-IIa (N-acetylglucosaminyltransferase II deficiency); CDGIIb (Glucosidase I deficiency); GDP-fucose transporter defect. CGG-IIa results in neurological diseases; CDG-IIb causes severe developmental problems, generally with a fatal outcome in newborns. GDP-fucose transporter defect causes developmental problems and neurological defects (Jaeken and Matthijs, 2001).

Part VIII: N-linked glycosylation and KCNE1

Asparagine-linked (N-linked) glycosylation is important for assembly, trafficking and stability of some K^+ conducting subunits. Most ion channels and their auxiliary subunits are N-glycosylated and the functional role of N-glycan addition varies dramatically among proteins. Glycosylation can modify the elementary properties of some channels and increase functional diversity (Watanabe et al., 2003) . At the same time glycosylation can modulate channel function through effecting its assembly and trafficking (Khanna et al., 2001; Khanna et al., 2004; Cotella et al., 2010; Egenberger et al., 2010; Hegle et al., 2010).

The extracellular N-terminus of KCNE peptides contain at least one and up to three consensus sequences for N-linked glycosylation (Figure 1.4***A***) (Abbott and Goldstein, 2001; McCrossan and Abbott, 2004). The glycosylation site nearest to the N-terminus (within 10 residues) is absolutely conserved in all mammalian KCNE peptides. E1 has two N-linked glycosylation consensus sites at residues N5 and N26, both of which are glycosylated in native tissues (Finley et al., 2002). Structure-function studies have shown that the minimal KCNE1 includes the first glycosylation site, which is essential for KCNQ1-KCNE1 complex formation and function (Takumi et al., 1991; Abbott and Goldstein, 1998; Freeman et al., 2000). Moreover, the JLNS mutation, T7I, prevents glycosylation at the first N-linked glycosylation site on E1 (Schulze-Bahr et al., 1997). An SNP in the equivalent threonine in KCNE2 (T8A) provokes drug-induced LQTS with

the commonly prescribed antibiotic, sulfamethoxazole (Sesti et al., 2000b; Park et al., 2003).

The two glycosylation sites on KCNE1 (N5 and N26) are conserved in all mammals (Figure 1.4***B***). However, only mutations in the first sequon (first sequon is also conserved among the KCNE family (Figure 1.4***A***)), are capable of causing Long QT Syndrome. Structure-function deletion scans have demonstrated residues between 1-9 (encompassing the first sequon) and 40-94 are indispensable for KCNE1 function. Surprisingly, despite the intriguing possible role of the first N-linked glycosylation site in KCNQ1/KCNE1 channel trafficking and function, little is known about either of the KCNE1 sequons. I will present the requirements for KCNE1 trafficking and cell surface expression in Chapter II and Appendix II. I will then explain the relative importance of the two consensus N-linked glycosylation sites on KCNE1 in Chapter III. Finally, I will present additional structural and functional data showing a likely pattern that could explain the relative importance of the first glycosylation site in Chapter IV.

CHAPTER II

KCNE1 subunits require co-assembly with K^+ channels for efficient trafficking and cell surface expression*

Contributors to the work presented in Chapter II:

The author of this thesis, Tuba Bas constructed and characterized the C-terminally HA tagged KCNE1 peptide that allowed the authors to observe the cell surface expression and membrane localization of KCNE1 in immunostaining experiments. Kshama D. Chandrasekhar performed the experiments.

* Chandrasekhar, K. D., Bas, T., and Kobertz, W. R. 2006. KCNE1 subunits require co-assembly with K^+ channels for efficient trafficking and cell surface expression. *J Biol Chem*. 281: 40015-40023.

ABSTRACT

KCNE peptides are a class of type I transmembrane β-subunits that assemble with and modulate the gating and ion conducting properties of a variety of voltage-gated K^+ channels. Accordingly, mutations that disrupt the assembly and trafficking of KCNE-K^+ channel complexes give rise to disease. The cellular mechanisms responsible for ensuring that KCNE peptides assemble with voltage-gated K^+ channels have yet to be elucidated. Using enzymatic deglycosylation, immunofluorescence, and quantitative cell surface labeling experiments, we show that KCNE1 peptides are retained in the early stages of the secretory pathway until they co-assemble with specific K^+ channel subunits; co-assembly mediates E1 progression through the secretory pathway and results in cell surface expression. We also address an apparent discrepancy between our results and a previous study in human embryonic kidney cells, which showed wild type KCNE1 peptides can reach the plasma membrane without exogenously expressed K^+ channel subunits. By comparing KCNE1 trafficking in three cell lines, our data suggest that the errant E1 trafficking observed in human embryonic kidney cells may be due, in part, to the presence of endogenous voltage-gated K^+ channels in these cells.

INTRODUCTION

Voltage-gated K^+ channels have diverse physiological roles ranging from repolarization of excitable tissues to salt and water homeostasis in epithelial cells. To achieve such functional diversity, many K^+ channels function as membrane-embedded complexes made up of pore-forming α-subunits and tissue-specific regulatory β-subunits. The KCNE type I transmembrane peptides are a class of small β-subunits that assemble with and modulate the function of several types of voltage-gated K^+ channels (McCrossan and Abbott, 2004). KCNE1 (E1) is the founding member of the family and has been shown to form complexes with Kv3.1, Kv3.2, Kv4.2, Kv4.3, HERG, and KCNQ1 (Q1) K^+ channels (Barhanin et al., 1996; Sanguinetti et al., 1996; McDonald et al., 1997; Zhang et al., 2001; Deschenes and Tomaselli, 2002; Lewis et al., 2004). When E1 assembles with Q1, the complex produces the slowly activating cardiac I_{Ks} current and is the exclusive pathway for endolymphatic K^+ recycling in apical membranes of strial marginal and vestibular dark cells (Marban, 2002; Wangemann, 2002). Conversely, unpartnered Q1 channels are ill-equipped to perform either function because they open and close too quickly to maintain the rhythmicity of the heartbeat and are significantly inactivated and nonconducting at the resting membrane potential of inner ear cells (Pusch et al., 1998). The biological importance of the proper Q1-E1 complex formation is further underscored by the inherited mutations in either Q1 or E1 that disrupt the

assembly and/or trafficking of the complex and give rise to cardiac arrhythmias, most notably long QT syndrome (Splawski et al., 2000). An autosomal recessive form of long QT syndrome also causes neural deafness (Tyson et al., 2000).

Although proper K^+ channel function requires completely assembled complexes at the plasma membrane, the cellular mechanisms that ensure K^+ channel α-subunits combine with membrane-embedded β-subunits are starting to be elucidated. For the ATP-sensitive K^+ channels (Kir6.1 and 6.2), which assemble with sulfonylurea receptors (sulfonylurea receptors 1/2A/2B) in a 4:4 stoichiometry, unpartnered channel and receptor subunits are stringently held in the endoplasmic reticulum (ER) via a RXR retention signal (Zerangue et al., 1999). Once an octameric complex is formed, the K_{ATP}-sulfonylurea receptor complex is permitted to exit the ER and traffic to the cell surface.

In contrast, E1 subunits in complexes with voltage-gated K^+ channels may traffic differently than their K_{ATP} counterparts. Two different studies suggest that Q1-E1 complex formation occurs at the plasma membrane, which would require both proteins to traffic through the secretory pathway independently (Romey et al., 1997; Grunnet et al., 2002). More recently, it was proposed that Q1-E1 assembly occurs in the ER because mutant E1 proteins could retain Q1 channels there (Krumerman et al., 2004). However, unpartnered wild type E1 proteins freely exited the ER and migrated to the cell surface, an observation inconsistent with an ER-based assembly. A significant caveat with all of the above studies was that KCNE trafficking was studied in either *Xenopus* oocytes or human embryonic kidney (HEK) 293B cells, both of which possess endogenous

transcripts of voltage-gated K^+ channels that have been shown to assemble with KCNE subunits (Sanguinetti et al., 1996; Jiang et al., 2002a).

Here, we examine the assembly and trafficking of wild type E1 subunits in the presence and absence of Q1 channels in Chinese hamster ovary (CHO) and African green monkey kidney (COS-7) cells, both of which are revered for their ~~–e~~lectrical tightness" or lack of measurable endogenous K^+ currents (Lesage et al., 1993). Using these cells, we find that the majority of E1 protein is localized to the ER when expressed alone. Co-expression with Q1 subunits promotes E1 protein trafficking through the secretory pathway, resulting in robust cell surface expression. Moreover, these results demonstrate that Q1-E1 complex formation occurs early in the secretory pathway and that unpartnered E1 subunits do not efficiently progress past the ER and *cis*-Golgi compartments until they assemble with Q1 channel subunits.

RESULTS

Active retention of unassembled membrane protein subunits is one mechanism by which a cell ensures that membrane-embedded K^+ channel complexes are properly assembled before the proteins arrive at their final cellular destination (Ellgaard and Helenius, 2003). Distinguishing cellular markers for ER-resident proteins are immature *N*-linked glycans. The ER utilizes these high mannose oligosaccharide handles to promote protein folding, oligomerization, quality control, retention, and trafficking (Helenius and Aebi, 2001). Once *N*-linked glycoproteins reach the Golgi, however, they are no longer subject to the rigorous quality control systems of the ER and migrate through medial and *trans*-Golgi compartments relatively unabated while acquiring complex modifications to their *N*-linked glycans (Helenius and Aebi, 2001). Because KCNE peptides have two well conserved *N*-linked glycosylation consensus sites, we utilized this hallmark of ER residency to determine the cellular locales of E1 peptides expressed alone, with Q1, and with KCNQ4 (Q4), a K^+ channel previously shown not to assemble with E1 (Figure 2.1) (Melman et al., 2004). Transient expression of E1 alone in CHO cells gave rise to two strong bands at 16 and 22 kDa (though faint, higher molecular mass bands can be seen on this intentionally well developed, but not overexposed Western blot). When expressed with Q4, a similar banding pattern was observed with an additional band at 19 kDa. In contrast, expression with Q1 affords an additional, higher molecular mass band at ~40 kDa. The presence of this 40-kDa band was independent of

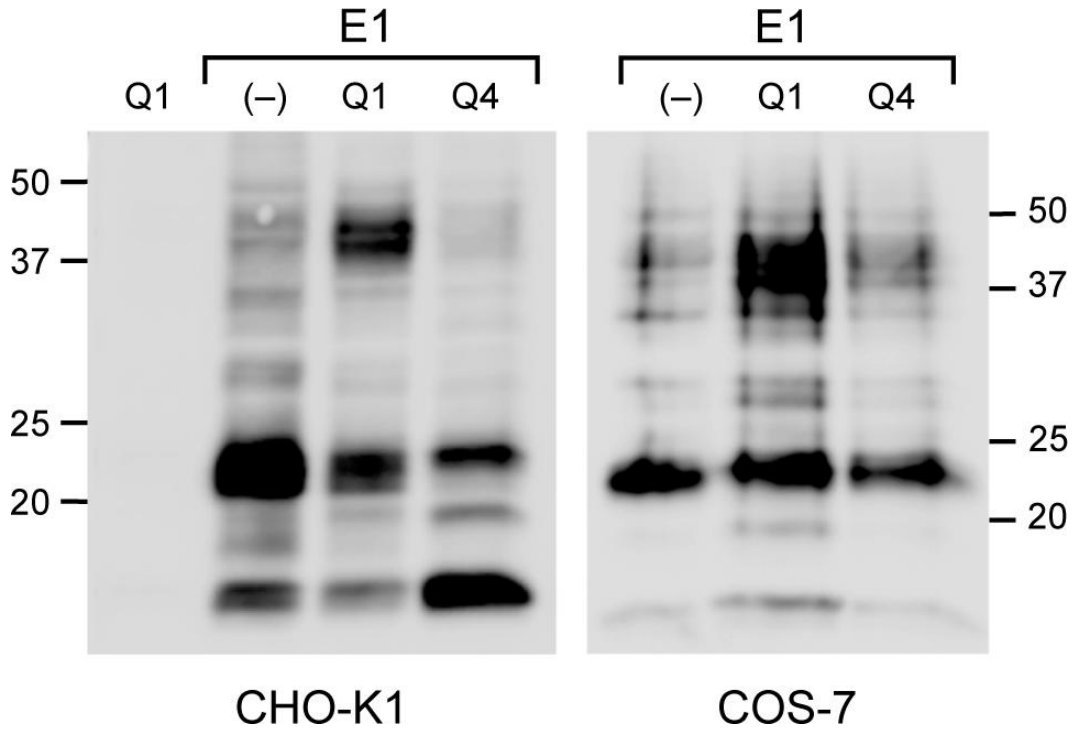
E1
E1
Q1
(–)
Q1
Q4
(–)
Q1
Q4
50
37
25
20
50
37
25
20
CHO-K1
COS-7

Figure 2.1: KCNE1 peptides migrate differently on denaturing gels when expressed with specific K^+ channel subunits. Immunoblots of HA-tagged E1 peptides from solubilized CHO cells or COS-7 cells transfected with Q1, E1, Q1/E1, or Q4/E1 DNA. Expression of E1 alone or with Q4 yields two intense bands at 16 and 22 kDa in CHO cells and one band at 22 kDa in COS-7 cells. Q1/E1 co-expression results in the appearance of an equally strong band at ~40 kDa. Q1 was transfected alone to serve as a negative control.

the detergent lysis mixture used but only occurred in abundance when E1 was co-expressed with Q1. The abundance of the higher molecular mass form of E1 was dependent on the ratio of Q1-E1 DNA used for transient transfection. Limiting amounts of Q1 DNA yielded all three forms of E1 protein as shown in Figure 2.1; optimizing the Q1-E1 DNA ratio (Experimental Procedures) afforded primarily the higher molecular mass species (Figure 2.2; see also (Figure 2.4). We also observed the same gel banding patterns for E1 in COS-7 cells (Figure 2.1).

The multiple bands and differences in gel shift mobility suggested that E1 peptides were differentially glycosylated depending on the presence of specific K^+ channel subunits. We therefore determined whether the gel shift mobility difference that was observed with Q1-E1 co-expression was due to maturation of the glycans on E1. The maturity of *N*-linked glycoproteins can be readily determined using two different glycosidases. Endo H is a glycosidase that removes the high mannose (immature) glycan found on ER and *cis*-Golgi proteins but is unable to process the complex (mature) glycoform once the protein reaches the medial Golgi in the biosynthetic pathway. In contrast, PNGase F is an endoglycosidase that removes all *N*-linked oligosaccharides. Treatment of the E1 samples with either Endo H or PNGase F reduced the 22-kDa band to 16 kDa, consistent with the loss of two immature glycans (Figure 2.2). Thus, when E1 is expressed alone, the majority of the *N*-linked glycan is immature; indicating that unpartnered E1 is localized to the ER and/or *cis*-Golgi. Enzymatic deglycosylation of the Q1-E1 sample afforded a different result. Treatment with Endo H had no effect on the higher molecular mass band. However, the two faint bands centered at ~20 kDa collapsed

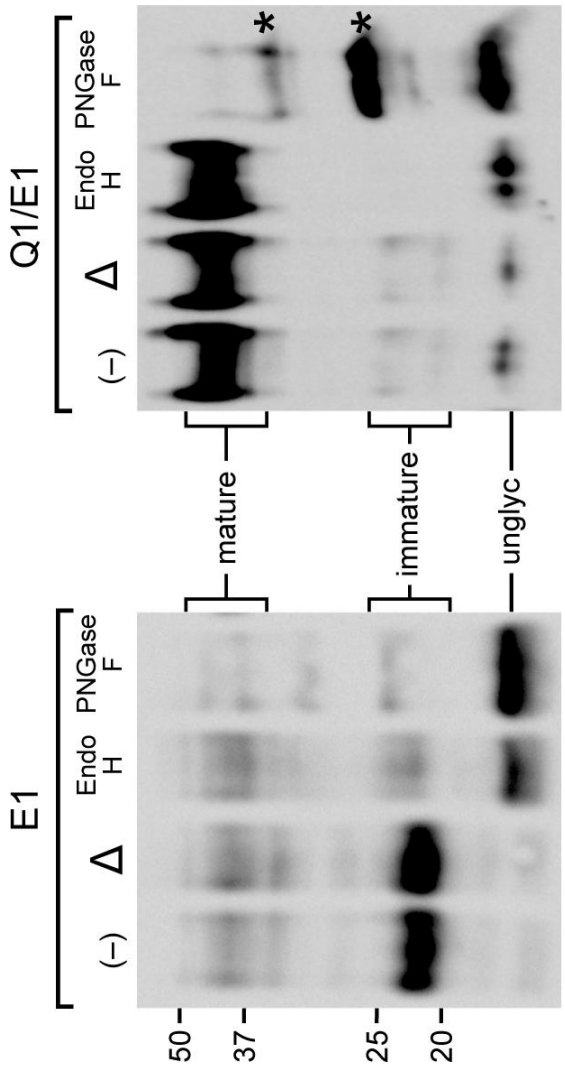
E1
Q1/E1
(–)
Δ
Endo H
PNGase F
mature
immature
unglyc
*
*
50
37
25
20

Figure 2.2: KCNE1 glycopeptides are predominantly immature until they assemble with KCNQ1 subunits. Immunoblot of enzymatic deglycosylation of E1 *N*-linked glycopeptides in the presence and absence of expressed Q1. The samples were left untreated (–), heat-treated (Δ) to 95°C for 5 min, digested with Endo H, or PNGase F and separated by SDS-PAGE (15%). Mature, immature, and unglycosylated (*unglyc*) samples are indicated as determined by enzymatic deglycosylation. Asterisks (*) denote PNGase F digestion products that consistently migrated slower than immature and unglycosylated protein, which may be due to an additional post-translational modification.

to the unglycosylated form (16 kDa), identifying these two bands as E1 glycoproteins with one and two immature glycans. Heating the samples (95 °C for 5 min) did not effect any of the bands, suggesting that the higher molecular mass band was not due to protein aggregation. All of the glycosylated forms of E1, however, were susceptible to PNGase F treatment, indicating that the higher molecular mass form of E1 possessed mature *N*-linked oligosaccharides. Because maturation of *N*-linked glycoproteins occurs in the medial and *trans*-Golgi, the presence of mature glycans in only the Q1-E1 sample shows that co-assembly with Q1 facilitates E1 peptide progression through the secretory pathway. Although the PNGase F-treated E1 protein was deglycosylated, several residual bands were observed (indicated by the *asterisks*). Prolonged treatment with PNGase F, the addition of more enzyme, varying the concentration of SDS in the gel loading buffer, or heat denaturation did not change the intensity or mobility of these bands (data not shown). The residual banding is not partial digestion of the individual *N*-linked glycans because PNGase F directly cleaves the oligosaccharide from the peptide backbone (Lemp et al., 1990). It is possible that one of the two mature *N*-linked glycans on E1 is totally inaccessible to the enzyme; however, we have observed these similar bands with PNGase F-treated E1 mutants that possess only one *N*-linked glycosylation site (data not shown). These bands do not correspond to immature E1, because they have a slightly slower mobility that can be readily observed in either the E1 or the Q1-E1 PNGase F-treated samples. Moreover, PNGase F treatment of the E1 sample demonstrates that this enzyme cleaves both immature *N*-linked glycans efficiently. These additional bands were also resistant to a subsequent phosphatase or neuraminidase (to

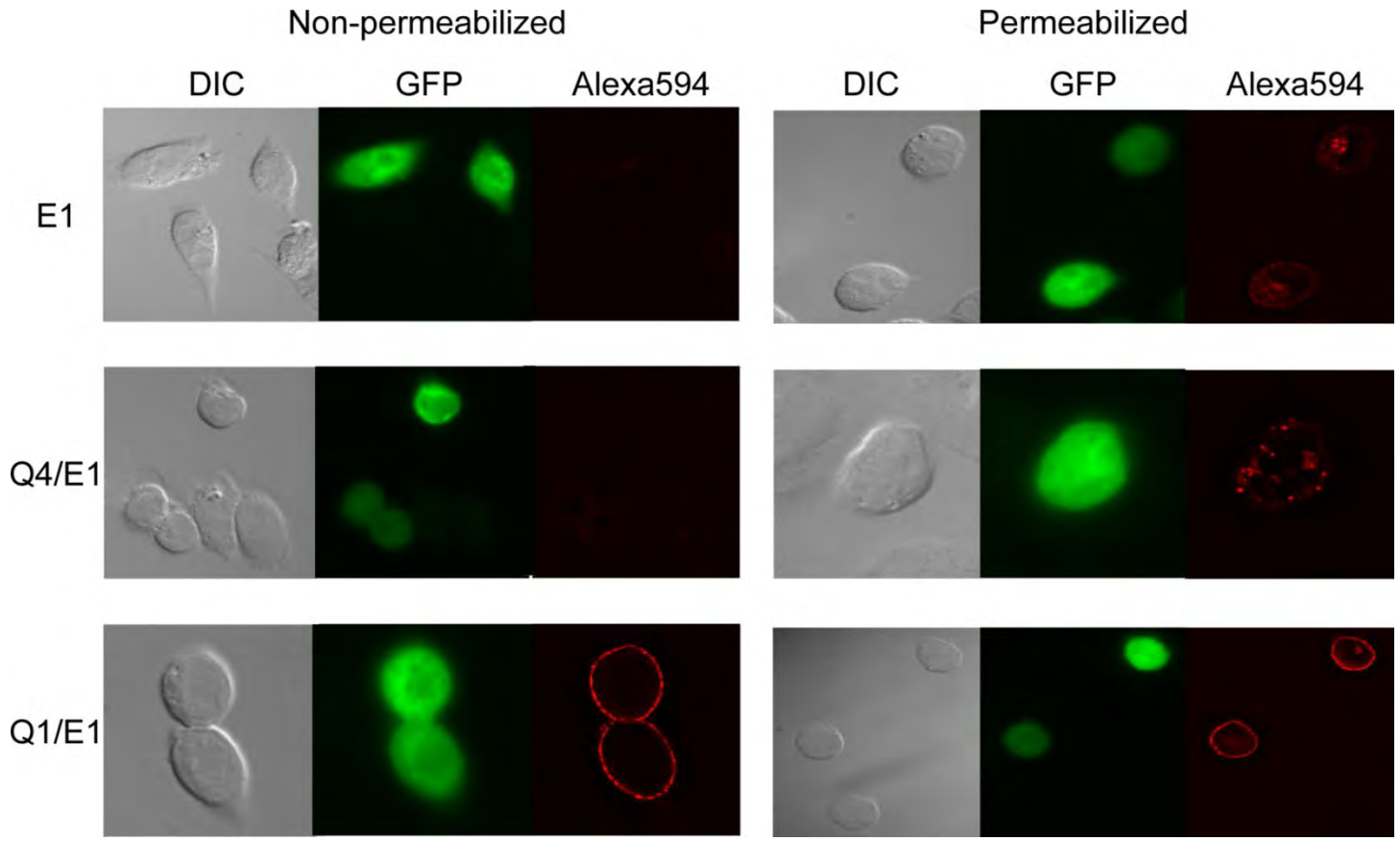
Non-permeabilized
Permeabilized
DIC
GFP
Alexa594
DIC
GFP
Alexa594
E1
Q4/E1
Q1/E1

Figure 2.3: Cell surface expression of KCNE1 requires co-expression with K^+ channel subunits that assemble with KCNE peptides. Cell surface immunostaining of E1 expressed alone or with Q4 or Q1 in CHO cells is shown. The cells were fixed and left intact to visualize cell surface staining or permeabilized to visualize total cellular staining. The images shown are single 0.4-μm planes through the center of each cell. Differential interference contrast (DIC) images show both untransfected and transfected cells. Green fluorescent protein (*GFP*) images identify transfected cells. Alexa 594 images show E1 protein staining with Alexa 594-conjugated antibodies. The fluorescent images were captured using the same exposure time and rendered identically to qualitatively compare the fluorescent intensities between panels. Note the strong cell surface staining for the Q1/E1 panels (non-permeabilized and permeabilized), whereas the E1 and Q4/E1 permeabilized panels show mostly punctate staining, indicative of intracellular distribution.

remove sialic acid residues from *O*-linked glycans) treatment (data not shown) and may be due to the presence of another type of post-translational modification.

Because maturation of *N*-linked glycans on E1 requires co-expression with Q1, we determined whether cell surface expression of E1 was also dependent on expression with specific K^+ channel subunits. Cell surface expression of E1 protein was visualized by immunofluorescence with permeabilized and nonpermeabilized cells using an extracellularly HA-tagged version of E1 (Wang and Goldstein, 1995). In nonpermeabilized cells, no cell surface labeling of E1 was observed when E1 was expressed alone or with Q4 (Figure 2.3, *E1* and *Q4/E1 panels*). Co-transfection with green fluorescent protein DNA verified that the absence of cell surface staining was not a result of untransfected cells. Permeabilization of the cells confirmed that the majority of the E1 protein was intracellular, as evidenced by the punctate staining. In contrast, co-expression with Q1 resulted in striking cell surface staining of E1 in intact and permeabilized cells (Figure 2.3, *Q1/E1 panels*).

The plasma membrane protein levels of E1 were then quantitated by cell surface biotinylation. To minimize labeling of intracellular proteins and membrane recycling, cells expressing E1 with or without Q1 were labeled with a membrane-impermeant, amine-reactive biotin derivative at 4 °C. When co-expressed with Q1, E1 shows robust cell surface expression Figure 2.4*A*. Moreover, no immature E1 was ever observed on the plasma membrane, which is consistent with the enzymatic deglycosylation assays Figure 2.2. Little to no protein was observed at the cell surface when E1 was expressed alone. To account for cell rupture during biotinylation, the ER-resident protein calnexin

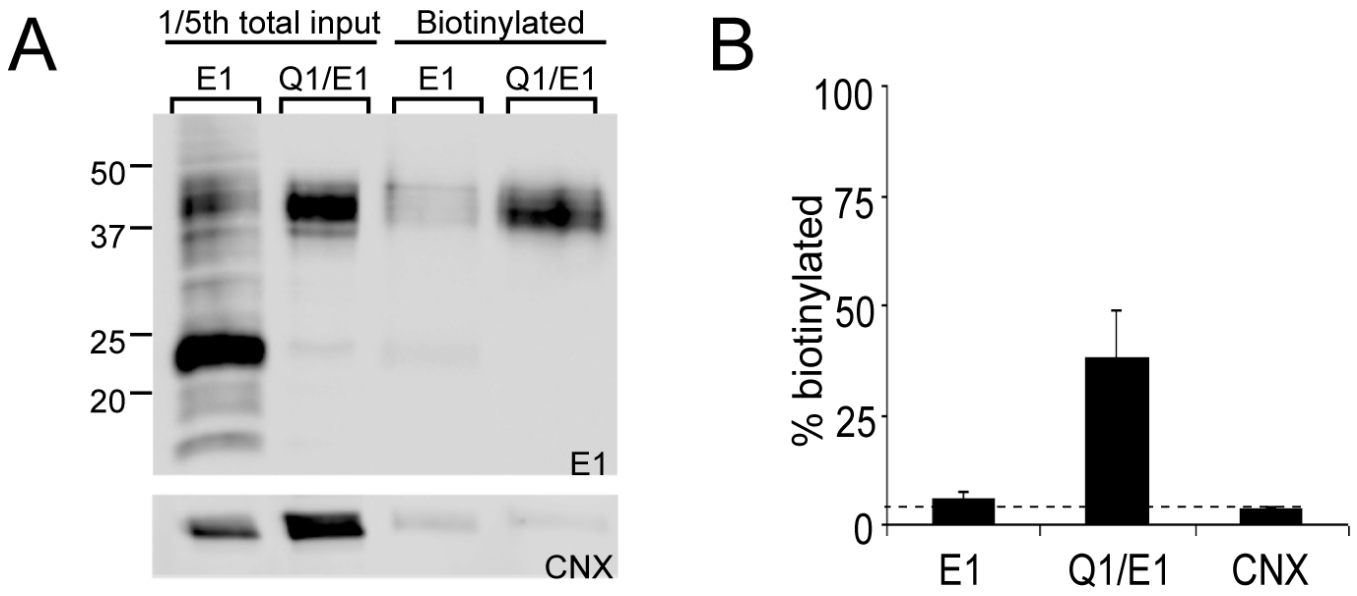
A
1/5th total input
Biotinylated
E1
Q1/E1
E1
Q1/E1
50
37
25
20
E1
CNX
B
100
75
50
25
0
% biotinylated
E1
Q1/E1
CNX

Figure 2.4: Quantification of the KCNE1 plasma membrane protein by cell surface biotinylation. (***A)*** a representative immunoblot of E1 expressed in CHO cells with and without Q1 channel subunits. Transfected cells were labeled with a membrane-impermeant biotin reagent and subsequently lysed, and the biotinylated proteins were isolated from 75μg of total protein. Lanes identified as one-fifth of the total input are 15μg of each sample lysate that was set aside to quantitate the total amount of biotinylated proteins. Biotinylated lanes are the streptavidin-bound proteins that were eluted from the beads and separated by SDS-PAGE (15%). The calnexin (*CNX*) immunoblot shows that the majority of the cells remained intact during the biotinylation procedure. (***B***) quantification of the biotinylated E1 proteins. The percentage of biotinylated protein was calculated by dividing the band intensities in the biotinylated lane by the band intensities in the one-fifth total input lane, which were multiplied by five. There was no significant difference between background calnexin labeling and cell surface labeling of E1 when the peptide was expressed alone. Co-expression with Q1 results in 34±11%E1 protein on the cell surface after subtracting for background cell lysis (calnexin control).The *error bars* are standard error measurement (S.E.M.) from three immunoblots. The *dotted line* indicates background biotinylation, which was calculated from calnexin staining (4±1%).

was used as an internal control in all experiments. The percentage of E1 protein at the cell surface was quantitated as a ratio of biotinylated proteins over the total protein input shown in Figure 2.4*B*. For Q1-E1, ~35% of E1 protein was at the cell surface after background subtraction. For E1 alone, the percentage of protein detected on the cell surface by biotinylation was within error of background calnexin labeling.

Because E1 does not reach the plasma membrane when it is expressed alone, we determined its intracellular localization. Results from enzymatic deglycosylation (Figure 2.2) narrow the spectrum of intracellular locales to the ER and/or *cis*-Golgi because the glycans on E1 were predominately immature. Initial examination of the intracellularly localized E1 protein by immunofluorescence afforded weak overall staining. The strongest signals were punctate in nature and not reminiscent of ER staining, as can be seen in the E1 permeabilized cells in Figure 2.3. Accordingly, E1 did not co-stain with ER markers (data not shown). These observations did not correlate with the strong protein expression seen in Western blots (Figure 2.1). We wondered whether antibody accessibility to the E1 HA tag was being prevented by lumenal proteins binding to the E1 N terminus because this extracellular tag is positioned between the two *N*-linked glycosylation consensus sequences (Wang and Goldstein, 1995). Thus, we repositioned the HA tag to the intracellular C terminus of E1 (Appendix II). This C-terminal construct behaved similarly to the extracellularly tagged construct in all aspects; it assembled with Q1 channel subunits to afford the cardiac I_{Ks} current and required co-expression with Q1 to reach the cell surface with mature *N*-linked glycans (Appendix II). In contrast to the extracellularly tagged E1 construct, visualization of the C-terminally HA-tagged E1

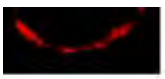

Figure 2.5: Intracellular distribution of KCNE1 peptides in CHO cells. (***A***) co-localization of E1 with intracellular markers. CHO cells expressing E1 alone were labeled for E1 along with an ER marker, calnexin (*CNX*), a *cis*-Golgi network marker (β'-COP), or a *trans*-Golgi network marker, EYFP-Golgi (YFP-Golgi). (***B***) co-immunoprecipitation (*IP*) of E1 with anti-Q1 antibody. Digitonin-solubilized CHO cells expressing E1 alone (E1) or co-expressed with Q1 (Q1/E1) were incubated with (+) or without (–) anti-Q1 antibody. One-fifth of the total detergent solubilized lysate (*1/5th Input*) and the precipitates were analyzed by SDS-PAGE.

protein by immunofluorescence gave strong perinuclear staining (Figure 2.5*A*). Counterstaining with calnexin and overlaying the images showed that the majority of E1 protein co-stains with this ER marker, although some E1 protein did not. E1 also co-stained with the *cis*-Golgi marker, β′COP (Palmer et al., 1993); however, the majority of the E1 protein stained in a pattern similar to calnexin. Little to no co-staining was observed when E1 was expressed with EYFP-Golgi, which localizes to the *trans*-Golgi network.

The intracellular staining of E1 showed that the majority of the protein resides in the ER when it is expressed alone. We determined whether Q1 subunits could co-assemble with the immature glycoforms of E1 found in the ER. Figure 2.5*B* shows that all glycoforms, mature, immature, and unglycosylated, co-immunoprecipitate with Q1. Immunoprecipitation of E1 required co-expression with Q1 because no bands were observed when E1 was expressed alone.

To verify that there are inherent differences in cellular trafficking of E1 in HEK cells *versus* CHO and COS-7 cells and not variability in experimental design, reagents, or constructs, we also examined E1 protein expression and trafficking in HEK cells. Unlike in CHO and COS-7 cells, expression of E1 in HEK cells primarily afforded the higher molecular mass species when it was expressed alone or with Q1 (Figure 2.6). Treatment with Endo H and PNGase F confirmed that this species contained mature *N*-linked glycosylation. As we observed with CHO and COS-7 cells, PNGase F digestion of E1 peptides from HEK cell lysates resulted in bands (indicated by the *asterisks*) that migrated slower than both immature and unglycosylated protein. Nonetheless, these

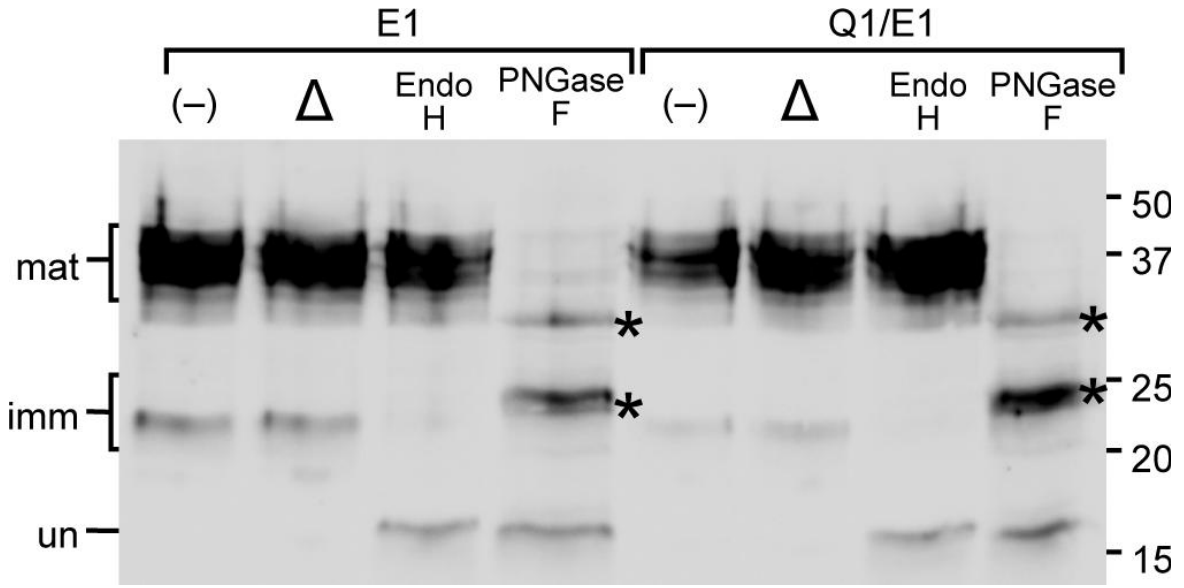
E1
Q1/E1
(–)
Δ
Endo H
PNGase F
(–)
Δ
Endo H
PNGase F
mat
imm
un
*
*
*
*
50
37
25
20
15

Figure 2.6: KCNE1 glycopeptides in HEK cells mature when expressed with or without K^+ channel subunits. Shown is an immunoblot of enzymatic deglycosylation of E1 peptides from SDS-solubilized HEK cells transfected with E1, Q1/E1, or Q1 (negative control) DNA. Expression of E1 with or without Q1 channel subunits results in robust expression of a 37 kDa band that was identified as the mature *N*-linked glycan after enzymatic deglycosylation. The samples were left untreated (–), heat-treated (Δ) to 95 °C for 5 min, digested with Endo H or PNGase F, and separated by SDS-PAGE (15%). Mature (*mat*), immature (*imm*), and unglycosylated (*un*) samples are indicated as determined by enzymatic deglycosylation. The asterisks (*) denote PNGase F digestion products that consistently migrated slower than unglycosylated or immature, which was also observed in CHO (Figure 2.2) and COS-7 (data not shown).

results show that the *N*-linked glycans on E1 peptides in HEK cells mature without transiently expressed K^+ channel subunits.

Given that E1 peptides in HEK cells exit the ER and traffic through the Golgi without co-expressed K^+ channel subunits, we determined whether these peptides were reaching the plasma membrane. Using immunofluorescence, some cell surface staining was observed for E1 when expressed alone (Figure 2.7*A*). However, the number of fluorescent cells and the intensity of cell surface staining were noticeably less than what was observed for Q1-E1. Quantitation of the cell surface proteins using biotinylation confirmed this qualitative observation. When E1 was expressed alone, 4 ± 2% of the protein was at the cell surface after calnexin subtraction; co-expression with Q1 increased the E1 cell surface protein to 22 ± 3%.

The combination of weak cell surface expression and the overwhelming maturation of the *N*-linked glycans on E1 when it is expressed in HEK cells prompted us to examine its intracellular distribution. The C-terminally HA-tagged version of E1 was expressed in HEK cells and overlaid with a panel of intracellular markers (Figure 2.7*B*). Negligible co-staining was observed with the ER marker, calnexin. Modest co-staining was observed with β′COP, but a substantial amount of E1 co-localized with EYFP-Golgi in the *trans*-Golgi network. However, in all merged images, there was some E1 protein that did not co-stain with any of the markers used. In total, these results in HEK cells demonstrate that the E1 protein traffics through the ER and to the Golgi apparatus without an exogenously expressed K^+ channel.

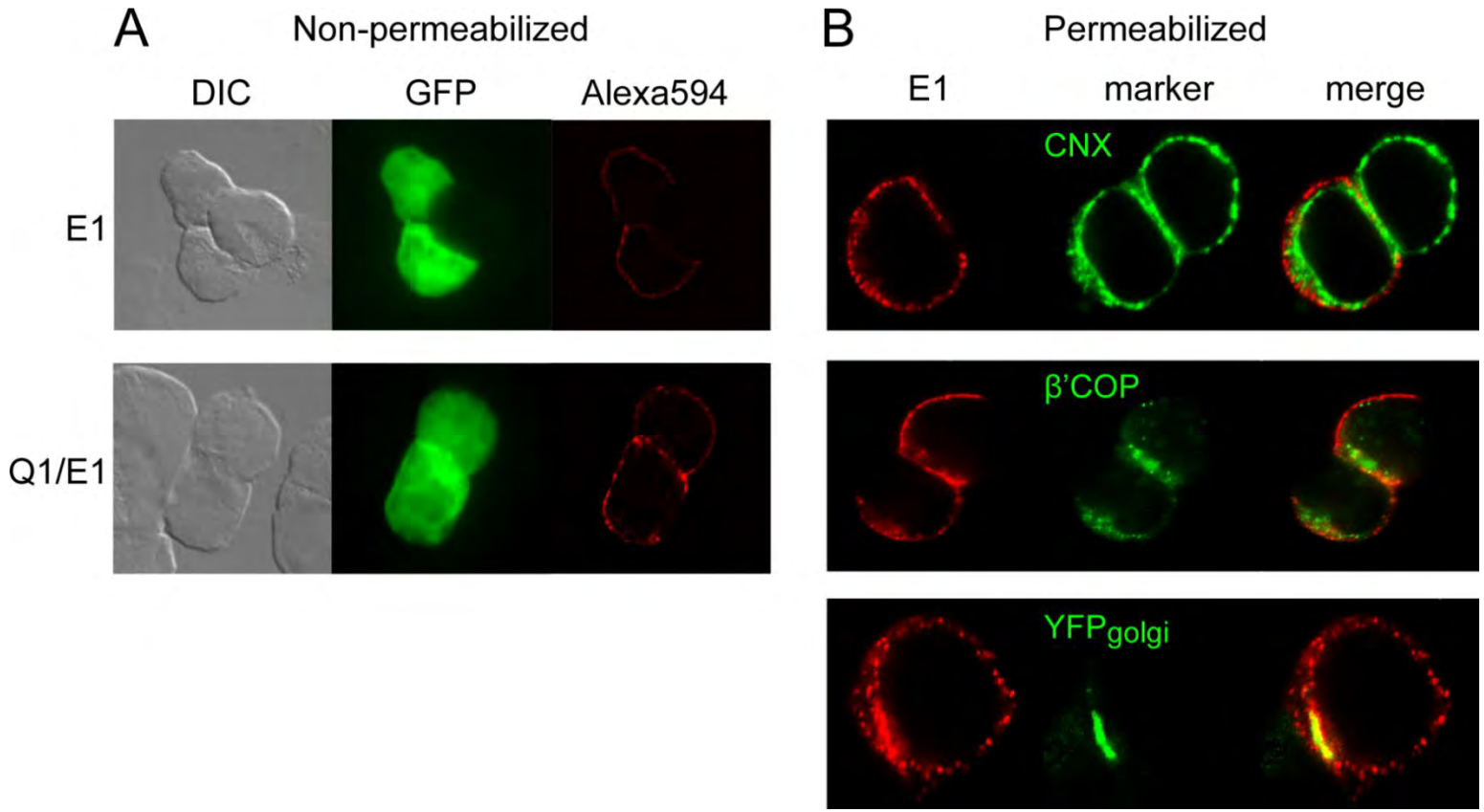
A
Non-permeabilized
DIC
GFP
Alexa594
E1
Q1/E1
B
Permeabilized
E1
marker
merge
CNX
β'COP
YFPgolgi

Figure 2.7: Solitary KCNE1 peptides traffic to the *trans*-Golgi in HEK cells and depend on KCNQ1 K^+ channel subunits for cell surface expression. (***A***) cell surface immunostaining of E1 in HEK cells. Intact cells transfected with E1 or Q1-E1 DNA were fixed, labeled with Alexa 594-conjugated antibodies, and visualized by wide field microscopy. The images shown are single 0.4-μm planes through the center of each cell. Differential interference contrast (*DIC*) panels show both transfected and nontransfected cells. Green fluorescent protein (*GFP*) panels identify transfected cells. Alexa 594 panels show cell surface staining of E1. (***B***) co-localization of E1 with intracellular markers. HEK cells expressing E1 alone were labeled for E1 along with an ER marker, calnexin (*CNX*), a *cis*-Golgi network marker (β'-COP), or a *trans*-Golgi network marker, EYFP-Golgi (YFP_{Golgi}). Note that the calnexin/E1 panels have two cells, but only the bottom cell expresses E1.

DISCUSSION

We studied the trafficking of E1 peptides through the biosynthetic pathway by following the maturation of the oligosaccharides on E1 because *N*-linked glycan processing is intimately tied to cellular compartmentalization (Helenius and Aebi, 2001). By expressing E1 alone, with Q1, or with Q4 (a K^+ channel that does not assemble with E1), we determined that E1 glycoproteins do not mature unless they are co-expressed with K^+ channel subunits that assemble with KCNE peptides. In addition, cell surface expression of E1 was also co-dependent on Q1 subunit expression, which was demonstrated in both qualitative and quantitative cell surface labeling experiments. Moreover, only the mature form of E1 was ever observed at the cell surface, indicating that the immature E1 protein bands observed at ~20 kDa do not correspond to E1 protein in functioning Q1-E1 complexes at the plasma membrane. Our results in CHO and COS-7 cells recapitulate what has been observed in *Caenorhabditis elegans* where a KCNE homolog requires its corresponding K^+ channel subunits to reach the cell surface (Bianchi et al., 2003).

The presence of immature *N*-linked glycans on E1 indicates that these proteins have yet to traffic beyond the *cis*-Golgi in the biosynthetic pathway and strongly suggests that unpartnered E1 peptides are actively prevented from trafficking past these early compartments in the secretory pathway. Co-localization experiments using a panel of intracellular markers place the majority of the E1 protein in the ER and a small fraction in

the *cis*-Golgi. Although these results cannot rule out Q1-E1 complex assembly in the *cis*-Golgi, the sheer abundance of unpartnered E1 peptides in the ER and co-immunoprecipitation of the immature and unglycosylated E1 with Q1 strongly suggest that Q1-E1 complex assembly occurs in the ER. An ER-based assembly for Q1-E1 complexes directly contradicts two previous functional studies where it was proposed that complex assembly occurs at the plasma membrane (Romey et al., 1997; Grunnet et al., 2002). The basis for this proposal was that *Xenopus* oocytes expressing unpartnered Q1 K^+ currents could be converted to KCNE-modulated currents within 24 h by a subsequent injection of KCNE mRNA. However, this functional change was the only evidence in support of this hypothesis. The cell surface and ER lifetimes of Q1 protein were not measured, nor was it directly shown that previously unpartnered, plasma membrane Q1 channels acquired newly synthesized KCNE peptides. The fact that the majority of the unassembled E1 peptides reside in the ER, possess immature *N*-linked glycans, and do not reach the cell surface in the absence of Q1 channel subunits eliminates a plasma membrane-based assembly mechanism for Q1-E1 complexes.

Enzymatic deglycosylation assays also revealed that E1 peptides potentially possess another post-translational modification, because we routinely observed digestion products that migrated slower than unglycosylated E1 (Figures 2.2 and 2.5) in all three cell lines: CHO, COS-7, and HEK. These bands appeared whether the E1 peptide possessed either or both *N*-linked glycosylation sites. In addition, changing the detergent composition used for cell lysis or the concentration of SDS in the loading buffer did not change the migration or intensity of these bands. The modification may be specific to E1

because PNGase F treatment of KCNE3 peptides co-expressed with Q1 channels in *Xenopus* oocytes (Gage and Kobertz, 2004), and CHO cells are completely digested to unglycosylated peptides (Gage and Kobertz, unpublished results). The retarded migration is not due to phosphorylation because treatment with phosphatase had no effect on the mobility of these bands. These residual bands were also resistant to a subsequent neuraminidase treatment, suggesting that if *O*-linked glycans are present on E1, the removal of terminal sialic acids does not change the mobility of the protein on a denaturing gel. Neuraminidase treatment of the *N*-linked glycans on Q1-E1, however, did show a subtle redistribution of the heterogenous E1 mature bands consistent with the removal of sialic acid residues (data not shown).

Previous studies of E1 trafficking in HEK cells observed that wild type E1 peptides could readily exit the ER with or without a co-expressed K^+ channel (Krumerman et al., 2004). In light of our contrasting results using CHO and COS-7 cells, we re-examined the cellular processing of E1 protein in HEK cells. As was previously reported, E1 peptides exited the ER without the exogenous expression of K^+ channels subunits. Using immunofluorescence, E1 protein could be detected at the plasma membrane in some cells; however, quantitative analysis of the cell surface population by biotin labeling revealed that the expression of E1 alone was barely detectable after background subtraction (4 ± 2%) and was considerably lower when compared with co-expression with Q1 (22 ± 3%). Visualization of the intracellular distribution of E1 in HEK cells by immunofluorescence showed that the majority of the protein has trafficked past both the ER and *cis*-Golgi. Some E1 protein is localized to the *trans*-Golgi network;

however, a fair amount of E1 does not co-stain with any of the secretory pathway markers used. The presence of E1 protein in the ER and *cis*- and *trans*-Golgi leaves open the possibility that Q1-E1 complex assembly in HEK cells may not be confined to the early compartments of the secretory pathway. This series of experiments suggests that the majority of the E1 protein in HEK cells exits the ER but is trapped in the *trans*-Golgi or is trafficked to another compartment in the cell. Redistribution of E1 peptides to intracellular vesicles may be an ancillary mechanism that occurs in HEK cells to redirect unassembled, mature E1 peptides to recycling and degradation compartments.

These contrasting results suggest that there are inherent differences in KCNE trafficking in HEK *versus* CHO or COS-7 cells. Traditionally, the biochemical investigation of K^+ channel α- and β- subunits has been performed in HEK cells because copious amounts of protein can be generated; however, these cells have been avoided for electrophysiological studies because endogenous voltage-gated K^+ currents can be measured (Jiang et al., 2002a). It is now known that some of these K^+ channels can assemble with KCNE peptides, including E1 (Lewis et al., 2004). The presence of native K^+ channels in HEK cells could explain the enigmatic trafficking of E1. In HEK cells, E1 peptides do not reach the plasma membrane unaccompanied but assemble with endogenous K^+ channel subunits in the secretory pathway. This inference harkens back to the initial discovery of E1 by expression cloning in *Xenopus* oocytes, where exogenously introduced E1 peptides assembled with endogenous Q1 channel subunits and trafficked to the plasma membrane producing the cardiac I_{Ks} current (Takumi et al., 1988; Folander et al., 1990). The low cell surface expression of E1 supports the idea that

it forms complexes with limiting amounts of endogenous K^+ channel subunits. However, the lack of immature E1 observed in our immunoblots suggests that protein overexpression may also contribute to the artificial ER exit of E1 in HEK cells. Whether cell surface expression of E1 is mediated by endogenous K^+ channels or by overwhelming the retention/retrieval machineries of the cell, studying the assembly and trafficking of KCNE peptides in HEK cells should be avoided.

The ER has two well known mechanisms for retaining misfolded and unassembled protein subunits: recognition of ER retention/retrieval signal sequences and chaperone-mediated retention of *N*-linked glycoproteins. The best studied ER retention signal to date is the RXR motif, which has been shown to regulate the ER exit of K_{ATP} channel subunits and sulfonylurea receptors (Zerangue et al., 1999). ER retention through this motif is a stringently controlled mechanism because neither protein can escape the ER with this signal sequence exposed. E1 peptides do not possess such a motif nor are they exquisitely retained in the ER when overexpressed in CHO or COS-7 cells, because faint bands that corresponded to mature glycoprotein were always observed with solitary expression of E1 (Figures 2.1 and 2.2). Because we also observe some E1 protein in the *cis*-Golgi, it is possible that E1 is subject to ER retrieval. E1 does possess a KK*XX* sequence, which is a known ER retrieval signal sequence (Ellgaard and Helenius, 2003); however, the juxtaposition of this motif to the transmembrane domain suggests that it may function only as a membrane stop transfer signal (Shikano and Li, 2003). It is likely that E1 peptides are, in part, retained in the ER via their *N*-linked glycans through the calnexin/calreticulin quality control pathway, which has been shown to aid in the

stability and ER exit of K^+ channel α-subunits (Khanna et al., 2004). A calnexin/calreticulin association with the E1 N terminus would also explain the lack of ER staining that we observed with the extracellularly HA-tagged E1 construct, which necessitated repositioning of the tag. If E1 peptides are retained in the ER by calnexin or calreticulin, this mechanism would be applicable to all KCNE peptides because the *N*-linked consensus site closest to the N terminus is conserved throughout the family. It is also feasible that multiple retention/retrieval machineries are acting on unassembled E1 peptides or that Q1-E1 co-assembly promotes active export of the complex from the ER.

The goal in preventing unassembled K^+ channel α- and β- subunits from leaving the ER is to ensure the formation of fully assembled K^+ channel complexes because unpartnered K^+ channels would have inappropriate gating and ion conducting properties. Although our results show that unpartnered E1 peptides reside primarily in the ER, homotetrameric Q1 channels have been shown to exit the ER and function at the plasma membrane in several different ion channel expression systems, including CHO and COS-7 cells (Pusch et al., 1998; Tinel et al., 2000; Melman et al., 2001). In E1 knock-out mice, however, Q1 channels do not traffic to the apical membranes of vestibular dark cells, where they would normally be found with E1 in wild type cells (Nicolas et al., 2001). In addition, RNA interference experiments in *C. elegans* suggest that the stability of the K^+ channel complex is dependent on the presence of both pore-forming and KCNE-like subunits (Bianchi et al., 2003). The discordant observation of unpartnered Q1 channels at the cell surface in expression systems may be due to Q1 channels leaking from the ER as a result of overexpression. Consistent with swamping the ER with

overexpressed protein is the fact that the majority of the Q1 protein in expression systems is intracellular (Schroeder et al., 2000). Moreover, Q1 expressed in *Xenopus* oocytes or CHO cells is not *N*-linked glycosylated (Gage and Kobertz, unpublished results) and thus not subject to glycosylation-dependent ER retention. An alternative explanation for the ER exit of unpartnered Q1 channels is that E1 protein synthesis always precedes Q1 subunit expression in native tissues. With this temporal control, the ER is always chock full of E1 peptides that can readily assemble with newly synthesized K^+ channel subunits. This mechanism alleviates the need to retain unpartnered Q1 channels as long as the rate of co-assembly with E1 is faster than ER exit of the homotetrameric channel. There is some *in vivo* evidence in the developing ear to support this notion, because E1 protein is expressed in embryonic mouse vestibular dark cells 24 h before the Q1 protein (Nicolas et al., 2001).

Many studies have shown that modulation of voltage-gated K^+ channels by KCNE peptides provides the functional diversity required for these complexes to work in the nervous system, muscle, colon, ear, and heart; however, for proper biological function these complexes must reach the plasma membrane fully assembled. Our results show that E1 peptides cannot advance past the *cis*-Golgi until they assemble with Q1 channel subunits, which is the first step in the assembly and trafficking of KCNE-K^+ channel complexes. Given that mutations in KCNE peptides effect the assembly and trafficking of the entire K^+ channel complex and cause long QT syndrome, identifying the cellular machineries that directly ensure the proper assembly and trafficking of healthy KCNE-K^+

channel complexes will be critical for following and interpreting the aberrant assembly and trafficking of diseased complexes.

This study laid the foundation of the next chapter where we investigated the N-linked glycosylation behavior of the two sequons on KCNE1.

EXPERIMENTAL PROCEDURES

Plasmids and cDNAs. Human Q1 and E1 were subcloned into pcDNA3.1(-) (Invitrogen). Two hemagglutinin A (HA)-tagged versions of E1 were used. For cell surface immunofluorescence experiments, an extracellular HA tag (YPYDVPDYA) was incorporated in the E1 N terminus between residues 22 and 23 (Wang and Goldstein, 1995). For intracellular immunolocalization experiments, an HA tag was appended to the E1 C terminus via a SGSG linker. Biochemical experiments were performed with both HA constructs. For consistency, only the data from the extracellularly tagged version is shown.

Cell Culture and Transfections. Chinese Hamster Ovary-K1 (CHO) cells were cultured in F-12K nutrient mixture (Invitrogen). HEK cells and African green monkey kidney (COS-7) cells were cultured in Dulbecco's modified Eagle's medium (Sigma). All of the media were supplemented with 10% fetal bovine serum (Hyclone) and 100 units/ml penicillin/streptomycin (Invitrogen). For biochemical analysis, the cells were plated at 60-75% confluency in 35-mm dishes. After 24 h, the cells were transiently transfected at room temperature with E1 alone, Q1-E1, or Q4-E1 at a ratio of 0.5 μg/1.5 μg with 8 μl of Lipofectamine (Invitrogen) for CHO cells or at a ratio of 0.25 μg/0.25 μg (COS-7 cells), 1.25 μg/2.5 μg (HEK cells) with 10 μl of Lipofectamine 2000 (Invitrogen). Empty pcDNA 3.1(-) plasmid DNA (0.5 μg for CHO, 0.25 μg for COS-7, and 1.25 μg for HEK) was co-transfected in samples containing only E1 DNA to keep the

total transfected DNA constant in all wells. To increase the amount of E1 protein with complex glycans in CHO cells, 0.75 μg of Q1 DNA was used in the co-transfection. For immunofluorescence studies, the cells were plated at 50% confluency onto sterile 12-mm glass coverslips (untreated for CHO cells, poly-d-lysine treated for HEK cells) in 24-well plates. For cell surface immunofluorescence, the cells were transiently transfected with E1 alone, Q1-E1, or Q4-E1 by scaling down the DNA (optimized ratio for CHO cells) and lipid levels by one-fifth; 0.2 μg of a vector containing green fluorescent protein was co-transfected to serve as a transfection control. For co-localization with ER and *cis*-Golgi markers, 0.3 μg of E1 was transfected; to visualize *trans*-Golgi, 0.3 μg of EYFP-Golgi (Clontech) was also transfected. Co-localization studies were performed 24 h post-transfection. For all other experiments, the cells were used 48 h post-transfection.

Cell Lysis and Western Blot Analysis. The cells were washed in ice-cold PBS (3 × 2 ml) and lysed at 4 °C in three different detergent buffers: 1% SDS lysis buffer (10 mm Tris·HCl, pH 7.5, 150 mm NaCl, 1 mm EDTA, 1% SDS (w/v)), 1.5% digitonin lysis buffer (20 mm Tris·HCl, pH 7.4, 140 mm NaCl, 10 mm KCl, 1 mm $MgCl_2$, 1.5% digitonin), and RIPKA lysis buffer (10 mm Tris·HCl, pH 7.4, 140 mm NaCl, 10 mm KCl, 1 mm EDTA, 1% Triton X-100, 0.1% SDS, 1% sodium deoxycholate). All of the detergent buffers were supplemented with protease inhibitors, 1 mm phenylmethylsulfonyl fluoride, and 1 μg/ml each of leupeptin, pepstatin, and aprotinin. For expression gels, CHO cells were lysed in 300 μl of 1% SDS buffer, and COS-7 cells were lysed in 250 μl of RIPKA buffer. Cell debris was pelleted in a microcentrifuge (16,100 × *g* for 10 min at room temperature). The supernatants were diluted with SDS-

PAGE loading buffer containing 100 mm dithiothreitol, separated on a 15% SDS-polyacrylamide gel, and transferred to nitrocellulose (0.2 μ; Schleicher & Schuell). The membranes were blocked in Western blocking buffer (5% nonfat dry milk in Tris-buffered saline containing 0.2% Tween 20 (TBS-T)) for 30 min at room temperature and then incubated with rat anti-HA (Roche Applied Science) (1:750) in Western blocking buffer overnight at 4 °C. The membranes were washed in TBS-T (four times for 5 min) and incubated with goat anti-rat horseradish peroxidase-conjugated antibody (Santa Cruz Biotechnology, Inc.) (1:2000) in Western blocking buffer for 45 min at room temperature. The membranes were subsequently washed with TBS-T (four times for 5 min). Horseradish peroxidase-bound proteins were detected by chemiluminescence using SuperSignal West Dura Extended Duration Substrate (Pierce) and a Fujifilm LAS-3000 CCD camera.

Endo H and PNGase F Deglycosylation Analysis. The cell lysates (30 μl) were diluted to 0.5% SDS with water and raised to 1% Nonidet P-40 (for PNGase F analysis only), 1% β-mercaptoethanol, 50 mm sodium citrate, pH 5.5 (for Endo H analysis) or 50 mm sodium phosphate, pH 7.5 (for PNGase F analysis) and then digested with Endo H_f (1 μl) or PNGase F (2 μl) (New England BioLabs, Inc.) for 30 min at 37 °C. The samples were then raised to 100 mm dithiothreitol and 3.5% SDS before resolving by SDS-PAGE (15% gel) and analyzed by Western blot.

KCNE1 Co-immunoprecipitation. The cells were washed in ice-cold PBS (3 × 2 ml) and lysed at 4 °C in 250 μl of 1.5% digitonin buffer. The cell debris was pelleted in a microcentrifuge (16,100 × *g* for 15 min at room temperature). 30 μl of cell lysate was

incubated with 5 μl of anti-Q1 antibody (Santa Cruz Biotechnology, Inc.) for 2 h at room temperature. The samples were bound to protein G beads (Pierce) for 2 h at room temperature to separate out antibody-bound protein complexes from the cell lysate. The beads were washed (three times with 500 μl) in digitonin-free wash buffer (20 mm Tris·HCl, pH 7.4, 140 mm NaCl, 10 mm KCl, 1 mm $MgCl_2$. Co-immunoprecipitated proteins were eluted from the beads using 1× SDS-PAGE loading buffer with 200 mm dithiothreitol for 15 min at room temperature. One-fifth of the total input used for the co-immunoprecipitation assay and eluted proteins were resolved by SDS-PAGE (15% gel) and analyzed by Western blot.

Immunofluorescence. For visualization of intact cells, the cells were first labeled with rat anti-HA antibody (1:200) in culture medium for 30 min at 37 °C. The cells were rinsed quickly in warm PBS (3 × 2 ml) before fixing in 4% paraformaldehyde (10 min at room temperature). The cells were then blocked in blocking solution (PBS containing 5% normal goat serum (Vector Laboratory, Inc.), 1% IgG-free bovine serum albumin (Sigma)) for 30 min at room temperature. For permeabilized samples, the cells were first washed in PBS (3 × 2 ml) and then fixed in 4% paraformaldehyde (10 min at room temperature). The cells were blocked in Triton blocking buffer (blocking solution containing 0.2% Triton X-100) and then incubated with rat anti-HA antibody (1:500) in Triton blocking buffer for 1 h at room temperature. Nonpermeabilized and permeabilized samples were then washed with PBS (3 × 5 min) and incubated with goat anti-rat Alexa Fluor 594-conjugated antibody (Molecular Probes) (1:2000) in blocking solution or Triton blocking solution, respectively, for 45 min at room temperature. The cells were

then washed with PBS (two times for 5 min; then for 1 h). The coverslips were dried at 37 °C for 45 min before mounting on slides with ProLong® Gold Antifade mounting solution (Molecular Probes). For co-staining with intracellular markers, the cells were fixed in 100% methanol at -20 °C for 8 min, rehydrated in PBS for 5 min, and blocked overnight in SeaBlock Blocking buffer (Pierce). The cells were first incubated with rabbit anti-calnexin (Stressgen) (1:500) or concentrated mouse serum from monoclonal antibody CM1A10 for β′ coatomer protein (anti-β′COP) (Palmer et al., 1993; Gomez et al., 2000) (1:10) in SeaBlock Blocking buffer at room temperature for 90 min. The cells were then washed with PBS (3 × 10 min) and incubated with donkey anti-rabbit Alexa Fluor 488-conjugated antibody (1:500) or donkey anti-mouse Alexa Fluor 488-conjugated antibody (1:250) (Molecular Probes) in SeaBlock blocking buffer at room temperature for 90 min. The cells were washed in PBS (three times for 10 min) and labeled for E1 as described above with rat anti-HA (1:100) followed by goat anti-rat Alexa Fluor 594-conjugated antibody (1:500) in SeaBlock blocking buffer. After a final set of PBS washes (three times for 10 min), the coverslips were mounted on slides with Vectashield® mounting medium (Vector Laboratories). All of the cells were visualized using a Zeiss Axiovert 200M microscope with a 63 × 1.4 N.A. oil immersion objective. *z* stacks were generated by obtaining optical sections through the samples 0.4 μm apart along the *z* axis. Deconvolution of *z* stack images was performed with a constrained iterative algorithm on Slidebook 4.0 software (Intelligent Imaging Innovations) using a measured point spread function. The images are displayed as single 0.4-μm planes through the center of each cell.

Cell Surface Biotinylation. The cells were rinsed with ice-cold PBS^{2+} buffer (four times with 2 ml; PBS containing 1 mm $MgCl_2$, 0.1 mm $CaCl_2$) at 4 °C to arrest membrane internalization. The cells were then incubated with 1 mg/ml sulfo-NHS-SS-biotin (Pierce) in PBS^{2+} buffer twice for 15 min at 4 °C. To quench the excess biotinylation reagent, the cells were washed quickly (three times with 2 ml) with quench solution (PBS^{2+} containing 100 mm glycine) and then incubated with quench solution twice for 15 min at 4 °C. The cells were lysed in RIPKA buffer for 30 min at 4 °C. Cell debris was removed by centrifugation (16,100 × *g* for 10 min at 4 °C). Total protein in each sample was quantitated by BCA analysis. Of these samples, 75 μg of total protein was separated by affinity chromatography on 25 μl of Immunopure® immobilized streptavidin beads (Pierce) overnight at 4 °C, whereas 15 μg was saved as an input control to determine the percentage of biotinylated proteins. The beads were washed (three times with 500 μl) in 0.1% SDS wash buffer (10 mm Tris·HCl, pH 7.4, 150 mm NaCl, 1 mm EDTA, 0.1% SDS). Biotinylated proteins were eluted from the beads using 2× SDS-PAGE loading buffer with 200 mm dithiothreitol for 15 min at 55 °C. The inputs and eluted proteins were resolved by SDS-PAGE (15% gel) and analyzed by Western blot. The images of nonsaturated bands were captured on a Fujifilm LAS-3000 CCD camera, and the band intensities were quantitated using MultiGauge V2.1 software (FujiFilm). An ER-resident protein, calnexin, was used as a control to determine the percentage of cell rupture that occurred during the labeling process. Background cell lysis was quantitated as a ratio of biotinylated calnexin protein to total input calnexin.

The percentage of E1 protein on the cell surface was calculated from the ratio of avidin-bound protein to total input protein after background lysis subtraction.

CHAPTER III

Post-Translational N-Glycosylation of Type I Transmembrane KCNE1 Peptides: Implications for Membrane Protein Assembly in the Endoplasmic Reticulum

Contributors to the work presented in Chapter III:

The author of this thesis, Tuba Bas performed all the experiments other than electrophysiological studies and the proteosomal inhibitor experiment. Kshama Chandrasekhar did the preliminary work. Anatoli Lvov provided electrophysiology data. Yuan Gao performed the proteosomal inhibitor experiment.

* Bas, T., Chandrasekhar, K. D., Lvov, A., Gao, Y, Gilmore, R., and Kobertz, W. R. 2010. Post-Translational N-Glycosylation of Type I Transmembrane KCNE1 Peptides: Implications for Disease. *Manuscript in Preparation*.

ABSTRACT

N-linked glycosylation of membrane proteins is critical for their proper folding, co-assembly and subsequent matriculation through the secretory pathway. Here we examine the kinetics and efficiency of N-linked glycan addition to type I transmembrane KCNE1 K^+ channel β-subunits, where point mutations that prevent N-glycosylation give rise to disorders of the cardiac rhythm and congenital deafness. We show that KCNE1 has two distinct N-linked glycosylation sites: a traditional co-translational site and a consensus site ~ 20 residues away that unexpectedly acquires N-linked glycans after protein synthesis (post-translationally). Mutations that prevent N-glycosylation at the co-translational site concomitantly reduce post-translational glycosylation, resulting in a large population of unglycosylated KCNE1 peptides that do not reach the cell surface with their cognate K^+ channel. This long range disruption of post-translational N-glycan addition directly explains how a single point mutation can prevent N-glycosylation at multiple consensus sites, providing a new biogenic mechanism for human disease. These results demonstrate that post-translational N-glycosylation in the endoplasmic reticulum is a cellular mechanism that ensures type I transmembrane proteins acquire the maximal number of glycans needed for proper membrane protein assembly and trafficking.

INTRODUCTION

Asparagine-linked (N-linked) glycosylation is a highly-conserved protein modification that eukaryotic cells utilize for the proper folding, assembly and trafficking of membrane and secreted proteins. The initial attachment of N-linked glycans to polypeptides occurs in the endoplasmic reticulum (ER), where the oligosaccharyltransferase (OST) complex efficiently transfers a high mannose oligosaccharide onto asparagine residues within the primary sequence N-X-T/S-Y (sequon, where X and Y can be any natural amino acid other than proline) (Marshall, 1972; Silberstein and Gilmore, 1996). Although commonly referred to as a post-translational protein modification, N-linked glycosylation in mammalian cells typically occurs during translation as the nascent polypeptide is threaded through the translocation tunnel into the ER lumen (Weerapana and Imperiali, 2006). Recently, however, one of the mammalian isoforms (STT3B) of the active site subunit of the ER resident OST complex has been shown to mediate post-translational N-glycosylation of a secreted protein, human blood coagulation factor VII (Ruiz-Canada et al., 2009). To date, factor VII is the only reported full-length protein that is post-translationally N-glycosylated in mammalian cells with intact N-glycosylation machinery (Bolt et al., 2005). Factor VII curiously contains two distinct sequons: one sequon is modified co-translationally whereas the second sequon is modified post-translationally, yet the biological significance of a protein harboring both a co- and post-translational sequon is unclear.

Besides the structurally-distorting proline residue, three other factors can reduce or eliminate N-glycosylation of sequons. (1) Residues at the X-position: NXS sequons with negatively-charged (Asp and Glu) and hydrophobic (Trp and Leu) at the X-position are poorer substrates for the OST complex (Shakin-Eshleman et al., 1996; Kasturi et al., 1997). (2) Proximity to the C-terminus: sequons within ~ 60 residues of the C-terminus often elude the OST complex, as the chain-terminated protein is believed to more rapidly enter the ER lumen through the translocation tunnel (Nilsson and von Heijne, 2000). (3) Proximity to a transmembrane domain: sequons that are less than 12 residues away from a transmembrane segment are inaccessible to the OST active site (Nilsson and von Heijne, 1993; Cheung and Reithmeier, 2007). Bioinformatic interrogation of the residues flanking sequons (up to 20 residues) has not identified any other sequence motifs that have long range effects on N-glycosylation efficiency (Gavel and von Heijne, 1990; Ben-Dor et al., 2004).

KCNE1 (E1) is the founding member of a family type I transmembrane K^+ channel β-subunits that have multiple sequons in their extracellular N-termini. E1 peptides have two sequons at N5 and N26, both of which are obligatorily glycosylated in native tissues as well as in standard electrophysiological expression systems (Finley et al., 2002; Chandrasekhar et al., 2006; Teixeira et al., 2006). E1 co-assembles with KCNQ1 (Q1) K^+ channels to produce the slowly activating cardiac I_{ks} current (Barhanin et al., 1996; Sanguinetti et al., 1996) and to recycle potassium in apical membranes of strial marginal and vestibular dark cells in the inner ear (Wangemann, 2002). A mutation that disrupts the sequon at N5 (T7I), gives rise to an inherited autosomal recessive form

of Long QT Syndrome (LQTS), a disorder of the cardiac rhythm that is accompanied with neural deafness, Jervell-Lange-Nielsen Syndrome (JLNS) (Schulze-Bahr et al., 1997). An SNP in the equivalent threonine in KCNE2 (T8A) provokes drug-induced LQTS with the commonly prescribed antibiotic, sulfamethoxazole (Sesti et al., 2000a; Park et al., 2003). However, the biogenic mechanism that underlies the importance for glycosylation at this absolutely conserved sequon remains to be elucidated.

Given the genetic linkage between N-glycosylation and KCNE biology, we determined the efficiency and kinetics of N-glycosylation of the two closely-spaced sequons in E1 and the effects of N-glycan occupancy on co-assembly with K^+ channel subunits and cell surface expression. By comparing wild type to a panel of E1 glycosylation mutants in metabolic labeling experiments, we found that the N-terminal sequon (N5) acquires its N-linked glycan during translation whereas the second glycan is primarily added to the internal sequon (N26) post-translationally. Unlike co-translational glycosylation, post-translational glycosylation was significantly effected by long range mutations since ablation of the N-terminal sequon inhibited N-glycan attachment to the internal sequon. Moreover, E1 subunits harboring the LQTS mutation, T7I, exit the translocational tunnel unglycosylated where co-assembly with Q1 inhibits post-translational glycosylation. These results provide a new biogenic mechanism for channelopathies and demonstrate a need for post-translational glycosylation of membrane proteins in the endoplasmic reticulum.

RESULTS

N-glycan Occupancy of KCNE1 Sequons

The addition of N-linked glycans via oligosaccharyltransferase (OST) to nascent polypeptides in the ER translocation tunnel is conserved from yeast to humans. Accordingly, the initial attachment of N-linked glycans to the two N-terminal sequons in E1 is identical in a wide range of cells from native (cardiomyocytes and inner ear cells) to traditional expression systems (Xenopus oocytes, HEK-293, CHO-K1 and COS-1 mammalian cells) (Gage and Kobertz, 2004; Chandrasekhar et al., 2006; Teixeira et al., 2006; Wu et al., 2006). To examine the two N-linked glycoforms of E1 individually (Figure 1**A**), we made an initial panel of single glycosylation mutants that would result in glycan addition to either the N-terminal sequon (N26Q) or the internal sequon (N5Q, T7I) and compared them to wild type E1 (WT). We first examined these E1 mutants without a cognate K^+ channel in order to follow N-glycosylation without interference from co-assembly with K^+ channel subunits. To do this, we expressed these E1 constructs in CHO cells since these cells lack endogenous voltage-gated K^+ channel subunits that assemble with E1 peptides (Chandrasekhar et al., 2006). Transient expression of a C-terminal, HA-tagged WT peptide yielded two strong bands at 17 and 23 kDa on a Western blot (Figure 3.1***B***, left), which we confirmed with enzymatic deglycosylation (Figure 3.S1) were the unglycosylated and immaturely N-linked

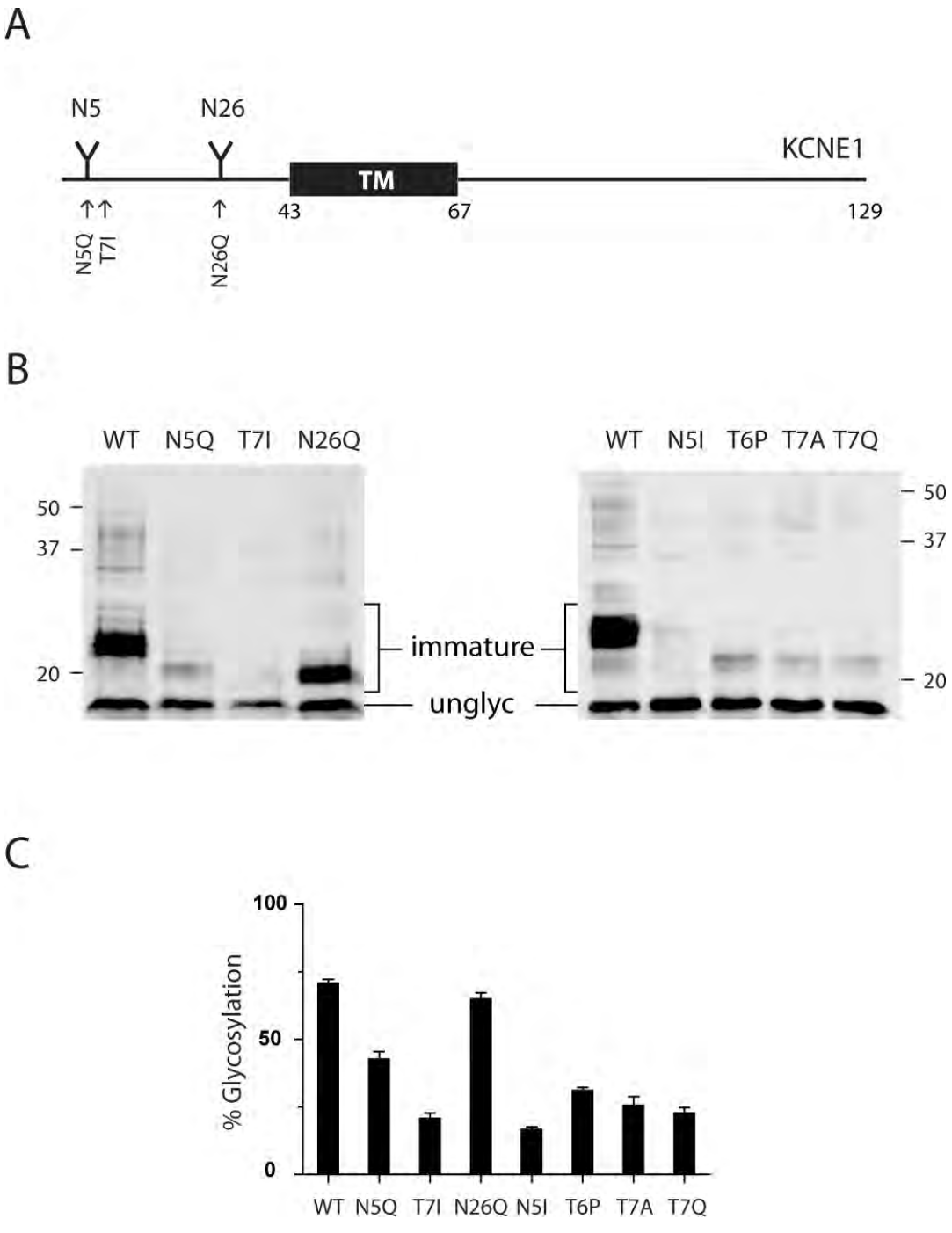
A
N5
N26
KCNE1
TM
43
67
129
N5Q
T7I
N26Q
B
WT
N5Q
T7I
N26Q
WT
N5I
T6P
T7A
T7Q
50
37
20
immature
unglyc
C
% Glycosylation
100
50
0
WT
N5Q
T7I
N26Q
N5I
T6P
T7A
T7Q

Figure 3.1: Differential N-linked glycosylation of WT and mutant KCNE1 peptides. (***A***) Schematic representation of KCNE1. The glycosylation mutants N5Q, T7I and N26Q are indicated by arrows. TM, transmembrane domain. (***B***) Immunoblots of WT and glycosylation mutant E1 peptides from solubilized CHO cells. Immature and unglycosylated (unglyc) are denoted. (***C***) Bar graph of the percentage of glycosylated WT and mutant E1 peptides. Error bars are SEM from n = 3 – 6 immunoblots.

glycosylated peptides, respectively (Chandrasekhar et al., 2006). Ablation of the N-terminal sequon (N5Q, T7I) unexpectedly prevented glycosylation of the internal sequon, resulting in mostly unglycosylated protein. In contrast, disruption of the internal sequon (N26) had no significant effect on glycosylation of the N-terminal sequon, though as expected, the mono-glycosylated protein migrated faster than doubly-glycosylated WT.

Since there was a significance difference in hypoglycosylation between the hydrophilic N5Q and hydrophobic T7I mutants (Figure 3.1***C***), we disrupted the N-terminal sequon with various residues to determine how mutations at the N-terminal sequon effect glycosylation at the internal site twenty residues away. Substitution of asparagine for isoleucine (N5I) reduced glycosylation at the internal site similarly to T7I (Figure 3.1***B***, right). Mutation to residues less hydrophobic than isoleucine (T7A or T7Q) afforded slightly more glycosylated E1 peptide than the isoleucine mutants; however, the differences were not statistically significant (Table 3.S1). Distorting the N-terminal sequon with proline (T6P) had an intermediate reduction of glycosylation, falling significantly between the isoleucine mutants and N5Q. This trend (T7I, N5I > T6P > N5Q > WT) suggests that hydrophobic disruption of N-terminal sequon has a long range effect on glycosylation of the internal site, resulting in a bolus of unglycosylated E1 peptides.

Cellular Stabilities of WT and Mutant KCNE1 Peptides

To identify the cellular mechanism responsible for the large population of unglycosylated protein observed with the N-terminal sequon mutants (N5Q, T7I), we first determined whether the singly-glycosylated mutants had different protein stabilities.

Cells expressing WT and mutant peptides were metabolically-labeled with ^{35}S for 10 min, chased with cold media, and the E1 peptides were isolated by immunoprecipitation at various times (Figure 3.2***A***). The total protein (unglycosylated and glycosylated) for each time point was normalized in a way to make each data set comparable to one another, plotted and fitted to a single exponential decay (Figure 3.2***B***). Since the zero time point is diluted with partially synthesized peptides (Hershey, 1991), the 5 min chase point was defined as maximally-labeled protein for the glycosylation mutants; for WT, the 10 min time point was used due to the delay in protein decay (Figure 3.2***B***). We also plotted the raw data for two WT data sets and calculated the decay rates individually and showed that the decay rates were within the range of the normalized average decay rate calculated for WT (Figure 3.S2***A***, Figure 3.S2***B*** and Table 3.1). Surprisingly, the WT and the single site glycosylation mutants had experimentally similar protein stabilities (Table 3.1). Moreover, this similarity in protein stability did not change when we measured the decay of just the singly-glycosylated form of N26Q. These results show that protein stability does not significantly contribute to the glycosylation ratios observed with the single site glycosylation mutants.

Co- and Post-translational N-Glycosylation of KCNE1 Peptides

We next determined whether the N-glycosylation rates of WT and the mutant E1 peptides were different. To follow the rapid kinetics of N-linked glycosylation, we metabolically-labeled cells using 2 min pulses. This shorter pulse allowed us to differentiate between co- and post-translational N-linked glycosylation since all of the E1 polypeptides initiated during the pulse will be completed by the 5 min chase

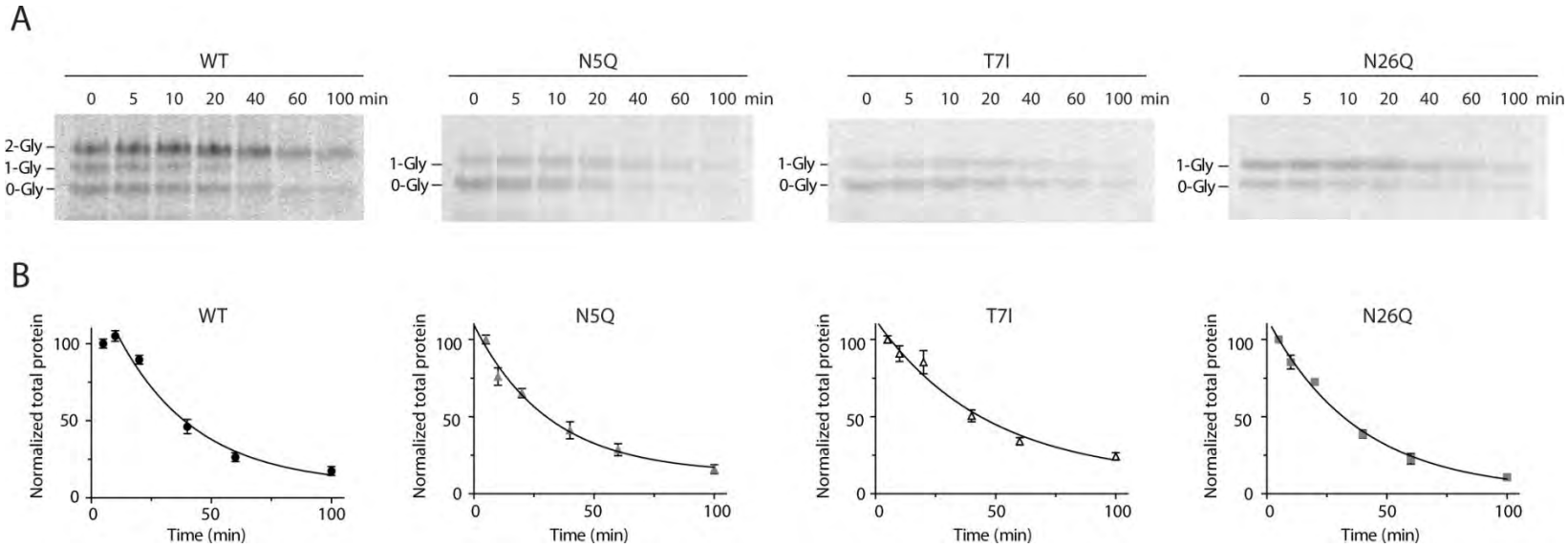
A
WT
N5Q
T7I
N26Q
0 5 10 20 40 60 100 min
2-Gly
1-Gly
0-Gly
B
Normalized total protein
Time (min)
0
50
100

Figure 3.2: Protein stability of WT and KCNE1 glycosylation mutants are similar. (***A***) Representative fluorographs for WT and glycosylation mutants. Metabolically-labeled CHO cells were chased for the indicated times and the E1 peptides were immunoprecipitated, separated by electrophoresis, and detected by autoradiography. 2-Gly: doubly glycosylated; 1-Gly: singly glycosylated; 0-Gly: unglycosylated. (***B***) Graphs of densitometric analysis. The total protein at each time point was quantified by densitometry, normalized to the total protein at 5 min (except WT: 10 min) and plotted versus chase time. WT: closed circles; N5Q: gray triangles; T7I: open triangles; N26Q: gray squares are mean ± SEM (n = 3 – 4) for each chase point for WT, N5Q, T7I and N26Q respectively. Data were fitted to a single exponential and tabulated in Table 3.1.

Table 3.1. Protein decay and post-translational glycosylation rates of KCNE1 peptides[1]		
KCNE1 peptide	τ protein decay (min) ^{ns}	τ post-translational glycosylation (min) ^{ns}
WT	33 ± 4	8.5 ± 2.0
N5Q	33 ± 5	15 ± 5
T7I	46 ± 3	20 ± 4
N26Q	38 ± 2	ND
N26Q (1-gly)	37 ± 3	NA

[1]Data are from 3 – 5 individual experiments. Data were fitted to a single exponential. Values are mean ± SEM. [ns]Indicates that the rates were not significantly different from each other (one-way ANOVA with Tukey post-hoc analysis ($p > 0.5$)) ND, not detectable; NA, not applicable.

(Hershey, 1991). Figure 3.3***A*** shows a time course for WT and mutant E1 peptides. At each chase time point, the different glycosylation states were plotted as a percentage of the total protein (Figure 3.3***B***). For WT, the doubly-glycosylated form of the protein steadily increased whereas the singly- and unglycosylated forms decreased over the duration of the 20 min time course. The increase in doubly-glycosylated E1 after the 5 min chase indicates that N-linked glycans were attached after translation. Therefore, we used the E1 mutants to determine which N-linked glycosylation site(s) were responsible for the slower, post-translational glycosylation of WT. For N26Q, the singly glycosylated form was the most abundant within the first 5 minutes, consistent with N-linked glycan addition to the N-terminal sequon during translation. Conversely, N5Q and T7I were poorly glycosylated during the protein translation time window, resulting in predominately unglycosylated protein. However, for both N5Q and T7I, the singly glycosylated form exponentially increased over 5 – 20 min whereas the glycosylation state of N26Q remained constant after 5 min (Figure 3.3***B***, Table 3.1). This kinetic difference in N-linked glycan addition identified the internal glycosylation site as a source of the post-translational glycosylation observed with WT E1. Moreover, the use of proteosomal inhibitors did not change this outcome, indicating that the kinetic differences in N-linked glycan addition were not due to protein decay (Figure 3.S3***A*** and Figure 3.S3***B***). We also plotted the raw data for each WT glycoform and showed that after 5 min, the fully glycosylated form of WT E1 increased (Figure 3.S4***A*** and Figure 3.S4***B***). Overall, these results demonstrate that the glycosylation timing and efficiency at the two sequons on E1 are different: N-linked glycans are readily added to the

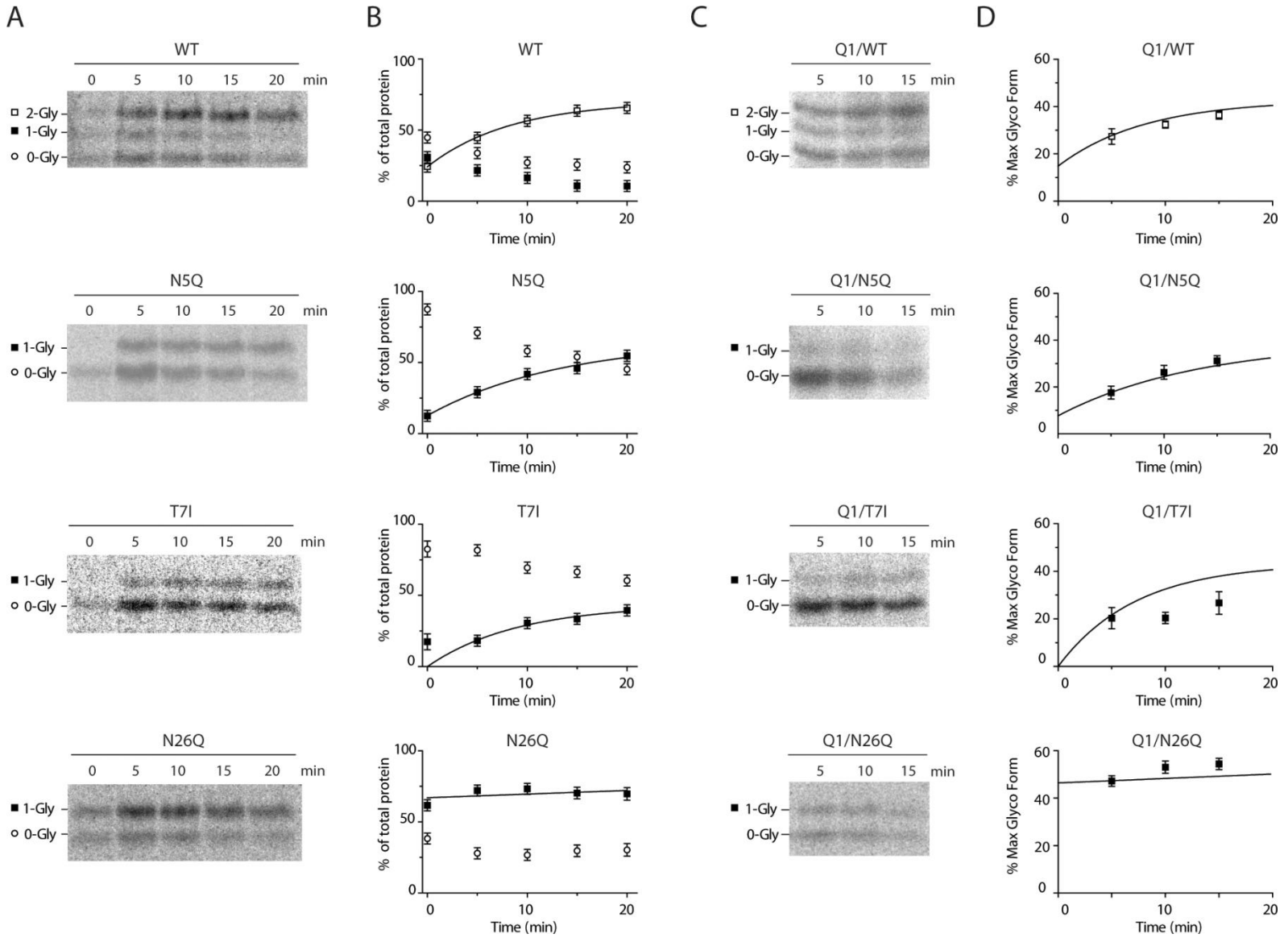
A
WT
0 5 10 15 20 min
2-Gly
1-Gly
0-Gly
N5Q
0 5 10 15 20 min
1-Gly
0-Gly
T7I
0 5 10 15 20 min
1-Gly
0-Gly
N26Q
0 5 10 15 20 min
1-Gly
0-Gly
B
WT
% of total protein
Time (min)
N5Q
% of total protein
Time (min)
T7I
% of total protein
Time (min)
N26Q
% of total protein
Time (min)
C
Q1/WT
5 10 15 min
2-Gly
1-Gly
0-Gly
Q1/N5Q
5 10 15 min
1-Gly
0-Gly
Q1/T7I
5 10 15 min
1-Gly
0-Gly
Q1/N26Q
5 10 15 min
1-Gly
0-Gly
D
Q1/WT
% Max Glyco Form
Time (min)
Q1/N5Q
% Max Glyco Form
Time (min)
Q1/T7I
% Max Glyco Form
Time (min)
Q1/N26Q
% Max Glyco Form
Time (min)

Figure 3.3: KCNE1 peptides are co- and post-translationally N-glycosylated. (***A***, ***C***) CHO cells were pulsed for 2 min, chased for the indicated times and the E1 peptides were immunoprecipitated, separated by electrophoresis, and detected by autoradiography. Representative fluorographs for WT and E1 mutants expressed alone (***A***) and with Q1 channel subunits (***C***). (***B***) Graphs of densitometric analysis for Fig. 3.3A. The percentage of the different glycoforms with respect to total protein is plotted for each time point. After 5 min, the fully glycosylated forms of WT, N5Q and T7I increased whereas N26Q remained constant. The increase in glycosylation was fitted to a single exponential and tabulated in Table 3.1. N26Q is a linear fit for comparison purposes. Data (n = 3 – 5) are mean ± SEM for each chase point. (***D***) Graphs of densitometric analysis for Fig. 3.3C. The percentage of the maximally glycosylated form of WT (two) and the E1 mutants (one) with respect to total protein is plotted for each time point. The fits from Fig. 3.3B were scaled to compare the post-translational glycosylation rates in the presence of Q1 channel subunits. Data (n = 3 – 5) are mean ± SEM for each chase point. Glycosylation states in all panels are labeled: 2-Gly: open square; 1-Gly: closed square; 0-Gly: open circle.

N- terminal sequon during translation whereas glycosylation of the internal site is delayed and less efficient.

Since KCNE peptides are regulatory subunits that co-assemble with K^+ channel subunits in the ER (Krumerman et al., 2004; Chandrasekhar et al., 2006), we next determined whether the presence of K^+ conducting subunits effected post-translational glycosylation of E1 peptides. Cells co-expressing Q1 channel subunits with WT and mutant E1 peptides were pulsed for 2 min and chased at different times to observe post-translational glycosylation (Figure 3.3***C***). Although co-expression with Q1 channel subunits eventually leads to N-glycan maturation in the Golgi complex (*vide infra*), the chase time points needed to detect post-translational glycosylation are too short to observe maturely glycosylated E1. Thus, in these experiments, the immature form of E1 is predicted to be the end glycoform as shown in Figure 3.3***C***. The maximally-glycosylated form of the E1 peptides in the presence of Q1 was calculated from the pulse chase data in Figure 3.3***C***, plotted in Figure 3.3***D***, and compared to post-translational glycosylation of solitary E1 peptides by re-plotting the curves from Figure 3.3***B***. Co-expression with Q1 reduced the overall glycosylation efficiency of the E1 peptides; however, the rate of post-translational glycosylation of WT and N5Q was unaffected. As expected, the glycosylation of N26Q was also relatively unaffected by Q1 co-expression since this mutant primarily acquires its N-glycans during translation. In striking contrast, post-translational glycosylation of T7I was strongly inhibited, suggesting that co-assembly with Q1 channel subunits prevents the OST from attaching an N-linked glycan to the T7I internal sequon.

Consequences of KCNE1 Hypoglycosylation

We subsequently determined whether the compounded hypoglycosylation of the E1 mutants altered their ability to traffic to the cell surface with Q1 subunits. Given the contrasting differences in the current profiles between unpartnered Q1 channels and Q1/E1 complexes (Figure 3.4***A***), we initially used electrophysiology to measure the function of WT and mutant Q1/E1 complexes. Unpartnered Q1 channels give rise to small currents that rapidly activate as well as inactivate with depolarization. In contrast, Q1/E1 complexes have larger currents that slowly activate over many seconds and show no measurable signs of inactivation. Thus, co-assembly with E1 bestows the Q1 channel with the appropriate properties to maintain the rhythmicity of the heartbeat and provide salt and water transport in the inner ear. Co-expression of Q1 with the glycosylation mutants afforded currents that were an amalgam of unpartnered Q1 channels (Figure 3.4***B***, arrowheads) and Q1/E1 complexes. Since the amount of unpartnered Q1 currents varied from cell to cell for each individual mutant, we measured the currents from several cells and normalized current activity relationships for the E1 mutants to WT (Figure 3.4***C***). The systematic decrease in maximal current of the glycosylation mutants followed the hypoglycosylation trend (Figure 3.1***C***), consistent with fewer Q1/E1 complexes functioning at the cell surface.

To directly measure the plasma membrane expression of the mutant E1 peptides co-expressed with Q1 channel subunits, we used cell surface biotinylation. This biochemical approach also allowed for the identification of the E1 glycoforms present on the plasma membrane. Cells expressing WT and mutant Q1/E1 complexes were labeled

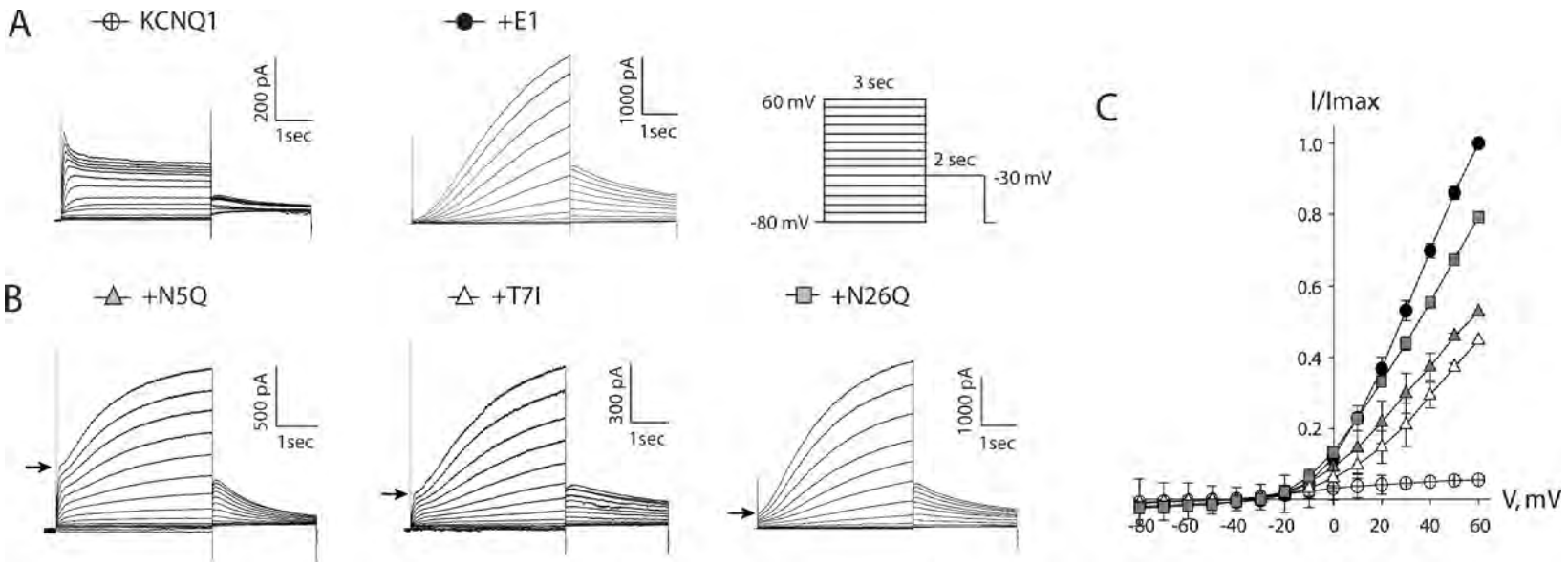
A
KCNQ1
200 pA
1sec
+E1
1000 pA
1sec
3 sec
60 mV
2 sec
-30 mV
-80 mV
B
+N5Q
500 pA
1sec
+T7I
300 pA
1sec
+N26Q
1000 pA
1sec
C
I/Imax
1.0
0.8
0.6
0.4
0.2
-80
-60
-40
-20
0
20
40
60
V, mV

Figure 3.4: Current properties of KCNQ1 channels co-expressed with KCNE1 glycosylation mutants. (***A***) Representative families of I_{Q1} and I_{Ks} currents recorded from CHO cells using the following voltage protocol: the currents were evoked by 3-s depolarization pulses from a holding potential of -80 mV to test voltages –70 to +60 mV in 10-mV increments at an interpulse interval of 30 s. The depolarization pulses were followed by repolarization to –30 mV for 2 s to monitor tail currents. Cells were transfected with a KCNQ1 plasmid only (KCNQ1) or cotransfected with WT KCNE1 (+E1). (***B***) Representative families of currents recorded from cells expressing KCNQ1 and the KCNE1 mutants (+N5Q, +T7I or +N26Q). Arrow is showing the instantaneous current. (***C***) Relative mean peak currents (I/I_{max}) were normalized to the maximal WT I_{ks} (+E1) and plotted as a function of the pulse voltage (V). Data (n = 3 – 5) are mean ± SEM.

with a membrane impermeant, amine-reactive biotin reagent at 4 ˚C to prevent membrane recycling and minimize labeling of intracellular proteins. The biotinylated proteins were isolated with streptavidin beads (Beads) and normalized to their respective endogenous calnexin (CNX) signal (½ Input) to compare the cell surface expression of WT to the E1 mutants (Figure 3.5). To verify that the cells remained intact during biotinylation, we also monitored for labeling of the ER-resident protein, CNX (Beads), and subtracted out this background intracellular labeling to calculate the normalized cell surface expression in Figure 3.4***B***. E1 peptides with a single glycan attached to the N-terminal sequon (N26Q) had cell surface expression that was similar to WT (Figure 3.5) and was dependent on co-expression with Q1 (Figure 3.S5). In contrast, E1 mutants lacking the N-terminal sequon (N5Q, T7I) were challenging to detect at the plasma membrane even when they were co-expressed with Q1.

We next used enzymatic deglycosylation to determine which glycoforms of the mutants were present at the plasma membrane. As we have previously shown with WT Q1/E1 complexes, E1 peptides are post-translationally modified in the Golgi, resulting in a strong, but diffuse band centered between 37 and 50 kDa, which is due in part to the maturation of the N-linked glycans (Chandrasekhar et al., 2006). Using deglycosylation enzymes (Figure 3.S1***B***), we identified the unglycosylated, immaturely and maturely N-glycosylated forms of WT and mutant E1 peptides, which are denoted in Figure 3.5***A***. Although all three glycoforms of WT and the E1 mutants were present in the cells (Figure 3.5***A***, ½ Inputs), only maturely N-glycosylated protein was detected at the cell surface over background calnexin labeling. Moreover, the abundance of intracellular,

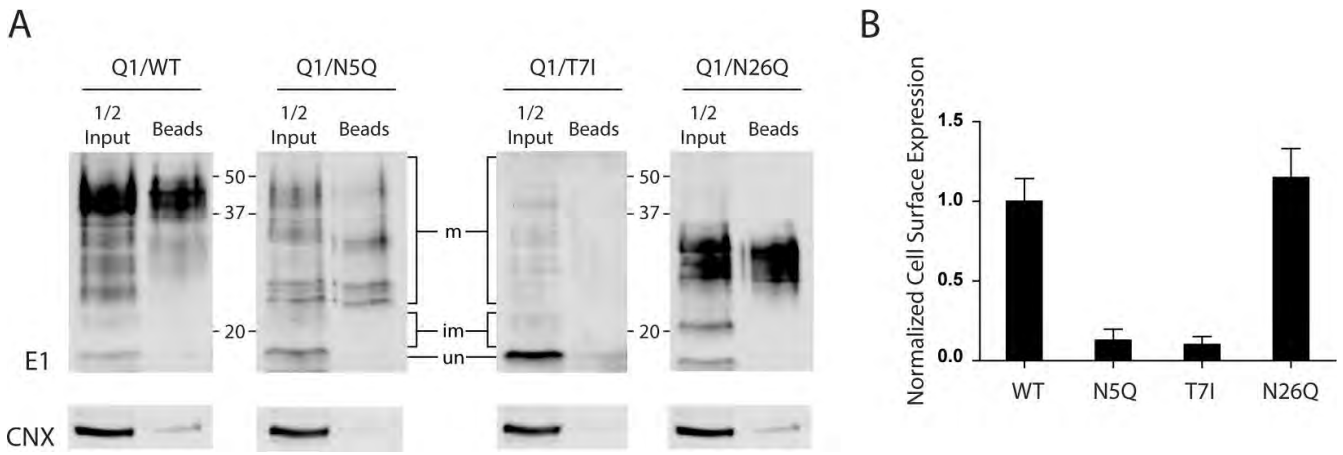
A
Q1/WT
Q1/N5Q
Q1/T7I
Q1/N26Q
1/2 Input
Beads
50
37
20
m
im
un
E1
CNX
B
Normalized Cell Surface Expression
1.5
1.0
0.5
0.0
WT
N5Q
T7I
N26Q

Figure 3.5: Mature KCNE1 glycopeptides reach the plasma membrane. (***A***) Representative immunoblots of WT and the glycosylation mutants co-expressed with KCNQ1. Transfected CHO cells were labeled with a membrane impermeable biotin reagent, lysed, and the biotinylated proteins were isolated with streptavidin beads. Lanes denoted as (½ input) are half the sample lysate that was set aside to quantitate the total amount of biotinylated proteins. (Beads) lanes represent the streptavidin-bound proteins that were isolated and separated by SDS-PAGE. The calnexin (CNX) immunoblots were used both to determine the amount of background lysis and to compare the cell surface expression of the mutants to WT. The mature (m), immature (im) and unglycosylated (un) forms of the E1 glycopeptides were identified by enzymatic deglycosylation (Figure 3.S1). (***B***) Quantification of the biotinylated E1 proteins on the cell surface. Band intensities for biotinylated E1 proteins were calculated as described in the Experimental Procedures and normalized to input calnexin for the corresponding data set. The error bars are SEM from n = 3 – 4 immunoblots.

unglycosylated T7I peptides in the presence of Q1 channel subunits is consistent with inhibiting post-translational glycosylation of T7I in Figure 3.3***D***. In total, these results demonstrate that cell surface expression of E1 peptides requires the acquisition of at least one N-linked glycan to reach the plasma membrane. Thus, mutations that directly prevent co- and reduce post-translational N-glycosylation result in a large population of unglycosylated E1 peptides, which severely reduces the number of Q1/E1 channel complexes at the cell surface.

DISCUSSION

Motivated by the genetic evidence that the N-terminal sequon in KCNE peptides plays an important role in cardiac biology (Schulze-Bahr et al., 1997; Sesti et al., 2000a; Park et al., 2003), we individually examined the kinetics and extent of N-linked glycosylation of the two E1 sequons. The results from our investigation provide four mechanistic insights into the biogenesis and N-glycosylation of these type I transmembrane peptides. (1) The two N-linked consensus sites on E1 are handled differently in the ER: glycans are added to the N-terminal sequon during translation whereas the glycans are predominately attached to the internal site after translation has been completed. (2) Post-translational glycosylation of E1 peptides lacking a co-translational site is less efficient, compounding hypoglycosylation and resulting in a majority of unglycosylated peptides. (3) Co-assembly with Q1 channel subunits additionally inhibits post-translational glycosylation of some mutant E1 peptides. (4) Unglycosylated E1 peptides do not reach the cell surface with or without Q1 K^+ channels. Thus, mutations that inhibit co-translational N-glycosylation reduce the population of functioning Q1/E1 complexes at the cell surface, providing a biogenic mechanism for Long QT and Jervell-Lange Nielsen Syndromes

Post-Translational Glycosylation of Properly Folded KCNE subunits

Post-translational glycosylation has been historically associated with cells that have compromised N-glycosylation machinery (Duvet et al., 2002) or that express

truncated glycoproteins (Kolhekar et al., 1998). All E1 constructs used here are full-length. Moreover, post-translational glycosylation yields the predominant glycoform of E1—the doubly glycosylated form—which folds and assembles with Q1 subunits to afford K^+ channel complexes that generate the hallmark cardiac I_{Ks} current (Figure 3.5). Similarly, post-translational glycosylation of E1 is neither a cell-specific artifact nor a result of depleting the key components of the N-glycosylation pathway. Post-translational glycosylation of E1 was observed in several standard mammalian cell lines (Figure 3.S6***A*** and Figure 3.S6***B***), consistent with the conservation of the STT3B subunit, which has been recently shown to attach N-glycans to secreted proteins after translation (Ruiz-Canada et al., 2009). We also tried to detect post-translational glycosylation in native cells (cardiomyocytes); however, the low endogenous expression of E1 combined with the short radioactive pulse (2 min) did not produce enough labeled protein from an entire rat heart (data not shown). Although exogenous expression of E1 was needed to generate a detectable protein signal, it did not saturate the co-translational machineries or deplete the dolichol-linked oligosaccharides since co-translational glycosylation of endogenous cathepsin C was unaffected. (Figure 3.S6***C***). Taken together, these results suggest that post-translational glycosylation of E1 is a native mechanism that affords assembly-competent regulatory subunits essential for proper electrical excitability.

Proteins with Distinct Co- and Post-translational Sites

To date, only one full-length protein has been identified that has distinct co- and post-translational N-linked glycosylation sites, yet the spacing between the two sites in this secreted, water soluble protein is over 170 residues (Bolt et al., 2005). For a type I

transmembrane peptide with closely-spaced N-linked consensus sites, the cellular mechanisms that define co- and post-translational glycosylation sequons on E1 are likely to be different. One possible explanation for distinct co- and post-translational sequons is that the E1 N-terminus is oriented in the ER translocation tunnel such that the OST complex has access to only the N-terminal sequon. Similarly, the internal sequon could simply be occluded by the translocation tunnel. Previous investigations have utilized the ―rule of 14" for membrane proteins: N-linked consensus sequences need to be at least 12-14 residues away from a transmembrane domain to be a substrate for the OST complex (Nilsson and von Heijne, 1993; Cheung and Reithmeier, 2007). However, the E1 internal sequon satisfies this rule, as it is 18 residues away from the predicted start of the transmembrane segment. Moreover, the E1 internal sequon is glycosylated, it just occurs after translation. Our results suggest the ER proteins responsible for post-translational glycosylation have a different set of structural requirements that define which consensus sites are acceptable substrates.

Post-Translational versus Post-Translocational N-glycosylation

We have shown that the internal sequon of E1 acquires N-linked glycans after translation, but do these modifications occur outside of the protein translocation tunnel? Although we cannot rule out the possibility that some glycans are post-translationally added when the fully-synthesized peptide resides in the translocation tunnel, two experimental observations support a mechanism where post-translational glycosylation occurs after the transmembrane segment slides into the hydrophobic confines of the membrane. Currently, there are two models for the timing of the lateral entry of a

transmembrane segment into the ER membrane based on photo-crosslinking studies. The first model requires the completion of translation before exiting the transloction pore (Do et al., 1996), whereas the second model suggests that certain transmembrane segments can enter the lipid environment before translation is terminated (Heinrich et al., 2000; McCormick et al., 2003). Thus, the observation of N-glycosylation events 10 – 15 minutes after translation of a ~ 150 residue type I transmembrane peptide (Figure 3.3***B***) is consistent with post-translocational glycosylation. Moreover, post-translational glycosylation of the T7I mutant was inhibited by co-expressing Q1 channel subunits (Figure 3.3***D***) that co-assemble with E1 peptides in the ER (Krumerman et al., 2004; Chandrasekhar et al., 2006). Since the protein translocation tunnel cannot simultaneously house a six transmembrane segment Q1 subunit and an E1 peptide, these data support the conclusion that post-translational glycosylation of type I transmembrane peptides occurs outside of the protein translocation tunnel.

Efficiency of Post-Translational N-glycosylation of Type I Transmembrane Peptides

The panel of E1 mutants that we examined revealed some basic structural requirements for post-translational glycosylation of type I transmembrane peptides. First, unlike co-translational glycosylation, long range point mutations (~20 residues) effect post-translational glycosylation, as ablation of the N-terminal sequon with more hydrophobic residues led to less post-translational glycosylation (Figure 3.1***C***). This trend is consistent with the best substrate for post-translational glycosylation, wild type E1, which is decorated with hydrophilic carbohydrates at its N-terminal sequon. Interestingly, we could not detect any post-translational glycosylation of the N26Q

mutant, which suggests that the N-terminal sequon is a poor substrate for post-translational glycosylation. This phenomenon has been previously observed with water soluble proteins where rapid protein folding sequesters the sequon from the OST complex (Ruiz-Canada et al., 2009). However, the N-terminus of E1 is not predicted to have a globular fold nor does it possess any lumenal cysteines for disulfide bond formation. While we could not directly measure post-translational glycosylation of N26Q (Figure 3.3***B***), the steady state populations (0 and 2 glycans) of WT peptides suggest that the N-terminal sequon acquires N-linked glycans post-translationally when the internal sequon is glycosylated. Differences in the degradation rates of the differently glycosylated WT peptides could also explain the lack of the singly glycosylated species; however, the degradation rates of WT and mutant E1 peptides were comparable in the absence of Q1 channel subunits (Figure 3.2). Nonetheless, these data hint that glycan occupancy directly effects post-translational glycosylation efficiency of type I transmembrane peptides.

Cellular Advantages of Doubly-Glycosylated Type I Transmembrane Peptides

The spacing of the N-linked glycosylation consensus sites in E1 is absolutely conserved among vertebrates. Moreover, 4 out 5 human KCNE peptides have at least two N-linked sites and the spacing between the sequons is relatively consistent (16 – 23 aa). A potential benefit of having two sequons is to increase the probability that KCNE peptides are at least singly glycosylated in the ER. KCNE peptides with only an N-terminal sequon would mimic the N26Q mutant, resulting in 30% unglycosylated protein, which is not a substrate for post-translational glycosylation (Figure 3.3***B***). Thus,

unglycosylated KCNE peptides having both sequons that elude the co-translational glycosylation machinery could still acquire at least one N-linked glycan post-translationally, thereby increasing the total pool of glycosylated KCNE peptides in the ER. Although we consistently observed ~ 5 – 10% more glycosylated wild type E1 protein compared to N26Q for the latest chase time points (Figure 3.3), this difference was not experimentally significant. Another potential advantage of a doubly-glycosylated KCNE peptide is that it would improve the interactions (via multivalency) between the lectin family of chaperones in the ER (Helenius and Aebi, 2001), which have been hypothesized to interact with E1 (Chandrasekhar et al., 2006). The initial delay in the decay of WT peptides that we observed is consistent with the notion that the chaperones that recognize N-linked glycans, calnexin and calreticulin, may be more avidly interacting with newly synthesized E1 peptides harboring two glycans (Figure 3.2*B*).

Biogenic Model for Long QT Syndrome

From our results, we propose a model for E1 peptide biogenesis, co-assembly with Q1 channel subunits, and its implications for Long QT and Jervell-Lange Nielsen Syndromes (Figure 3.6). In this model, WT peptides co-translationally acquire an N-terminal glycan before exiting the translocon. Once free from the proteinaceous environment of the translocon, post-translational glycosylation of E1 peptides either occurs before or after co-assembly with Q1 channel subunits (pathways ***a*** and ***b***, respectively). Once fully glycosylated, Q1/E1 complexes exit the ER and traffic to the plasma membrane. For WT peptides, we cannot rule out either pathway ***a*** or ***b*** since co-

expression with Q1 channel subunits had no significant effect on post-translational glycosylation. In contrast, post-translational glycosylation of T7I was inhibited by Q1 co-expression, which shunts the unglycosylated peptides towards co-assembly, resulting in a large population of unglycosylated Q1/T7I complexes that do not reside at the plasma membrane (Figure 3.6, T7I). Therefore, the lack of N-linked glycosylated E1 peptides in the heart would decrease the number of Q1/E1 complexes at the cell surface, leading to a reduction in the cardiac I_{Ks} current and a prolongation of the QT interval. Alternatively, a smaller population of assembly-competent E1 peptides could result in either unpartnered Q1 channels trafficking to the cell surface (as we observed in Figure 3.4*B*) or assembly with different KCNE peptides since the mRNA for all five KCNE peptides is expressed in heart (Bendahhou et al., 2005; Lundquist et al., 2005). Either scenario would result in ill-equipped Q1 channels, which would increase the probability of an arrhythmic event. A similar reduction of Q1/E1 complexes in the developing ear would prevent the proper potassium flux into and thus formation of the endolymphatic space. Given the absolute conservation of the N-terminal site in KCNE peptides, we predict that mutations that prevent N-linked glycosylation in other members of the KCNE family will also compromise K^+ channel complex assembly and give rise to channelopathies.

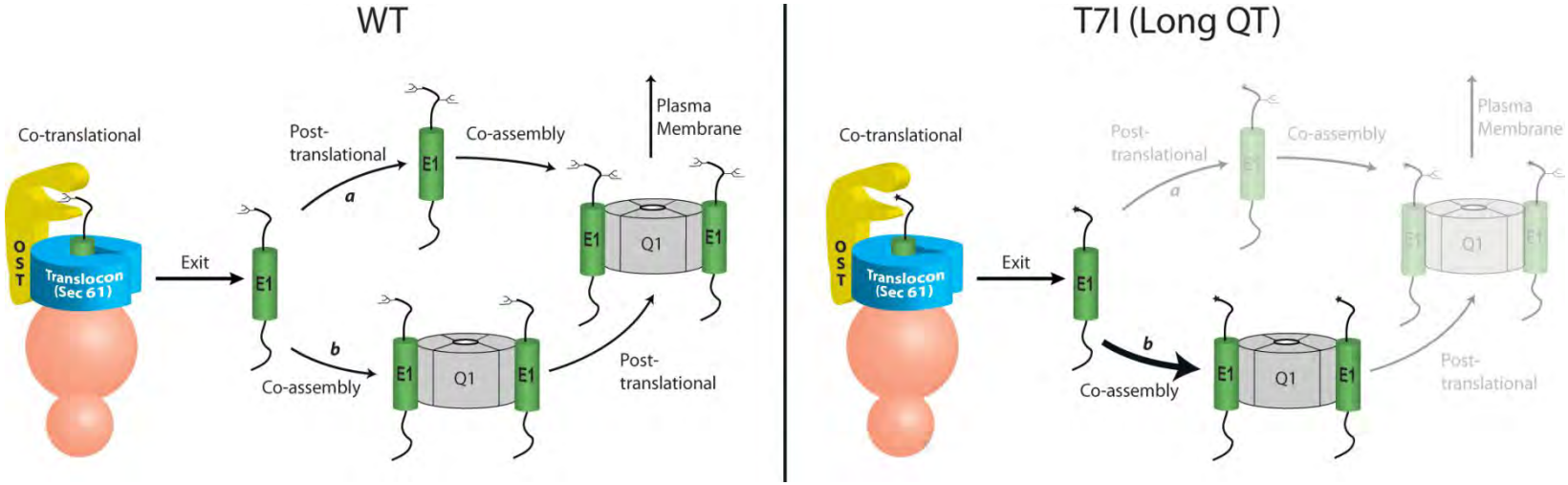
WT
Co-translational
OST
Translocon (Sec 61)
Exit
E1
Post-translational
a
Co-assembly
Plasma Membrane
b
Q1
T7I (Long QT)

Figure 3.6: Model of KCNE1 biogenesis, N-glycosylation and co-assembly with KCNQ1 channels. N-linked glycans are added to the N-terminal sequon (N5) of E1 peptides during translation (Co-translational) and laterally exit the translocon into the membrane. Post-translational glycosylation of WT peptides at N26 occurs either before (***a***) or after (***b***) co-assembly with Q1 channel subunits. Once fully glycosylated, the Q1/E1 complex exits the ER and traffics to the plasma membrane. For the Long QT mutation, T7I, post-translational glycosylation is inhibited by co-assembly with Q1 channel subunits resulting in Q1/E1 complexes that do not reside at the plasma membrane.

SUPPLEMENTARY MATERIAL

Table 3.S1. Statistical Analysis of Glycosylation Mutants[1]

	WT	N26Q	N5Q	T6P	T7A	T7Q	N5I	T7I
WT		ns	***	***	***	***	***	***
N26Q	ns		***	***	***	***	***	***
N5Q	***	***		*	***	***	***	***
T6P	***	***	*		ns	ns	**	*
T7A	***	***	***	ns		ns	ns	ns
T7Q	***	***	***	ns	ns		ns	ns
N5I	***	***	***	**	ns	ns		ns
T7I	***	***	***	*	ns	ns	ns	

[1]Data are from 3 – 6 individual experiments. Tukey's multiple comparison test was used to determine the significantly differently glycosylated mutants as ***, $p < 0.0001$; **, $p < 0.01$; *, $p < 0.05$ (one-way ANOVA with Tukey post-hoc analysis). ns indicates the E1 peptides were not significantly different from each other ($p > 0.05$).

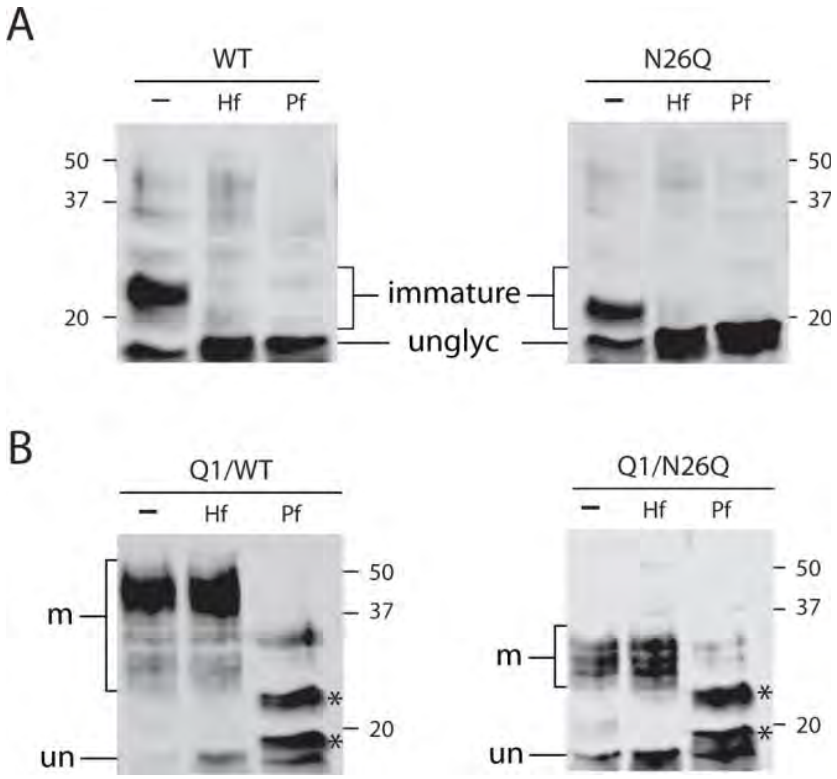
A
WT
N26Q
–
Hf
Pf
50
37
20
immature
unglyc
B
Q1/WT
Q1/N26Q
m
un
*

Figure 3.S1: Identification of the mature, immature and unglycosylated WT and N26Q KCNE1 peptides. Immunoblots are from enzymatic deglycosylation of WT and N26Q KCNE1 peptides. The samples were left untreated (–), digested with Endo H (H_f) or PNGase F (P_f). (***A***) E1 peptides expressed alone. Endo H susceptibility of the 23 kDa band (WT) and the 20 kDa band (N26Q) identified these bands as immaturely glycosylated E1 protein, which collapsed to the ~ 17 kDa unglycosylated form (unglyc). (***B***) E1 peptides co-expressed with Q1 subunits results in the appearance of higher molecular weight bands: WT: ~40 kdD; N26Q: 25 – 30 kD. Resistance to Endo H, but susceptibility to PNGase F identified these higher molecular weight bands as peptides with mature N-linked glycans (m). As was previously reported (Chandrasekhar et al., 2006), exhaustive digestion with PNGaseF results in a series of bands (denoted by asterisks) that are the result of an additional, as of yet unidentified post-translational modification.

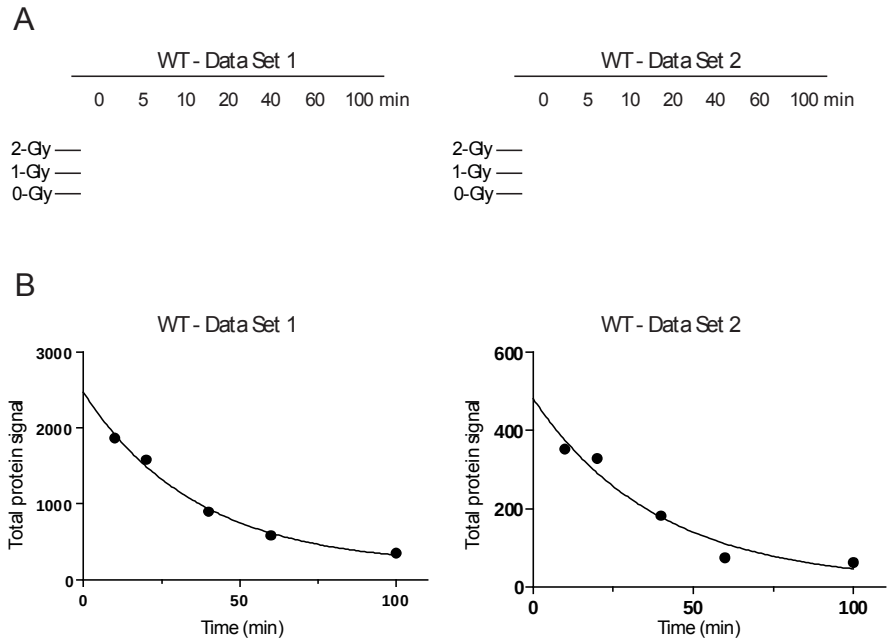

Figure 3.S2: Protein stability of WT KCNE1. ***A***) Representative fluorographs for two WT KCNE1 data sets. Metabolically-labeled CHO cells were pulsed for 10 min and chased for the indicated times. E1 peptides were immunoprecipitated, separated by electrophoresis, and detected by autoradiography. 2-Gly: doubly glycosylated; 1-Gly: singly glycosylated; 0-Gly: unglycosylated. (***B***) Graphs of raw data corresponding to the total protein (glycosylated and unglycosylated) from each data set (Figure 3.S2***A***) plotted as the total protein signal at each time point (0 and 5 min are excluded, since zero time point is diluted with partially synthesized peptides and protein decay is delayed within 10 min). Each signal was quantified by densitometry and plotted versus chase time. Data were fitted to a single exponential and the τ (min) value for Data Set1 is ~~3~~5.9" and Data Set2 is ~~3~~8.7" comparable to the WT τ value for the normalized average protein decay rate 33± 4 min (Table 3.1).

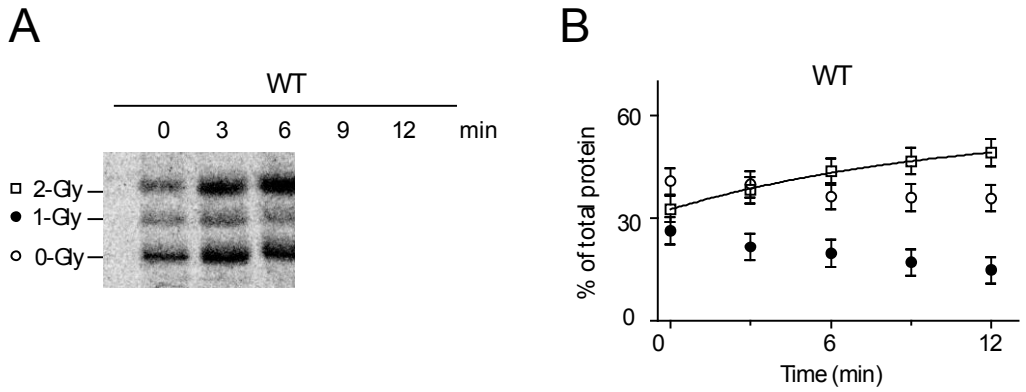

Figure 3.S3: Proteosomal inhibitor, MG132, did not change co- and post-translational N- glycosylation pattern of KCNE1 peptides. (***A***) Representative fluorograph for WT KCNE1 protein. CHO cells were starved, pulsed and chased in media containing 10 μM MG132 to inhibit proteosomal degradation. CHO cells were pulsed for 2 min, chased for the indicated times and the E1 peptides were immunoprecipitated, separated by electrophoresis, and detected by autoradiography. (***B***) Graphs of densitometric analysis for Figure 3.S3***A***. The percentage of the different glycoforms with respect to total protein is plotted for each time point. After 3 min, the fully glycosylated form of WT increased. Data (n = 5) are mean ± SEM for each chase point. Glycosylation states are labeled: 2-Gly: open square; 1-Gly: closed circle; 0-Gly: open circle.

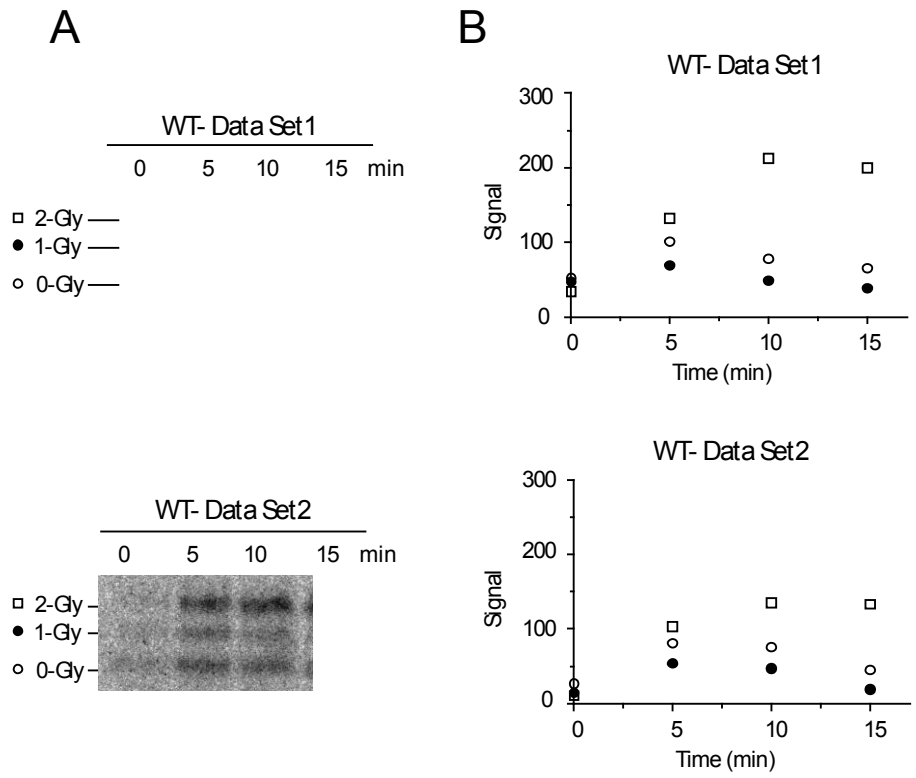

Figure 3.S4: Raw data showing the co- and post-translational N-glycosylation of KCNE1 peptides. (***A***) Representative fluorographs for WT E1 protein. CHO cells were pulsed for 2 min, chased for the indicated times and the E1 peptides were immunoprecipitated, separated by electrophoresis, and detected by autoradiography. (***B***) Graphs of raw data plotted as signal for Figure 3.S4***A***. Signal is plotted for each time point. After 5 min, the fully glycosylated forms of WT increased. Glycosylation states in all panels are labeled: 2-Gly: open square; 1-Gly: closed circle; 0-Gly: open circle.

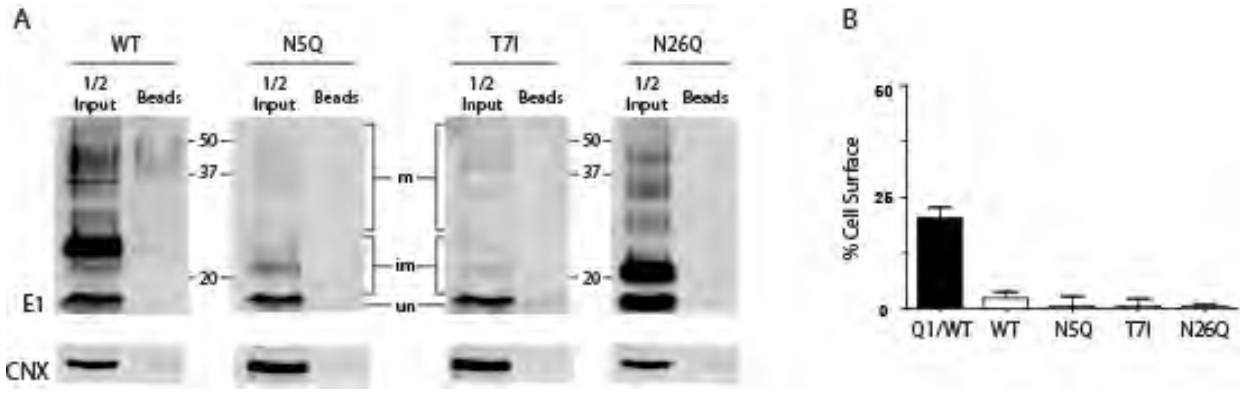
A
WT
N5Q
T7I
N26Q
1/2 Input
Beads
50
37
20
m
im
un
E1
CNX
B
% Cell Surface
60
25
0
Q1/WT
WT
N5Q
T7I
N26Q

Figure 3.S5: Cell surface expression of WT and mutant E1 peptides requires Q1 channels. (***A***) Representative immunoblots of WT and the glycosylation mutants. Transfected CHO cells were labeled with a membrane impermeable biotin reagent, lysed, and the biotinylated proteins were isolated with streptavidin beads. Lanes denoted as (½ input) are half of the sample lysate that was set aside to quantitate the total amount of biotinylated proteins. (Beads) lanes represent the streptavidin-bound proteins that were isolated and separated by SDS-PAGE. The calnexin (CNX) immunoblot was used to determine the amount of background lysis. The mature (m), immature (im) and unglycosylated (un) forms of the E1 glycopeptides were identified by enzymatic deglycosylation (Figure 3.S1). (***B***) Quantification of the biotinylated E1 proteins on the cell surface. To obtain the percentage of E1 protein on the cell surface, the percentage of CNX labeling was subtracted from the percentage of biotinylated E1 protein, which was determined by dividing the band intensities in the beads lane by twice the band intensity in the corresponding half input lanes. Statistically, there was no cell surface expression of E1 peptides when expressed alone: WT: 2.3 ± 1.5 %; N5Q: 0.5 ± 2.2; T7I: 0.3 ± 1.9; N26Q: 0.5 ± 0.2 (open bars). Cell surface expression of WT E1 protein co-expressed with Q1 is shown for comparison (Q1/E1: filled bar) where 20 ± 3 % of the E1 protein on the cell surface. The error bars are SEM from n = 3 – 4 immunoblots.

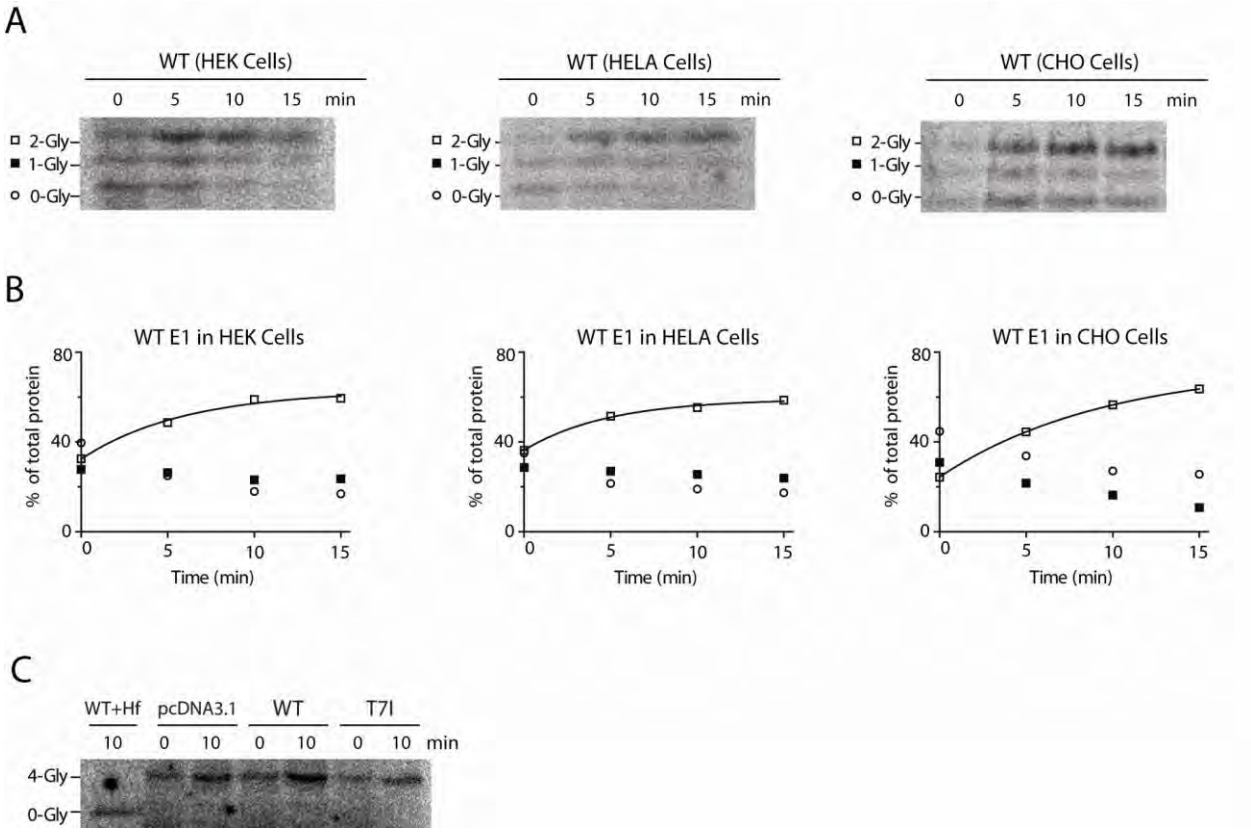
A
WT (HEK Cells)
0 5 10 15 min
2-Gly
1-Gly
0-Gly
WT (HELA Cells)
0 5 10 15 min
2-Gly
1-Gly
0-Gly
WT (CHO Cells)
0 5 10 15 min
2-Gly
1-Gly
0-Gly
B
WT E1 in HEK Cells
% of total protein
80
40
0
0 5 10 15
Time (min)
WT E1 in HELA Cells
% of total protein
80
40
0
0 5 10 15
Time (min)
WT E1 in CHO Cells
% of total protein
80
40
0
0 5 10 15
Time (min)
C
WT+Hf pcDNA3.1 WT T7I
10 0 10 0 10 0 10 min
4-Gly
0-Gly

Figure 3.S6: Post-translational N-glycosylation of exogenously-expressed KCNE1 peptides occurs in various cell types with fully functional co-translational machinery. (***A***) Cells were pulsed for 2 min, chased for the indicated times and the E1 peptides were immunoprecipitated, separated by electrophoresis, and detected by autoradiography. Representative fluorograph for WT E1 expressed in CHO cells is shown for comparison. (***B***) Graphs of densitometric analysis for Figure 3.S6***A***. The percentage of the different glycoforms with respect to total protein is plotted for each time point. After 5 min, the fully glycosylated forms of WT protein increased in all mammalian cell lines. Glycosylation states in all panels are labeled: 2-Gly: open square; 1-Gly: closed square; 0-Gly: open circle. (***C***) Representative fluorograph for human cathepsin C. HeLa cells transfected with empty vector (pcDNA3.1), WT or T7I were pulsed for 2 min, chased for the indicated times. Endogenous cathepsin C was immunoprecipitated, separated by electrophoresis, and detected by autoradiography. Only the fully glycosylated protein (4-Gly) was observed at 0 and 10 min chase points, demonstrating that plasmid-based expression of E1 peptides does not compromise the co-translational N-glycosylation machinery. Endo (Hf) lane was used to identify the unglycosylated protein (0-Gly).

EXPERIMENTAL PROCEDURES

Plasmids and cDNAs. Human Q1 and E1 were subcloned into pcDNA3.1(-) (Invitrogen). E1 constructs (wild type and mutants) possessed a C-terminal HA (YPYDVPDYA) epitope tag (Chandrasekhar et al., 2006). To produce the N5Q, N5I, T6P, T7I, T7A, T7Q and N26Q mutants, site-directed mutagenesis was performed using the QuickChange system (Stratagene) and the mutations were confirmed by DNA sequencing of the entire gene.

Cell culture and transfections. Chinese Hamster Ovary (CHO-K1) cells were cultured in F-12K nutrient mixture (Gibco – Invitrogen). HeLa cells and HEK Cells were cultured in Dulbecco's modified Eagle's medium (Sigma). All of the media were supplemented with supplemented with 10% fetal bovine serum (Hyclone) and 10^2 U/mL penicillin/streptomycin (Gibco – Invitrogen). Cells were plated at 60 – 75 % confluency in 35 mm dishes for all experiments except pulse-chase (60 mm). After 24 h, cells were transiently transfected at RT with Lipofectamine (Invitrogen) 8 µl per mL of Opti-MEMI (Gibco - Invitrogen) for CHO cells or (HeLa cells and HEK Cells) with 10 µl of Lipofectamine 2000 (Invitrogen) per mL of Opti-MEMI and returned to fresh media after 6 hr (2 hr for electrophysiology). DNA ratios (in µg): E1/empty pcDNA 3.1 plasmid: 1.25/1.25; Q1/E1 (Western Blots): 1.25/1.25; Q1/E1 (Pulse-chase): 0.75/1.75; Q1/E1 + pEGFP-C3 (electrophysiology): 0.5/2 + 0.25. Cells were used 48 h post-

transfection for Western Blots; 24 h for pulse-chase and electrophysiological experiments.

Cell lysis and Western Blot Analysis. Cells were washed in ice-cold PBS (3 × 2 mL) and lysed at 4°C in RIPKA buffer (in mM): 10 Tris·HCl, pH 7.4, 140 NaCl, 10 KCl, 1 EDTA, and 1% Triton-X, 0.1% SDS, 1% sodium deoxycholate and supplemented with protease-inhibitors: 1 mM phenylmethylsulfonyl fluoride (PMSF) and 1 µg/mL each of leupeptin, pepstatin and aprotinin (LPA). Lysates were diluted with SDS-PAGE loading buffer containing 100 mM DTT, loaded on a 15% SDS-polyacrylamide gel, transferred to a nitrocellulose membrane, and blocked in Western blocking buffer (5% nonfat dry milk in Tris-buffered saline containing 0.2% Tween-20 (TBS-T)) for 30 min at RT. Membranes were incubated overnight at 4°C with rat anti-HA (Roche) (1:750) in Western blocking buffer and washed in TBS-T next day and incubated with goat anti-rat horseradish peroxidase (HRP)-conjugated antibody (Jackson Immunoresearch Labs, Inc.) (1:2000) in Western blocking buffer for 45 min at RT. Membranes were washed with TBS-T and incubated with SuperSignal West Dura Extended Duration Substrate (Pierce) for 5min. HRP-bound proteins were detected by chemiluminescence using Fujifilm LAS-3000 CCD camera and quantified using the Image Gauge V2.1 software (Fujifilm).

Ezymatic deglycosylation assay. NP-40, BME, and reaction buffer (G5 for Endo H; G7 for PNGase F) were added to the cell lysates (20 µL), which were diluted with water such that the final concentrations were 1% for NP40 and BME. Endo Hf (2 µL) or PNGase F (1 µL) (New England BioLabs, Inc.) were added to the samples and incubated at 37°C for 30 min. The samples were brought to a final concentration of 100 mM DTT

and 1.3% SDS and were separated on an SDS-PAGE (15% gel) and analyzed by Western Blot as described above.

Cell surface biotinylation. Transfected cells were rinsed with ice-cold PBS^{2+} buffer (PBS containing 1 mM $MgCl_2$, 0.1 mM $CaCl_2$), incubated with 1 mg/mL sulfo-NHS-SS-biotin (Pierce) in PBS^{2+} buffer for 2 × 15 min at 4°C. The biotin reagent was quenched by washing with (3 × 2 mL) with quench solution (PBS^{2+} containing 100 mM glycine) and then incubated with quench solution for 2 × 15 min at 4°C. Cells were lysed in RIPKA buffer and cell debris was removed by centrifugation. For each sample, 75 µg of total protein was quantitated by BCA analysis and incubated with 25 µL of Immunopure® Immobilized streptavidin beads (Pierce) overnight at 4°C. One-half of the input (37.5 µg of total protein) was saved as a control for each sample. Beads were washed 3 X with 0.1% SDS buffer (500 µL) and biotinylated proteins were eluted first with 30 µl 2× SDS-PAGE and 200 µM DTT mix for 15 min at 55°C, then with 30 µl 200 µM DTT for 5 min at 55°C and the two elutions were combined to achieve 60 µl final volume. Half of the input and bead-eluted proteins were separated by SDS-PAGE, analyzed by Western Blot as described above, and quantified in the linear range. To compare the cell surface populations of WT to the mutant E1 peptides, the band intensities in the beads lanes were divided by twice the band intensity in the corresponding calnexin ½ input lanes and WT was normalized to 1. Since some cell lysis and intracellular labeling of proteins occurs during biotinylation, the amount of calnexin (CNX) labeling was first subtracted from each biotinylated E1 sample.

Pulse-chase Experiments. Cells were washed in PBS (2 × 2 mL) and starved in Dulbecco's modified Eagle medium (DMEM) high glucose (Gibco - Invitrogen) supplemented with 10% fetal bovine serum (Hyclone) and 102 U/mL penicillin/streptomycin (Gibco – Invitrogen) and 2 mM glutamine (Invitrogen) for 1 hour at 37°C. Then, 100 µCi/mL [^{35}S] methionine and [^{35}S] cysteine (MP Biomedicals, Inc.) was added to the starve media and the cells were pulsed 10 min for decay experiments and 2 min for post-translational glycosylation studies. After the radioactive pulse, cells were washed in PBS (2 × 2 mL) and chased in standard medium at various times. The cells were washed in PBS (2 × 2 mL) and lysed for 30 min at 4°C in 300 µL low salt lysis buffer consisting of (in mM): 50 Tris·HCl, pH 7.4, 150 NaCl, 20 NaF, 10 Na_3VO_4, and 1% NP-40, 1% CHAPS supplemented with protease-inhibitors (PMSF and LPA). To test proteosomal degradation 10 µM MG132 (Calbiochem) was used during 1 hour starvation and for the subsequent steps.

Radioimmunoprecipitation assay. Lysates were pelleted at 16,100 g for 10 min at RT and supernatant was precleared with a slurry of Immobilized Protein G Beads (Pierce) in lysis buffer rotating for 2 hours at 4°C. The beads were pelleted and the precleared supernatants were rotated overnight at 4°C with 25 µl Protein G Beads/ (1 µl) rat anti-HA (Roche) antibody mix or with 25 µl Protein G Beads/ (1 µl) goat anti-human cathepsin C (R&D Systems) antibody mix. The beads were pelleted at 16,100 g for 10 min at RT and washed 2 X in low salt lysis buffer and then with 2 X in high salt buffer consisting of (in mM): 50 Tris·HCl, pH 7.4, 500 NaCl, 20 NaF, 10 Na_3VO_4, and 1% NP-40, 1% CHAPS, followed by a final wash with low salt lysis buffer. For cathepsin C

enzymatic deglycosylation assay beads were resuspended in 400 µl low salt lysis buffer with Endo Hf (20 µL) (New England BioLabs, Inc.) and incubated at 37°C for 1 hour followed by a final wash with low salt lysis buffer. The washed and pelleted beads were eluted in 50 µL of 2 X SDS and 100 mM DTT mix at 55^{o}C for 15 min. Supernatants were separated by SDS-PAGE (15%) and visualized by autoradiography. Signals were captured on a FLA-3000 phosphorimager and quantified using the Image Gauge V2.1 software (Fujifilm). The rates of protein decay and post-translational glycosylation were fitted to a single exponential.

Perforated Patch Whole-Cell Recordings. IKCNQ1 and IKs were recorded in the whole-cell perforated patch configuration. Briefly, on the day of the experiment cells were seeded on the surface of cover glass and placed to a custom recording bath filled with a modified Tyrode's solution contained (in mM) 145 NaCl, 5.4 KCl, 10 HEPES, 5 $CaCl_2$ (pH 7.5 with NaOH). Transfected (eGFP-expressing) cells were selected using an Axiovert 40 CFL inverted light microscope (Zeiss). For the perforated patch configuration, a glass electrode (pipette resistance: 2.5-3.5 MΩ) filled with internal electrode solution contained (in mM) 126 KCl, 1 $MgSO_2$, 0.5 $CaCl_2$, 5 EGTA, 4 K_2-ATP, 0.4 GTP, 25 HEPES (pH 7.5 with CsOH), and 60 µg/ml Amphotericin B (Sigma; prepared in DMSO) was attached to the cell. Once a GΩ seal was achieved and access resistance was dropped to the level enough to record membrane potential (<15 MΩ), Tyrode's solution was replaced with the extracellular bath solution contained (in mM) 160 NaCl, 2.5 KCl, 2 CaCl2, 1 MgCl2, 8 glucose, and 10 HEPES (pH 7.5 with NaOH). Initially, the electrical access to the inside of the cell was monitored using 3-sec

depolarizing test pulse from the holding potential of -80 mV to +20 mV taken every 15 sec. Cells with pronounced rundown were discarded, and only those expressed stable currents were used. The I_{Q1} and I_{Ks} currents were elicited using a family voltage protocol described in Figure legend 4. All measurements were performed at room temperature (24±2°C).

CHAPTER IV

Investigating the Relative Importance of the two glycosylation sites on KCNE1: Structure-Function Deletion Scans and Positional Glycosylation Studies

Contributors to the work presented in Chapter IV:

The author of this thesis, Tuba Bas performed all the experiments, but the immunoblot for the the KCNE1 double mutant (N5Q;S28T) was kindly generated by Yuan Gao.

ABSTRACT

The KCNE peptides are a class of type I transmembrane N-linked glycoproteins that assemble with a variety of voltage-gated K^+ channels in a tissue specific manner. KCNE β-subunits modulate the gating and ion conducting properties of K^+ channels; formation of these heteromeric complexes enhances K^+ current diversity. In the heart and inner ear, KCNE1 co-assembles with KCNQ1 to form a voltage-gated K^+ channel complex. Genetic mutations in either KCNE1 or KCNQ1 give rise to inherited cardiac arrhythmicities and neural deafness, namely Romano-Ward and Jervell-Lange-Nielsen Syndrome (JLNS). The JLNS mutation, T7I, indirectly prevents glycosylation at one of the two N-linked glycosylation sites on KCNE1. In order to elucidate the positional importance of N-linked glycosylation of KCNE1, we constructed a C-terminally HA-tagged KCNE1 that behaves like the wild type KCNE1 protein in terms of channel assembly and function. Using this construct, we showed that the glycosylation site proximal to the KCNE1 N-terminus (N5) was critical for the formation of KCNE1 protein, whereas removal of the second glycosylation site (N26) had no significant effect on KCNE1 protein expression and assembly. To further investigate the structural requirements of KCNE1 glycosylation, we generated structure-function deletion scans of KCNE1 and performed positional glycosylation scanning mutagenesis. Examination of the biogenesis and complex formation of these mutants with the channel partner KCNQ1, will define the glycosylation window that is important for proper KCNE1 assembly and trafficking.

INTRODUCTION

Asparagine-linked (N-linked) glycosylation is the most common covalent modification in eukaryotic cells (Helenius and Aebi, 2004). In the endoplasmic reticulum (ER), N-linked glycosylation involves the transfer of high-mannose oligosaccharides onto asparagine residues within the primary sequence N-X-T/S (Marshall, 1972; Silberstein and Gilmore, 1996). This consensus sequence is recognized by oligosaccharyl-transferase (OST) complex for glycosylation as the first 12-14 residues of the nascent protein appear from the translocation pore into the lumen of the ER (Nilsson and von Heijne, 1993). The factors that effect the N-glycan transfer on the asparagine of N-X-T/S involve the residues at X-position, proximity to C-terminus and proximity to transmembrane domain. Negatively-charged residues (Asp and Glu), hydrophobic amino acids (Trp and Leu) and proline at the X-position are poorer substrates for the OST complex (Marshall, 1972; Shakin-Eshleman et al., 1996; Silberstein and Gilmore, 1996; Kasturi et al., 1997). The distance between the sequons and the C-terminus should be at least ~ 60 residues to give enough time for the OST complex to recognize sequon and for efficient co-translational glycosylation (Nilsson and von Heijne, 2000). Also, N-linked glycosylation sites should be more than 12 residues away from the transmembrane segment to be accessible to the OST active site (Nilsson and von Heijne, 1993; Cheung and Reithmeier, 2007). To date, there are no other identified sequence motifs that have long range effects on N-glycosylation efficiency (Gavel and von Heijne, 1990; Ben-Dor et al., 2004).

Although commonly referred to as a post-translational modification, N-linked glycosylation typically occurs during translation. Recently, however, post-translational N-glycosylation of a secreted protein, human blood coagulation factor VII, has been observed in cells with intact N-glycosylation machinery (Bolt et al., 2005; Ruiz-Canada et al., 2009). Factor VII has two sequons that are ~170 amino acids apart. Surprisingly the sequon closest to the N-terminus is modified co-translationally, whereas the second sequon is modified post-translationally. Unfortunately, the requirements of this relative behavior of the two N-linked glycosylation sites on Factor VII are not clear.

KCNE1 is a K^+ channel β-subunit that modulates the function of its partnering α-subunits in a tissue specific manner. In the heart, KCNE1 co-assembles with KCNQ1 (Q1) K^+ channels to produce the slowly activating cardiac I_{Ks} current (Barhanin et al., 1996; Sanguinetti et al., 1996). In the inner ear, the KCNE1/KCNQ1 channel complex recycles potassium (Wangemann, 2002). KCNE1 is a type I transmembrane glycoprotein with two sequons at N5 and N26 facing the extracellular media. Both glycosylation sites satisfy the known N-linked glycosylation rules: they are more than ~60 residues away from the C-terminus and more than ~12 residues away from the transmembrane domain. Only the sequon that is closest to the N-terminus is conserved in all KCNE family members (1-5) (Figure 1.4***A***). Patients with genetic mutations effecting the first sequon in KCNE proteins give rise to congenital or acquired Long QT Syndrome (LQTS) (Schulze-Bahr et al., 1997; Abbott and Goldstein, 2001; McCrossan and Abbott, 2004). Our studies showed that the first N-linked glycosylation site in KCNE1 is indespensible for proper protein expression and function (Chapter III). Moreover, the sequon closest to

the N-terminus is modified co-translationally and the internal N-linked glycosylation site is modified post-translationally just like Factor VII (Chapter III). Factor VII is a secreted, water soluble protein; therefore KCNE1 is the only known transmembrane protein that acquires glycans posttranslationallly. When comparing the two proteins it is hard to deduce any patterns for posttranslational glycosylation since the distance between the two sequons in Factor VII is ~170 residues, whereas in KCNE1 they are only 21 amino acids apart. What determines the differential N-linked glycosylation behavior of the two closely-spaced N-linked consensus sites on KCNE1 remains to be uncovered.

In this study, I have changed the microenvironments of the two N-linked glycosylation sites on KCNE1 in order to understand the relative importance of sequon position. In the structure-function deletion scans, I had two sets of mutants. In the first group I truncated the N-terminus, bringing it closer to the internal sequon (N26). In the second group I systematically brought the first sequon (N5) closer to the transmembrane domain through internal deletions. I also repositioned the internal sequon (N26) in a KCNE1 null glycosylation background (N5Q; N26Q) by sliding this consensus sequence (N26) closer to the N-terminus and away from the transmembrane domain. These experiments revealed a likely pattern that could reflect the differential glycosylation of the two sequons on KCNE1. Lastly, in order to make the internal glycosylation site (the post-translational glycosylation site) a more desirable substrate for OST complex (Kasturi et al., 1997), we changed the serine of the second sequon to a threonine (S28T). Surprisingly, we found that this change was enough to convert the post-translational glycosylation site to a co-translational glycosylation site on KCNE1.

RESULTS

N-terminal truncations

In Chapter III, we discovered that the N-terminal sequon is co-translationally glycosylated; whereas glycans are attached to the internal sequon predominantly post-translationally. What distinguishes the behavior of the two sequons remains to be elucidated. Therefore, in order to investigate the difference between the two sequons, we constructed a series of N-terminal truncation mutations of the KCNE1 protein (Figure 4.1***A***). We systematically brought the internal glycosylation site (N26) closer to the N-terminus to find the optimal distance required to rescue E1 protein expression. In order to prevent the interference of a probable internal start site, we used a mutant KCNE1 background, M27V, and confirmed that M27V had no effect on KCNE protein expression and function (Figure A2.5***A***, Appendix II). The expression and glycosylation state of the resultant mutant proteins were tested in CHO cells (Figure 4.1***B***).

Figure 4.1***B*** shows that E1 and Δ(2-4) bear two glycosylation sites when fully glycosylated, yielding a strong band at 23 kDa on a Western blot corresponding to the immaturely N-linked glycosylated peptides. N26Q;M27V both lacking the second sequon, served as positive control to follow monoglycosylated KCNE1. Unglycosylated E1 protein appears at ~17 kDa on a western blot, which was confirmed by enzymatic deglycosylation assays (Figure 3.S1, Chapter III). Unexpectedly, none of the N-terminal truncation mutants, Δ(2-10), Δ(2-16), Δ(2-22), were able to rescue the E1 protein

expression; therefore bringing the internal glycosylation site (N26) closer to the N-terminus was not sufficient for proper glycosylation. Elimination of the first glycosylation site by deletion has the similar effect as T7I mutation.

Internal deletions

Having demonstrated that the distance from the N-terminus was not the main criteria for efficient glycosylation of the internal sequon (N26) on KCNE1, we altered the distance from the transmembrane domain to determine the minimal distance required to keep the N-terminal sequon (N5) glycosylated. We made a panel of internal deletion mutants, systematically bringing the N-terminal glycosylation site (N5) closer to the transmembrane domain (Figure 4.2***A***). All constructs possessed N26Q, since we have previously shown that ablation of the internal sequon (N26) had no significant effect on glycosylation of the N-terminal sequon (Figure 3.1, Chapter III). 48 hours post-transfection, expression and glycosylation of E1 internal deletion mutants were analyzed on a western blot (Figure 4.2B). We used E1 and N26Q as positive controls, where we could follow the unglycosylated (17 kDa), monoglycosylated (20 kDa) and doubly glycosylated (23 kDa) forms of the E1 protein.

All internal deletion mutants, Δ(8-10), Δ(8-16), Δ(8-22), Δ(8-28) showed a reduction in glycosylation efficieny at N5 (Figure 4.2***B***). Unlike the expected strong band observed at 20 kDa corresponding to the monoglycosylated form of N26Q, the internal deletion mutants resolved as a smear above the unglycosylated band. Interestingly, even the three amino acid deletion Δ(8-10), was not tolerated, and resulted

A

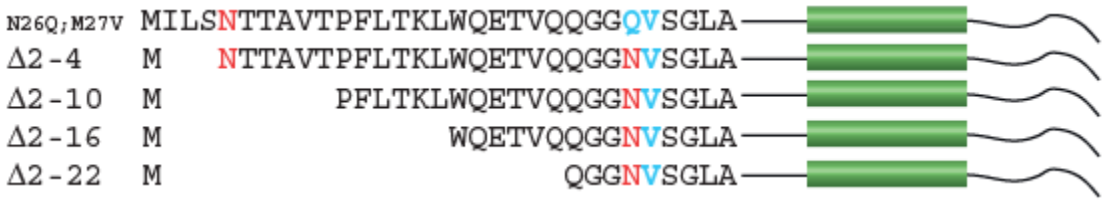
N26Q;M27V MILSNTTAVTPFLTKLWQETVQQGGQVSGLA
Δ2-4 M NTTAVTPFLTKLWQETVQQGGNVSGLA
Δ2-10 M PFLTKLWQETVQQGGNVSGLA
Δ2-16 M WQETVQQGGNVSGLA
Δ2-22 M QGGNVSGLA

B

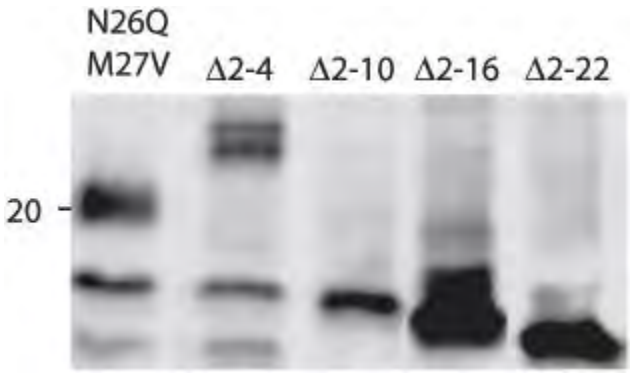
N26Q
M27V
Δ2-4
Δ2-10
Δ2-16
Δ2-22
20

Figure 4.1: **KCNE1 N-terminal truncation mutants were not efficiently glycosylated as N26Q**. ***A***. A panel of truncation mutants was made using PCR methods. The internal glycosylation site (N26) was systematically brought closer to the N-terminus in M27V background. The deletion mutants were named as the residue numbers of deleted amino acids in parenthesis following the mark –Δ". ***B***. CHO were cells transiently transfected with N26Q;M27V and the N-terminal truncation mutants (Δ(2-4), Δ(2-10), Δ(2-16), Δ(2-22)). After 48 hours, cells were lysed and samples were resolved on an SDS-PAGE. N26Q;M27V and Δ(2-4) served as positive controls, where we could follow the double and single glycosylated forms of the E1 protein. A ~23 kDa band, Δ(2-10), corresponds to the double glycosylated protein, ~20 kDa band (N26Q;M27V) monoglycosylated protein and ~17 kDa unglycosylated form (Figure 3. S1).

in an abundance of unglycosylated proteins corresponding to the 17 kDa band (Figure 4.2***B***). Moreover, the Δ(8-10) showed the most severe phenotype, which may be due to bringing the consensus N-linked glycosylation site right next to the structurally-distorting proline residue, P11 (*vide infra*). When co-expressed with the channel partner, KCNQ1, all mutants but Δ(8-10) showed a faint banding pattern between 25 and 37 kDa (data not shown). However, these bands did not exactly match the maturely monoglycosylated E1 protein (N26Q) and might be due to O-linked glycosylation of the KCNE1 peptides (personal communication with Kshama Chandrasakher).

Since large internal deletions were not well tolerated, and the smallest deletion Δ(8-10) may have been distrupted by P11, we decided to check the effect of small internal deletions on N5 while keeping the sequon farther from P11 (Figure 4.2***C***). We brought the N-terminal sequon one residue closer to the transmembrane domain in the Δ8 mutation and two residues closer with the Δ(8-9) deletion. We found that these small internal deletions were well tolerated. We observed an unglycosylated band at ~17 kDa and a monoglycosylated band at ~20 kDa (Figure 4.2***D***). Both Δ8 and Δ(8-9) behaved like N26Q.

Up to now our data implied that the exact position of N5 was critical for efficient glycosylation and within the protein sequence only small changes were tolerated for proper N-linked glycosylation.

A

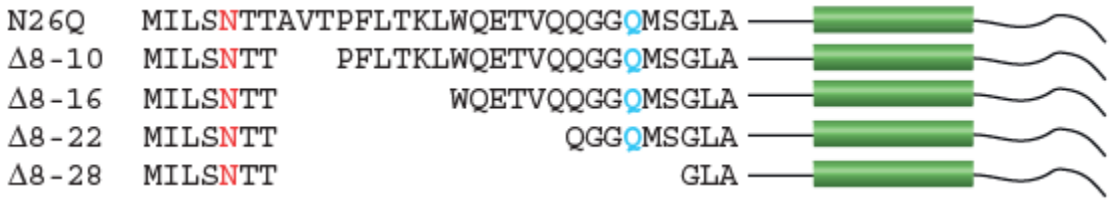
N26Q MILSNTTAVTPFLTKLWQETVQQGGQMSGLA
Δ8-10 MILSNTT PFLTKLWQETVQQGGQMSGLA
Δ8-16 MILSNTT WQETVQQGGQMSGLA
Δ8-22 MILSNTT QGGQMSGLA
Δ8-28 MILSNTT GLA

B

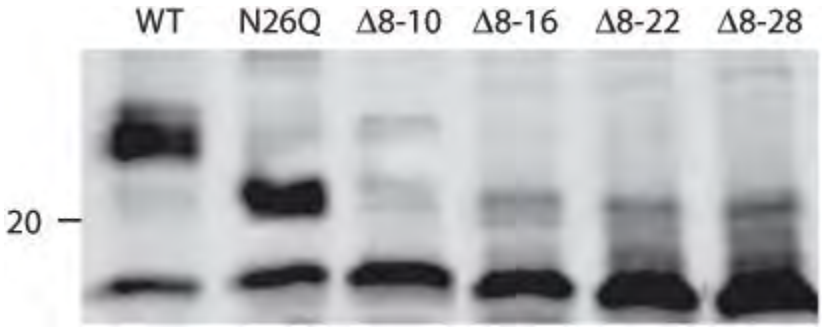
WT
N26Q
Δ8-10
Δ8-16
Δ8-22
Δ8-28
20

C

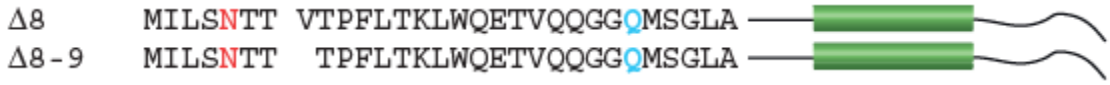
Δ8 MILSNTT VTPFLTKLWQETVQQGGQMSGLA
Δ8-9 MILSNTT TPFLTKLWQETVQQGGQMSGLA

D

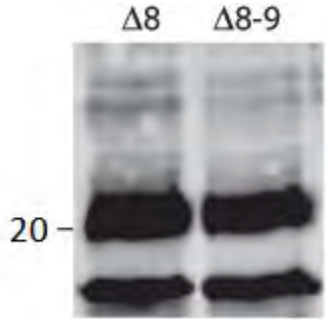
Δ8
Δ8-9
20

Figure 4.2: **Only single, Δ8 or double amino acid deletions, Δ(8-9) were allowed for effective glycosylation at N5**. (***A) & (C)***. A panel of internal deletion mutants was made using PCR methods. Transmembrane domain was brought closer to the N-terminal sequon (N5) systematically in N26Q background. The internal deletion mutants were named as the residue numbers of deleted amino acids in parenthesis following the mark "Δ". (***B) & (D)***. CHO cells were transiently transfectedwith WT, N26Q, and the internal deletion mutants (Δ(8-9), Δ(8-10) Δ(8-16), Δ(8-22), Δ(8-28)). After 48 hours, cells were lysed and samples were resolved on an SDS-PAGE. WT and N26Q served as positive controls, where we could follow the double and single glycosylated forms of the E1 protein when expressed alone (~23 kDa band (WT), double glycosylated protein; ~20 kDa band (N26Q) monoglycosylated protein; ~ 17 kDa (WT and N26Q) unglycosylated protein).

Positional glycosylation mutants

Since the N-terminal truncation mutants and the internal deletion mutants did not significantly improve our understanding of the differential behavior of the two N-linked glycosylation sites on KCNE1, we made a panel of positional glycosylation mutants to investigate the effect of changes in the microenvironment of the sequon (Figure 4.3***A*** & ***C***). Within the N5Q;N26Q;M27V background, we repositioned the sequon at residues 26-28, sliding this consensus sequence in triplets within the N-terminus. M27 was mutated to a valine in order to prevent replacing a probable internal translational start site (Figure A2.5***A***, Appendix II).

We examined the expression and glycosylation of the mutant E1 proteins (Figure 4.3***B*** & ***D***) 48 hours post-transfection. We observed a ~17 kDa band for unglycosylated E1 for all the positional glycosylation mutants (P1 through P6); however, only mutants P3 and P6 resolved to the 20 kDa monoglycosylated E1 protein (Figure 4.3***B*** & ***D***).

Knowing that one or two residue deletions were tolerated (*vide supra*), we wanted to test the effect of small amino acid changes on the first glycosylation site, rather than sliding the internal sequon (-NVS-) in triplets. Therefore, we constructed two more positional glycosylation mutants, P1a and P1b (Figure 4.3***E***). P1a and P1b resolved as monoglycosylated protein (Figure 4.3***F***), yet surprisingly the signal level was nowhere near that of the monoglycosylated glycoforms of P3 or P6 (Figure 4.3 ***B*** & ***D***).

A

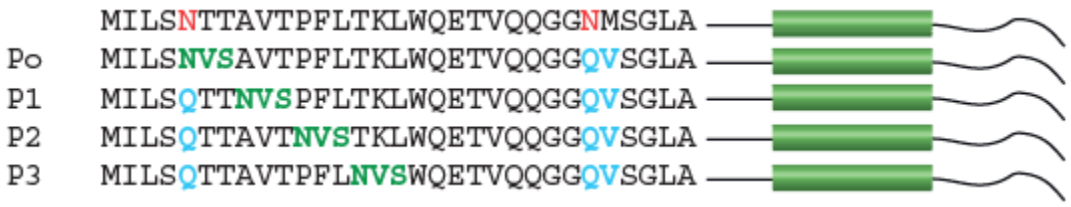
MILSNTTAVTPFLTKLWQETVQQGGNMSGLA
Po MILSNVSAVTPFLTKLWQETVQQGGQVSGLA
P1 MILSQTTNVSPFLTKLWQETVQQGGQVSGLA
P2 MILSQTTAVTNVSTKLWQETVQQGGQVSGLA
P3 MILSQTTAVTPFLNVSWQETVQQGGQVSGLA

B

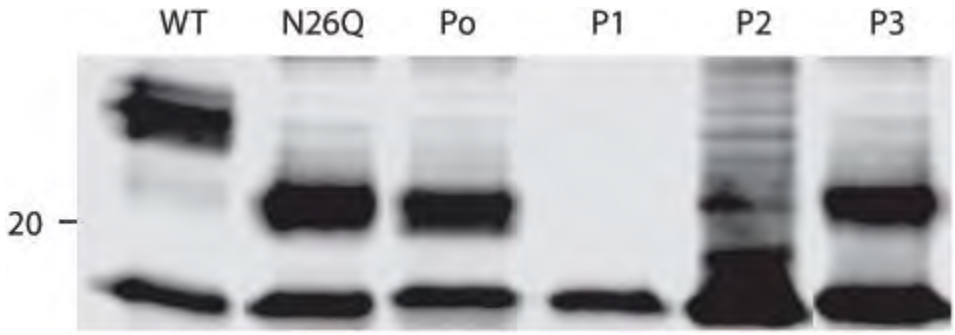
WT
N26Q
Po
P1
P2
P3
20

C


P4 MILSQTTAVTPFLTKLNVSTVQQGGQVSGLA
P5 MILSQTTAVTPFLTKLWQENVSQGGQVSGLA
P6 MILSQTTAVTPFLTKLWQETVQNVSQVSGLA

D

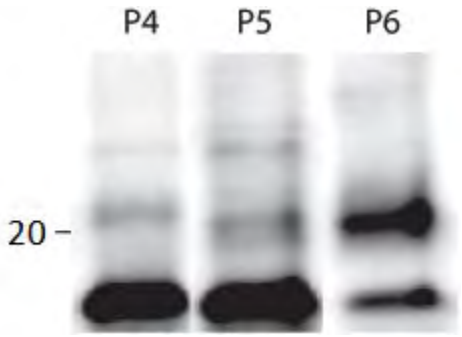
P4
P5
P6
20

E

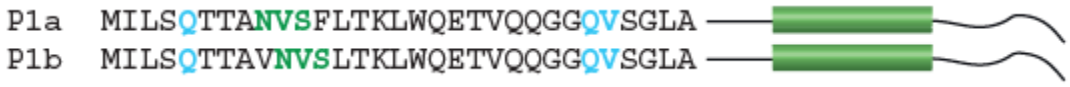
P1a MILSQTTANVSFLTKLWQETVQQGGQVSGLA
P1b MILSQTTAVNVSLTKLWQETVQQGGQVSGLA

F

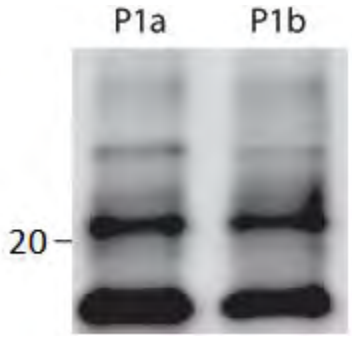
P1a
P1b
20

Figure 4.3: **Positional glycosylation mutants presented a 9 amino acid periodicity for efficient glycosylation**. (***A) & (C) & (E)***. A panel of positional glycosylation mutants were made and named as numbers indicating the position of the internal sequon (-NVS-) relative to the N-terminus following the mark "P". PCR methods were used to systematically move the consensus glycosylation sequence (-NVS-) in triple mutant background (N5Q;N26Q;M27V) towards the transmembrane domain. (***B) & (D) & (F)***. CHO cells were transiently transfected with WT, N26Q and the positional glycosylation mutants (Po, P1, P2, P3, P4, P5, P6, P1a, P1b). After 48 hours, cells were lysed and samples were resolved on an SDS-PAGE. WT, Po and N26Q served as positive controls, where we could follow different glycoforms of the E1 protein.

Changing the serine of the second sequon to a threonine

We wanted to test whether the internal sequon (N26) would be glycosylated more efficiently if S28 was replaced with a threonine residue (Figure 4.4***A***) (Kasturi et al., 1997). We expressed the N5Q; S28T double mutant in CHO cells alone and with KCNQ1. After 48 hours, we examined the cell surface expression and glycosylation of the double mutant E1 protein by performing cell surface biotinylation and resolving the samples on an SDS-PAGE. (Figure 4.4***B***). We observed a ~17 kDa band for unglycosylated E1 and a band at ~20 kDa, corresponding to the monoglycosylated E1 protein. In the presence of Q1, we observed the typical slow migrating bands at 25 – 30 kDa for mature monoglycosylated E1 protein that could also be detected on the cell surface. Surprisingly, changing the serine of the second sequon to a threonine (S28T) was sufficient to overcome the N5Q phenotype (Figure 4.4***B***). Moreover, we found that this change was enough to convert the internal post-translational glycosylation site on KCNE1 (N26) to a co-translational glycosylation site (Data not shown).

A

B

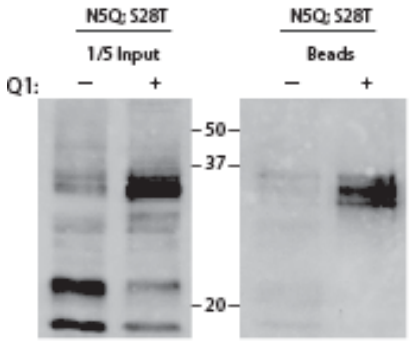

Figure 4.4: **Converting S28 to a threonine was sufficient to suppress N5Q phenotype**. (***A***) The internal sequon (N26) was changed to a better glycosylation site by mutating the S28 to a threonine (Kasturi et al., 1997) via site-directed mutagenesis in N5Q background. (***B***) N5Q;S28T was expressed in CHO cells alone and with KCNQ1 (Q1). Cell surface biotinylation assay (Experimental Procedures) was performed after 48 hours and the data was analyzed on a western blot. "1/5 of the input" lanes are showing the expression of the double mutant w and w/o Q1; "Beads" lanes are showing the bead-eluted proteins. ~17 kDa band corresponds to unglycosylated E1 protein and ~20 kDa band shows monoglycosylated E1 protein. In the presence of Q1, ~30 kDa band is indicative of mature monoglycosylated E1 proteins on the cell surface. (This data is kindly generated by Yuan Gao).

DISCUSSION

Previously, we have shown that the distruption of the N-terminal sequon (N5) and increasing its hydrophobicity had long range effects on the glycosylation of the internal sequon (N26) and prevented the efficient glycosylation of N26 (Figure 3.1***A*** and Figure 3.1***B***, Chapter III). To date, there are no other identified sequence motifs that have long range effects on N-glycosylation efficiency (Gavel and von Heijne, 1990; Ben-Dor et al., 2004). In order to understand the structural requirements that determine the relative N-glycosylation behavior of the two sites, N5 and N26, we changed the microenvironments of the two sequons on KCNE1.

Structure-function deletion scans were not conclusive

We performed structure-function deletion scans with two sets of mutants: N-terminal truncation mutants and internal deletion mutants. We wanted to see whether the relative position of the first glycosylation site (N5) to the N-terminus was responsible for the efficient glycosylation of this sequon. To test this, we designed N-terminal truncations to bring the N-terminus closer to the internal sequon (N26) in order to rescue the N5Q phenotype. Our results showed that none of the N-terminal truncation mutants, even the Δ(2-22) (in which N26 is four residues from M1) increased the glycosylation efficiency. We concluded that the relative distance from the N-terminus did not significantly contribute to the N-linked glycosylation at N5.

We then tested the internal deletion mutants. These mutants allowed us to systematically bring the first sequon (N5) closer to the transmembrane domain. We have observed a slightly better glycosylation pattern with the internal deletion mutants compared to N-terminal truncation mutants, yet still we did not see a robust monoglycosylated protein expression as N26Q. Only single or double amino acid deletions, Δ8 and Δ(8-9), allowed for an effective glycosylation at N5, suggesting a probable link between efficient glycosylation and the relative position of the sequon to the transmembrane domain.

Positional glycosylation mutants suggest a positional periodicity for N-glycosylation

Next, in a null glycosylation KCNE1 background (N5Q; N26Q) we changed the microenvironment of the internal sequon (N26) by repositioning it within the N-terminus. We moved the sequon at N26 closer to the N-terminus and away from the transmembrane domain in triplets in an effort to avoid distrupting helicity. These positional glycosylation scans showed that bringing the glycosylation site to every other 9th residue, namely P0, P3, P6, resulted in glycosylation. This suggested a periodicity for the efficient glycosylation of the sequon, which might be due to the accessibility of the sequon to the OST complex. Interestingly, the N-terminally HA-tagged KCNE1 introduces 9 amino acids between the residues Q22 and Q23, pushing the first glycosylation site 9 residues away from transmembrane domain. Functionality and glycosylation efficiency of this tagged KCNE1 protein also favors the same glycosylation pattern.

The glycosylation pattern observed with these mutants is now being tested by Yuan Gao in collaboration with the Gilmore Lab, through 2 min pulse-chase radioactive labeling experiments.

EXPERIMENTAL PROCEDURES

Plasmids and cDNAs. Human Q1 and E1 were subcloned into pcDNA3.1(-) (Invitrogen). E1 constructs (wild type and mutants) possessed a C-terminal HA (YPYDVPDYA) epitope tag (Appendix II). To produce the positional glycosylation mutants, site-directed mutagenesis was performed using the QuikChange® system (Stratagene). For deletion mutants a combination of PCR techniques, enzyme digestion and ligation procedures were utilized. All the mutations were confirmed by DNA sequencing of the entire gene.

Cell culture and transfections. Chinese Hamster Ovary (CHO-K1) cells were cultured in F-12K nutrient mixture (Gibco – Invitrogen). The media was supplemented with 10% fetal bovine serum (Hyclone) and 10^2 U/mL penicillin/streptomycin (Gibco – Invitrogen). Cells were plated at 60 – 75 % confluency in 35 mm dishes for all experiments. After 24 h, cells were transiently transfected at RT with Lipofectamine (Invitrogen) 8 µl per mL of Opti-MEMI (Gibco - Invitrogen) and returned to fresh media after 6 hr. DNA ratios (in µg): E1/empty pcDNA 3.1 plasmid: 1.25/1.25; Q1/E1 (Western Blots). Cells were used 48 h post-transfection for western blots.

Cell lysis and Western Blot Analysis. Cells were washed in ice-cold PBS (3 × 2 mL) and lysed at 4°C in RIPKA buffer (in mM): 10 Tris·HCl, pH 7.4, 140 NaCl, 10 KCl, 1 EDTA, and 1% Triton-X, 0.1% SDS, 1% sodium deoxycholate and supplemented with protease-inhibitors: 1 mM phenylmethylsulfonyl fluoride (PMSF) and 1 µg/mL each of leupeptin, pepstatin and aprotinin (LPA). Lysates were diluted with SDS-PAGE loading

buffer containing 100 mM DTT, loaded on a 15% SDS-polyacrylamide gel, transferred to a nitrocellulose membrane, and blocked in western blocking buffer (5% nonfat dry milk in Tris-buffered saline containing 0.2% Tween-20 (TBS-T)) for 30 min at RT. Membranes were incubated overnight at 4°C with rat anti-HA (Roche) (1:750) in western blocking buffer and washed in TBS-T next day and incubated with goat anti-rat horseradish peroxidase (HRP)-conjugated antibody (Jackson Immunoresearch Labs, Inc.) (1:2000) in western blocking buffer for 45 min at RT. Membranes were washed with TBS-T and incubated with SuperSignal West Dura Extended Duration Substrate (Pierce) for 5 min. HRP-bound proteins were detected by chemiluminescence using Fujifilm LAS-3000 CCD camera and quantified using the Image Gauge V2.1 software (Fujifilm).

Cell surface biotinylation. Transfected cells were rinsed with ice-cold PBS^{2+} buffer (PBS containing 1 mM $MgCl_2$, 0.1 mM $CaCl_2$), incubated with 1 mg/mL sulfo-NHS-SS-biotin (Pierce) in PBS^{2+} buffer for 2 × 15 min at 4°C. The biotin reagent was quenched by washing with (3 × 2 mL) with quench solution (PBS^{2+} containing 100 mM glycine) and then incubated with quench solution for 2 × 15 min at 4°C. Cells were lysed in RIPKA buffer and cell debris was removed by centrifugation. For each sample, 75 µg of total protein was quantitated by BCA analysis and incubated with 25 µL of Immunopure® Immobilized streptavidin beads (Pierce) overnight at 4°C. One-fifth of the input (37.5 µg of total protein) was saved as a control for each sample. Beads were washed 3 X with 0.1% SDS buffer (500 µL) and biotinylated proteins were eluted first with 30 µl 2× SDS-PAGE and 200 µM DTT mix for 15 min at 55°C, then with 30 µl 200 µM DTT for 5 min at 55°C and the two elutions were combined to achieve 60 µl final

volume. 1/5 of the input and bead-eluted proteins were separated by SDS-PAGE, analyzed by western blot analysis as described above.

CHAPTER V

DISCUSSION

CONCLUSIONS

The work presented in this thesis investigated the importance of KCNE1 N-linked glycosylation on KCNQ1/KCNE1 channel complex assembly, trafficking and function. Our findings show that nonglycosylated KCNE1 proteins are K^+ channel assembly incompetent and hypoglyosylated KCNE1 proteins are retained in the early secretory pathway. The assembly inept KCNE1 proteins prevent KCNQ1/KCNE1 channel complex trafficking and lead to a pool of unpartnered KCNQ1 channels on the cell surface providing a biogenic mechanism for Long Q T Syndrome. Moreover, we determined that the two consensus N-linked glycosylation sites on KCNE1 are glycosylated and show diverse biological properties. The N-terminal sequon is a traditional co-translational glycosylation site and indispensible for KCNQ1/KCNE1 assembly and function; whereas the internal sequon is a substrate for post-translational glycosylation machinery. To date KCNE1 is the only full-length type I transmembrane protein shown to have distinct co- and post-translational N-linked glycosylation sites and I am very proud to be part of this finding.

Chapter II laid the foundation for studying N-linked glycosylation of KCNE1. We showed KCNE1 peptides were N-glycosylated and we utilized glycan maturation as a tool for following KCNE1 trafficking through the secretory pathway. We found that E1

glycan maturation and cell surface expression were dependent on Q1 subunit expression. We demonstrated that when E1 was expressed alone the majority of the unassembled E1 peptides had immature *N*-linked glycans, were retained in the ER, and did not reach the cell surface. Only in the presence of Q1 was the maturely glycosylated form of E1 observed at the cell surface. Our results supported the previous observation regarding *Caenorhabditis elegans* KCNE1 homolog, where Bianchi *et al*. (2003) showed that KCNE1 needs corresponding K^+ channel subunit to reach cell surface.

KCNE1 has two consensus N-linked glycosylation sites; an N-terminal sequon (N5) and an internal sequon (N26). Both sequons in KCNE1 are conserved in all mammals and strikingly, the N-terminal sequon (N5) is conserved in all five KCNE family members (Figure 1.4, Chapter I). In addition, the mutations that prevent glycosylation at the N-terminal sequon on both KCNE1 and KCNE2 lead to Long QT Syndrome (Schulze-Bahr et al., 1997; Sesti et al., 2000b; Park et al., 2003). At this point I had enough background information to hypothesize that KCNE1 glycosylation at the N-terminal sequon is important for KCNQ1/KCNE1 channel assembly and proper function.

After showing KCNE1 was glycosylated and understanding the cellular machineries that ensure proper assembly and trafficking of KCNE-K^+ channel complexes in Chapter II, I asked the following questions: Does each consensus N-linked glycosylation site acquire glycans and is there anything special about the absolutely conserved N-terminal sequon? Therefore, I performed extensive biochemical analysis and examined the kinetics and extent of N-linked glycosylation of the two E1 sequons individually in Chapter III. I demonstrated that the unglycosylated E1 peptides do not

reach the cell surface with or without Q1 K^+ channels. I also showed that the two N-linked consensus sites on E1 were handled differently in the ER. The N-terminal sequon acquired glycans during translation, whereas the internal sequon acquired glycans mainly after translation. Moreover, I found that without the co-translational site post-translational glycosylation of E1 peptides was less efficient, resulting in the accumulation of unglycosylated KCNE1. In addition, the post-translational glycosylation efficiency of some mutant E1 peptides was considerably reduced through co-assembly with Q1 channel subunits. Finally, I showed that mutations that inhibit co-translational N-glycosylation reduced the population of functioning Q1/E1 complexes at the cell surface, which provided a biogenic mechanism for Long QT and Jervell-Lange Nielsen Syndromes.

Next, I wanted to examine the differential glycosylation behavior of the two KCNE1 sequons: I questioned the structural requirements that make the N-terminal sequon so indespensible and I wanted to find how disruption of the N-terminal sequon (N5) and/or increasing the hydrophobicity at this site had the observed unexpected long range effects on E1 glycosylation and how it reduced the glycosylation efficiency of the internal sequon (N26). Therefore, in Chapter IV, in order to explain this observed long range hydrophobic effect and to understand the relative N-glycosylation behavior of the two N-linked glycosylation sites (N5 and N26), I systematically changed the microenvironment of the two sequons on KCNE1. Our positional glycosylation scans showed that sliding the consensus N-glycosylation site to every other 9^{th} residue from the N-terminal sequon resulted in glycosylation; just like the functional N-terminally HA-

tagged KCNE1 that repositions the N-terminal sequon 9 residues away from the transmembrane domain. This periodicity might give us a hint about N-terminal sequon being a traditional glycosylation site and the internal sequon being a post-translational glycosylation site, yet requires further investigation. Figure 5.1 presents a likely pattern that could reflect the differential glycosylation of the two sequons on KCNE1. The periodicity of the efficient glycosylation mutants fits to an α-helical presentation of the N-terminus, placing the glycosylation mutants on the same side or exact opposite side of the first glycosylation site. At this stage, this hypothesis is quite premature and highly speculative, since the secondary structure of KCNE1 is still unknown. But this hypothesis could allow us to brainstorm and design new experiments. And if it is correct, this helical periodicity might be the reason why the first sequon is a traditional glycosylation site: by providing the correct interface for OST complex and by introducing the correct directionality for consensus N-linked glycosylation site recognition. Briefly, as N5 is coming out the translocon it is available for OST complex for glycan transfer. However, the second glycosylation site (N26) does not fit to the same helical presentation with the effective glycosylation mutants (Po, P3, P6) (Figure 5.1). Therefore, N26 is not presented to OST complex in optimal position and it can not get efficient co-translational glycosylation. According to this hypothesis, following translation, N26 can be recognized by post-translational glycosylation machinery as an unoccupied consensus N-linked glycosylation site and acquires glycans mainly post-translationaly.

In Appendix II, I demonstrated the characterization of the C-terminally HA-tagged KCNE1 that was used in the preceding chapters. C-terminally HA-tagged

KCNE1 allowed us to study two previously unobserved features of E1 glycoprotein: KCNE1 bears an internal translational initiation site and a proprotein convertase recognition site. In brief, I showed that KCNE1 has an internal translational start site, a methionine at position 27, in heterelogous expression systems. This was not observed in the long-used N-terminally HA-tagged E1, since the tag was four amino acids upstream of the M27. Therefore E1 protein that utilized M27 as the translation start site did not have a tag. In addition, I found a proteolytic cleavage site at the arginine cluster spanning the residues 32 through 38, which also bears the two known Long QT mutations (R32H and R36H) (Splawski et al., 2000; Napolitano et al., 2005). For the first time ever, we are showing that E1 has a proteolytic cleavage product that might be involved in KCNQ1/KCNE1 channel function; since mutations, indirectly preventing cleavage at this site, cause the Long QT Syndrome.

In Appendix I, I described a suppressor genetic screen using two temperature sensitive alleles of *mom-2*/Wnt. I designed these suppressor genetic screens to find additional components of the Wnt/Wingless signaling pathway that specify the endoderm tissue in *C. elegans*. I identified five intragenic suppressors and three extragenic suppressors of *mom-2*/Wnt embryonic lethality. We found a mutation in *ifg-1*, eIF4G homologue, as one of the extragenic suppressors, suggesting an intriguing connection between the Wnt signaling pathway and the translational machinery.

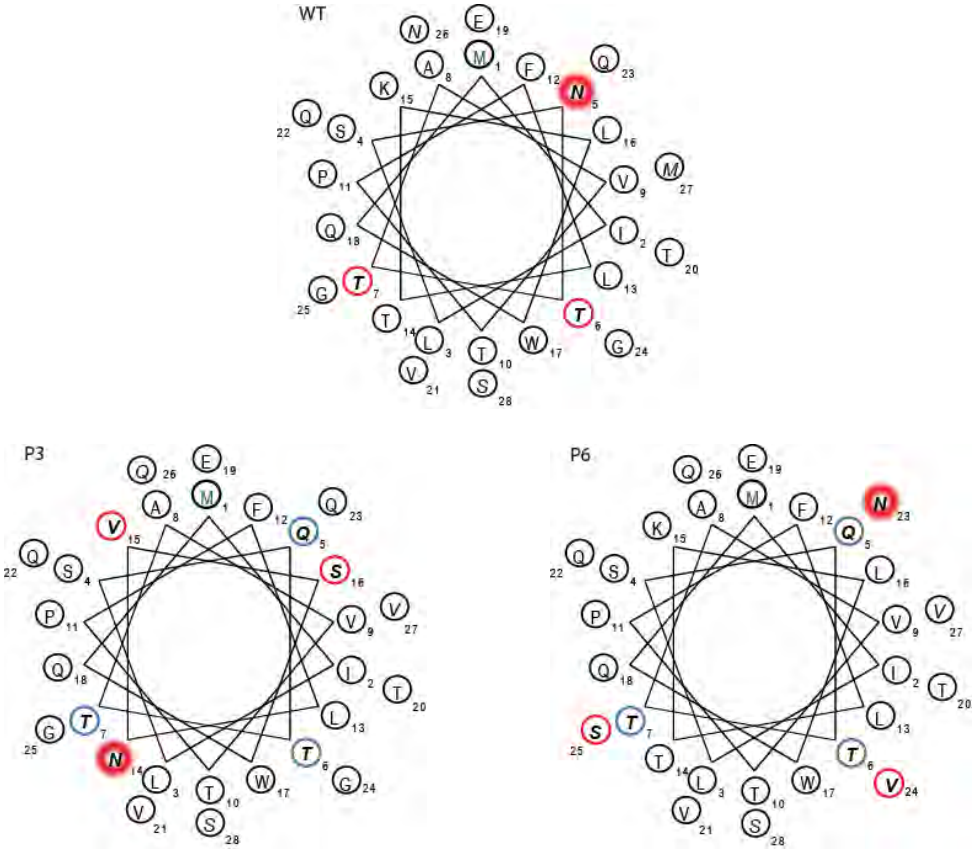

Figure 5.1: **The helical presentation of the two positional glycosylation mutants (P3 and P6) compared to WT KCNE1**. The positional glycosylation scans showed that bringing the glycosylation site to every other 9th residue from the N-terminal sequon (P0, P3, P6) resulted in glycosylation (Figure 4.3, Chapter IV). This periodicity could be fitted to an α-helical presentation of the N-terminus, placing the glycosylation mutants on the same side or exact opposite side of the first glycosylation site. In WT, the letters of the first glycosylation site are centered in red circles (-NTT-), in mutants, P3 and P6, the letters corresponding to these exact amino acid positions are circled in blue (-QTT-), emphasizing the background mutation (N5Q). The letters of the glycosylation sites in positional glycosylation mutants (P3 and P6) are placed in red circle.

Future Directions

Chapter II and III:

Does degradation of individual KCNE1 glycoforms (other than N26Q) play any role on observed glycosylation rates?

Though we have shown that the protein decay rates of WT KCNE1, glycosylation mutants (N5Q, T7I and N26Q) and mono-glycosylated N26Q were similar (Table 3.1 and Figure 3.2, Chapter III), it would be a safe approach to recapitulate the glycosylation rates observed with kinetic experiments (2 min pulse) in the presence of proteosome inhibitors. Inhibiting the ER-associated degradation (ERAD) pathway will help us to dissect glycosylation rates from the degradation rates of individual glycoforms. In our lab, Yuan Gao is tackling this question.

Do other members of the KCNE family acquire glycans co-translationally and/or post-translationally?

With the exception of KCNE4, all KCNE family members have multiple consensus N-linked glycosylation sites in their N-terminus and moreover, the N-terminal sequon (N5) is absolutely conserved among all five KCNE family members (Figure 1.4, Chapter I). Also, the distance between the N-terminal sequon and internal sequon is conserved (18-20 amino acids) in KCNE1, KCNE2, and KCNE5. KCNE3 has an

additional sequon located midway between the N-terminal sequon and the internal sequon.

It would be interesting to study the glycosylation sites on other KCNE family members through the same biochemical and functional approaches we used for KCNE1. The fact that the N-terminal sequon on KCNE1 is a traditional co-translational glycosylation site and the internal sequon is a substrate for post-translational glycosylation machinery raises the question whether the internal sequon(s) in other KCNE family members acquire glycans post-translationally. In addition, knowing that the genetic mutations that target the N-terminal sequon in both KCNE1 and KCNE2 lead to Long QT Syndrome, it would be interesting to know whether the absolutely conserved N-terminal sequon in all KCNE family members is a traditional co-translational glycosylation site. Consequently, KCNE peptides can be used as an invaluable tool to improve our knowledge of N-linked glycosylation. Examining the glycosylation sites on KCNE family of proteins and the effects of glycosylation on K^+ channel assembly and trafficking will help us understand the diseases related to hypoglycosylation of the channel subunits.

Is STT3B responsible for the post-translational glycosylation of the KCNE1 internal sequon?

Human coagulation factor VII (FVII) has two N-linked glycosylation sites: one of them acquires glycans co-translationally and the other post-translationally (Bolt et al., 2005). After this discovery, the Gilmore Lab demonstrated that STT3A is primarily

responsible for the co-translational glycosylation; whereas STT3B is important for both co-translational glycosylation and posttranslational glycosylation of FVII (Ruiz-Canada et al., 2009).

Since post-translational glycosylation of proteins with intact glycosylation machinery is a newly emerging field, it would be of great interest to determine which OST isoform is responsible for post-translational glycosylation of the internal sequon on KCNE1. In fact, our lab is pursuing this goal in collaboration with the Gilmore lab. I participated in the initiation of this project. We used RNA interference to knockdown the OST isoform of interest and performed 2 min pulse-chase radioactive analysis on WT KCNE1 to observe the changes in the KCNE1 glycosylation pattern. The initial data was not conclusive and requires optimization of the RNAi technique. Though, we are still in the early stages of this project, hopefully Yuan Gao will determine which OST isoform is responsible for post-translational glycosylation of the KCNE1 internal sequon.

Are there other transmembrane glycopeptides that acquire glycans post-translationally?

In order to understand: 1. The functional importance of post-translational glycosylation 2. why at times post-translational glycosylation is preferred over co-translational and vice versa, we need to create a database of glycoproteins that are post-translationally glycosylated. This hypothetical database might help us to deduce an algorithm that can identify the sequons that are substrates for co-translational and/or post-translational machinery. To achieve this goal, more proteins with post-translational N-

linked glycosylation sites have to be discovered. One way to overcome this caveat would be searching for proteins that exhibit sequence similarity to KCNE1 N-terminus. With this approach we were able to find one candidate gene that has sequence homology to N-terminus KCNE1: Homo sapiens transmembrane protein 10 (HTMP10). HTMP10 is a novel human brain-specific gene encoding a putative transmembrane protein of 141 amino acids. Also, HTMP10 has two potential N-linked glycosylation sites that require further investigation. It would be interesting to find similar proteins and analyze their N-linked glycosylation behavior to find a pattern for predicting post-translational glycosylation.

Chapter IV:

What are the biochemical and functional properties of positional glycosylation mutants, P3 and P6?

In order to make sure that the efficiently glycosylated positional glycosylation mutants are indeed behaving like WT KCNE1 and/or N26Q, we have to further characterize their biochemical and functional properties. Enzymatic deglycosylation assays must be performed to identify the different glycoforms (immature N-linked and mature N-linked glycans) of these mutants when expressed alone and with Q1. The cell surface expressions of P3 and P6 (co-expressed with Q1) should be tested through cell surface biotinylation assays. Finally, electrophysiological studies have to be performed to see whether Q1/P3 and/or Q1/P6 will give rise to WT Q1/E1 currents.

Do efficiently N-glycosylated positional glycosylation mutants (P3 and P6) acquire glycans post-translationally or co-translationally?

It would be interesting to know how P3 and P6 acquire glycans: co-translationally and/or post-translationally. In our lab, Yuan Gao has started analyzing the positional glycosylation mutants (including P3 and P6) using 2 min pulse-chase analysis. Preliminary results suggest that P6 acquires glycans co-translationally and P3 acquires glycans primarily co-translationally. If these findings are confirmed via upcoming experiments, it will be in favor of my periodicity–helical fit hypothesis (*vide supra*). These mutants acquire glycans co-translationally by attaining the optimal orientation during translation required for OST-complex recognition.

How can we test the structural requirements for post-translational glycosylation?

More structure-function studies will help us understand the requirements for post-translational glycosylation. By utilizing the differential behavior (co- vs post-) of the two N-linked glycosylation sites on KCNE1, following experiments can be designed: 1. Adding more amino acids between the transmembrane domain and the internal sequon (N26) can convert the post-translational glycosylation site (N26) to a co-translational glycosylation site (if the distance between the sequon and transmembrane domain has an effect on glycosylation). 2. Similarly, addition of transmembrane domains in tandem following E1 C-terminus might change the glycosylation behavior of the internal sequon (N26) by pushing this site out of the translocation channel and making it more accessible to OST-complex. 3. Transfering the two sequons on KCNE1 to a well-studied α-helical

type I transmembrane protein; placing them at the exact amino acid positions/distances relative to the N-terminus, transmembrane domain and each other and applying the positional glycosylation scans might allow us to examine the effect of protein secondary structure on glycosylation.

Which post-translational modifications are responsible for the slower migrating bands observed on the SDS-PAGE of internal deletion mutants when co-expressed with Q1?

When internal deletion mutants were co-expressed with KCNQ1 we observed slow migrating bands that require further characterization (data not shown). Enzymatic deglycosylation assays must be performed to identify the different glycoforms (O-linked, immature N-linked and mature N-linked glycans) of these E1 mutants.

Appendix II:

What are the effects of single (R32A, R33A, R36A) and double (R33A;R36A) arganine mutants on KCNE1 cell surface expression and Q1/E1 channel function?

The discovery of the proteolytic cleavage site spanning the residues that are prone to Long QT Syndrome on KCNE1 is quite promising and opens a new research direction. For starters, it would be interesting to know the biochemical properties of the single and double arganine mutants. For instance cell surface expression of these mutants can be tested using the cell surface biotinylation assays. If these mutants are expressed on the

plasma membrane, we can check the effect of these mutations on channel function through electrophysiological studies. If all the biochemical and functional properties of the arganine mutants turn out to be WT KCNE1 like, then this might suggest that the cleavage product might have a regulatory role in KCNE1 function. This brings up the next future direction: analyzing the E1 proteolytic cleavage product.

What is the functional role of the proteolytic cleavage product?

We can mimic the E1 cleavage product by designing an E1 mutant construct that removes the residues before and at the proteolytic cleavage cut site and introducing a new translational start site (methionine) before R36. We can characterize this mutant protein and its assembly with K^+ channel partner, KCNQ1 through biochemical analysis and test its role on KCNQ1/KCNE1 channel currents using electrophysiology. This study will provide answers to the following questions: 1. Can the mutant protein assemble with KCNQ1 and traffic to the cell surface? 2. Are the KCNQ1/Mutant channel currents similar to KCNQ1/KCNE1 channel currents? If the currents are not same, can this cleavage product be a negative regulator of KCNQ1/KCNE1 channels? This work will enhance our knowledge about E1 cleavage product; hence improve our understanding in Long QT mutations that prevent the cleavage of E1 peptide.

Final Words

To me the most amazing part of the work presented in this thesis was that it gave birth to many new ideas. I really enjoyed working with KCNE1. This small glycoprotein had/has a big story to tell us.

Appendix I

My work in Dr Craig C Mello's Lab – The first four years…

Screening for the suppressors of *mom-2*/ Wnt embryonic lethality*

Contributors to the work presented in Appendix I:

The author of this thesis, Tuba Bas conducted suppressor screens of *mom-2*/Wnt; isolated five intragenic suppressors and three extragenic suppressors and initiated the mapping of one of the extragenic suppressors of *mom-2*/Wnt, *ifg-1*. Dr Takao Ishidate helped conduct the suppressor screens. Dr Soyoung Kim mapped and cloned *ifg-1*, one of the extragenic suppressors of *mom-2*/Wnt, and performed its genetic analysis.

* Kim S **, **Bas T** **, Ishidate T, Sharma R, Shirayama M, and Mello CC. (** **equal contribution**). Screening for the suppressors mom-2 embryonic lethality: A connection between the Wnt signaling pathway and the translational machinery in C. Elegans. *Manuscript in preparation*.

ABSTRACT

The highly conserved Wnt/Wingless family of secreted glycoproteins regulates many aspects of animal development. In 4-cell stage *Caenorhabditis elegans* embryos Wnt signaling specifies endoderm by controlling the fate of EMS blastomere daughters. In order to identify additional regulators of the Wnt/Wingless signaling pathway in endoderm specification, we performed suppressor genetic screens with two temperature-sensitive alleles of *mom-2*/Wnt. Among 20 million chromosomes screened, five intragenic and three semi-dominant extragenic suppressors were isolated. Here, we report the identification of one extragenic suppressor as an allele of *ifg-1,* a homolog of eukaryotic translation initiation factor *eIF4G*. The allele *ifg-1(ne4271)* is associated with a substitution, arginine 745 to cysteine, at a highly conserved residue in the middle third domain essential for the translational activity. Genetic analyses using the *ifg-1* deletion allele and *ifg-1*(RNAi) show that *ifg-1(ne4271)* acts as loss-of-function for suppressing the *mom-2* phenotype. Furthermore *ifg-1(ne4271)* suppresses other mutants in the pathway such as *wrm-1*/β-catenin, *lit-1*/MAPKKK, NEMO, and *mom-4*/MAPK, placing *ifg-1* downstream of these molecules in the pathway. Our results imply a potential connection between the Wnt signaling pathway and the translational machinery.

INTRODUCTION

The Wnt signaling pathway is an evolutionarily conserved signal transduction pathway and consists of a protein network, where players take part in various stages of animal development including cell proliferation, cell fate specification, cell polarity and migration (Cadigan and Nusse, 1997; Wodarz and Nusse, 1998; Hobmayer et al., 2000; Moon et al., 2002; Nelson and Nusse, 2004). Several of these proteins are oncogenes, and mutant proteins lead to colorectal, hepatic, breast and skin cancers (Peifer and Polakis, 2000; Polakis, 2000; Logan and Nusse, 2004). In *C. elegans,* the Wnt signaling pathway acts early in development to specify endoderm (Rocheleau et al., 1997; Thorpe et al., 1997). In 4-cell stage embryos signaling from the posteriormost P2 blastomere polarizes the EMS cell to produce one of the daughter cells known as the endoderm founder cell E. In the absence of P2/Wnt signal, E adopts the fate of the other EMS daughter, the MS blastomere, and becomes progenitor of the mesodermal tissues rather than endoderm.

Previous genetic screens and studies using RNA-mediated genetic interference (RNAi) have identified a number of genes that are involved in P2/EMS signaling. Several of these genes define the components of the conserved Wnt/Wg signaling pathway, including *mom-1* (Porcupine), *mom-2* (Wnt/Wg), *mom-5* (Frizzled), *sgg-1 (gsk-3)*, *wrm-1* (β-catenin/Armadillo), *apr-1* (adenomatous polypopsis coli, APC), and *pop-1* (TCF/LEF) (Lin et al., 1995; Rocheleau et al., 1997; Thorpe et al., 1997). Genetic studies

also indicate that other signaling mechanisms contribute to the endoderm specification including the MAP kinase signaling factors, namely *mom-4* (TAK1, MAP kinase kinase related) and *lit-1* (Nemo, MAP kinase related) (Ishitani et al., 1999; Meneghini et al., 1999; Rocheleau et al., 1999; Shin et al., 1999), and the Src-signaling pathway (Bei et al., 2002). Although the discovery of these components has been a great template in understanding Wnt signaling pathway; the picture is far from being complete. So far, exactly how these pathways are orchestrated and what other players are involved remains a mystery.

In order to look for new components of Wnt signaling pathway we have initiated suppressor genetic screens beginning with the most upstream component MOM-2/Wnt. For these screens we have utilized two temperature sensitive (Ts) alleles of *mom-2*/Wnt (*ne834* and *ne874*), both exhibiting fully penetrant embryonic lethal phenotypes at 25^{o}C. We used ENU (N-Ethylinitrosourea) as the mutagen and screened for suppression of embryonic lethality at the nonpermissive temperature. For both alleles, suppressors were rare and we could isolate only five intragenic and three extragenic suppressors for the 20 million chromosomes screened. We identified one extragenic suppressor with a point mutation in *ifg-1* gene, a homolog of eukaryotic translation initiation factor *eIF4G* known to play a key role in translation. We also showed that the semi-dominant suppressor *ifg-1(ne4271)* is a loss-of-function allele, and functions downstream of *lit-1*/MAPKKK, NEMO and *wrm-1*/β-catenin. Our results reveal new insight into the function of Wnt signaling in endoderm specification, providing a link between the translational machinery and Wnt signaling pathway in early *C. elegans* embryos.

RESULTS

Isolation of maternal-effect suppressors of *mom-2*/Wnt

In order to screen for *mom-2* suppressors, we utilized two *mom-2*/Wnt Ts alleles, *ne834* and *ne874*, which were among the five alleles of *mom-2* isolated in a previous large scale Ts screen Figure A1.1 (Nakamura et al., 2005). Briefly, *mom-2* suppressors were isolated through careful selection of viable embryos at the non-permissive temperature, 25°C. After the ENU (N-**E**thyl-N-**N**itroso**u**rea) mutagenesis of parent hermaphrodites (Po) of *mom-2(ne834, ne874)*, dominant suppressors were collected in F1 generation and recessive suppressors were isolated in F2 generation Figure A1.2.

In *ne874* screening, among five million worms that were mutagenized at the permissive temperature, five independent suppressors (*TT1, TT2, TT3, TT4, TT5*) were recovered at the non-permissive temperature in F1 screening, and none in F2 generation. In *ne834* screening, we were unable to find any suppressors in the F1 generation. However, we were able to isolate three suppressors (*TT10, TT11, TT12*) among one million worms in the F2 generation (Table A1.1). Isolated suppressors in *ne834* suppressor screen showed weak suppression at 25°C with ~ 5% viability. When we lowered the temperature to 24 or 23 °C, we observed a significant increase in the suppression rate.

Figure A1.1: **The *mom-2* alleles suppressed *(ne834* and *ne874)* and the intragenic suppressors of *mom-2(ne874).*** Amino acid alignments of the two *mom-2* homologs (*C. elegans* and human). Amino acid substitutions for each intragenic suppressors are shown in red letters above each black box. The *mom-2(ne834)* and *mom-2(ne874)* mutations are in green letters. The double amino acid substitution in *TT5(ne3347)* are highlighted by the blue letters of *TT5*. Conserved residues are in orange letters.

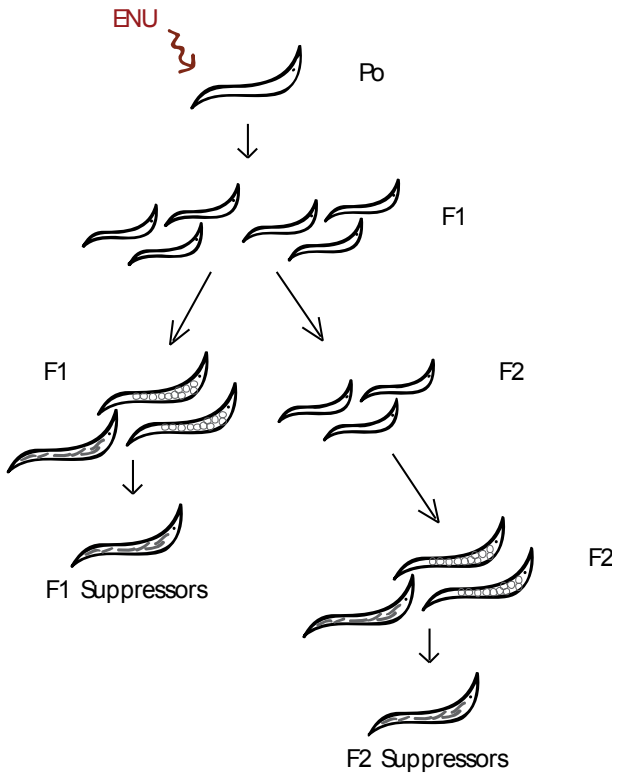

Figure A1.2: Schematic diagram of the screen for maternal-effect suppressors of *mom-2*/Wnt. Po *mom-2(ne834 and ne874)* animals in *lin-11* Hawaiian (CB4856) background were mutagenized by ENU (N-**E**thyl-N-**N**itroso**u**rea). After growing at permissive temperature (15°C), the F1 L4 stage animals were shifted to 25°C for 27 hrs then screened for worms with viable embryos, F1 suppressors. For F2 suppressors, the F2 L4 stage animals were shifted to 25°C for 27 hrs to look for animals with viable embryos inside the mother worms.

Table A1.1: **Statistics of *mom-2*(*ne874*) and *mom-2*(*ne834*) suppressor screens**

Suppressor	Screen	Number of worms screened	Chromosomal location
TT1(ne3346)	ne874 F1 screen	4 million	V
TT2(ne3343)	ne874 F1 screen	4 million	V
TT3(ne3344)	ne874 F1 screen	4 million	V
TT4(ne3345)	ne874 F1 screen	4 million	V
TT5(ne3347)	ne874 F1 screen	4 million	V
TT10	ne834 F2 screen	1 million	V
TT11	ne834 F2 screen	1 million	X
TT12	ne834 F2 screen	1 million	II

To determine the chromosomal locations of the suppressors, we used linkage analysis combined with SNP (**S**ingle **N**ucleotide **P**olymorphism) mapping method. The results showed that five suppressor strains from the *ne874* screening contained mutations that were tightly linked to *mom-2*. Whereas the three suppressors from *ne834* screening did not appear to be linked to *mom-2*. We further mapped these suppressors to determine their approximate chromosomal locations. We found that *TT10* was located far from the center of chromosome II, *TT11* was on chromosome X, and *TT12* was on the center of chromosome II. In addition, during these initial mapping procedures we were able to determine if the suppressors were functioning in a dominant or recessive manner. We showed that *TT10*, *TT11* and *TT12* were all weak dominant suppressors (semi-dominant).

Identification of intragenic suppressors of *mom-2(ne874)*

When we performed the linkage analysis on chromosome V, where *mom-2* is located, we found that the five suppressors (*TT1, TT2, TT3, TT4, TT5)* from *ne874* screen were tightly linked to the *mom-2* locus and could not be separated. In order to determine whether they were intragenic suppressors, we sequenced the *mom-2* locus in these five strains and found at least one second site mutation in all of the five suppressors (Figure A1.1). Surprisingly, *TT5* had two amino acid substitutions; methionine 235 to leucine and aspartic acid 239 to asparagine. Interestingly, we found that *TT4* had a substitution in cysteine 167 to tyrosine, which was the same mutation as that of another Ts *mom-2* allele, namely *ne834*. The two *mom-2* mutant alleles, *ne874* and *ne834*, replace cysteine

with tyrosine. The fact that removal of both cysteines simultaneously resulted in the suppression of the *mom-2* phenotype implies that both *ne874* and *ne834* eliminate a disulfide bond.

TT12 is associated with an R745C substitution in *ifg-1*/eIF4G

Linkage analyses and SNP assays showed that *TT12* was located around the center of chromosome II. In order to perform three-factor SNP mapping, we constructed a strain with *unc-83(e1414*) and *rol-1(e19)* in the *mom-2(ne834)* genetic background, which spanned the entire region from -2.98 to 6.65 on chromosome II. After crossing this mapping strain with *TT12* males, we isolated the recombinants in F2 generation, and tested for the suppression of *mom-2 (ne834)* and checked SNP loci to narrow down the location of the suppressor. After testing approximately 700 recombinants, we were able to locate *TT12* in a 9 cosmid interval on chromosome II (from T05H10 to Y1E3A). This interval held about 30 genes. Next, we sequenced the candidate genes to find the suppressor mutation. We found a point mutation in *ifg-1,* a homolog of eukaryotic translation initiation factor *eIF4G* (Figure A1.3). The *ifg-1(ne4271*) allele had an R745C substitution. Arginine 745 is highly conserved and is located in the eIF4A and eIF3 binding domain of eIF4G.

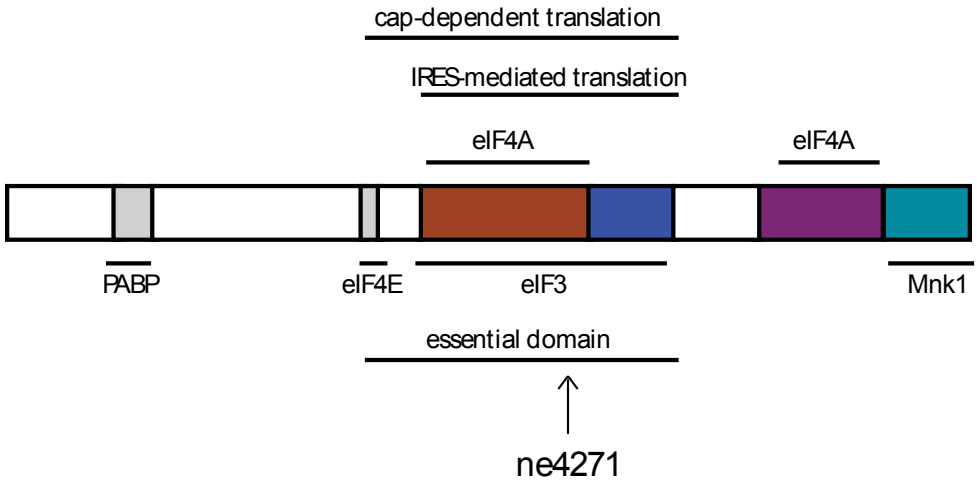

Figure A1.3: **The *mom-2(ne834)* suppressor, *ifg-1* is a homolog of *eIF4G***. Structure of eIF4G with the interaction domains for eIF4A (Lomakin et al., 2000; Morino et al., 2000), eIF3 (Korneeva et al., 2001), Mnk1 (Morino et al., 2000), PABP & eIF4E (Gingras et al., 1999). *TT12 (ne4271)* has a single amino acid change at Arginine 745 to Cysteine within the essential domain important for translational function and binding eIF4A and eIF3.

DISCUSSION

Wnt proteins are secreted glycoproteins that play essential roles during embryonic development. Many players of Wnt signaling pathway such as Wnt, Frizzed/LRP, Axin, GSK3, APC, β-catenin, and TCF/LEF have been found through the extensive genetic screens performed in Wnt pathways of *Drosophila* and *C. elegans*. Despite their undeniable role in identification of new components in Wnt signaling pathway, basic genetic screens have their weaknesses. For example some pathway regulators may not have an obvious *wnt*-related phenotype of their own and can be missed in a basic genetic screen. Also, using the same screening parameters over and over might lead to the saturation of a particular type of screen. Here, we describe a suppressor genetic screen, a powerful genetic approach to overcome these shortcomings and identify new Wnt pathway regulators. Another study that resulted in identification of new components was performed by DasGupta *et al*., where they used a genome-wide RNAi screening in *Drosophila* and found 238 candidate regulators of the Wnt signaling pathway, most of which had never been shown to be connected to Wnt signaling before (DasGupta et al., 2005).

In this study, we aimed to find additional components of the Wnt/Wingless signaling pathway to specify the endoderm tissue in *C. elegans* through suppressor genetic screen using two temperature sensitive alleles of *mom-2*/Wnt. In our screen, we identified 8 new potential regulators of the Wnt signaling pathway. When we

molecularly characterized the new loci, we found that five of them were intragenic suppressors and the rest were extragenic. The locus of one extragenic suppressor corresponded to *ifg-1*, which encodes the eukaryotic translation initiation factor eIF4G.

Intragenic suppressors

Intragenic suppressors have extra mutations within the same gene that restore function of the original mutant gene products. In our *mom-2(ne874)* (C139Y) suppressor screen, we identified five intragenic suppressors (*TT1, TT2, TT3, TT4, TT5*). Surprisingly, *TT4* turned out to have a second site mutation in C167 to a tyrosine, the same mutation of the Ts allele *mom-2(ne834)* (C167Y). Our suppressor screen allowed us to find out *mom-2(ne834)* itself acts as a suppressor of *mom-2(ne874)* in an allele specific manner. This finding strongly implies that the cysteine residues at positions 139 and 167 could be interacting with each other. A high proportion of the conserved cysteine residues in Wnt proteins suggest that they may be critical determinants of the final structure of proteins through the formation of intramolecular disulfide bonds.

Wnt proteins are highly hydrophobic. This property of Wnt proteins renders them insoluble; therefore they are extremely difficult to isolate and characterize. Well designed suppressor genetic screens might not only give us new Wnt regulators through extragenic suppressors, but might allow us to isolate intragenic suppressors that may help us understand the structural aspects of Wnt proteins *in vivo*.

Identification of the eukaryotic translational initiation factor *eIF4G* as a suppressor of *wnt*

In our *mom-2(ne834)* suppressor screen, we isolated an *eIF4G* allele as a semi-dominant suppressor of the *wnt* phenotype. The eukaryotic initiation factor, eIF4G, is a large modular protein and a key component in promoting ribosome binding to mRNA through serving as a docking site for the initiation factors and proteins involved in RNA translation. eIF4G is part of the eIF4F complex and acts as a scaffold for the other two members of this complex, namely eIF4E and eIF4A. Thus, the central role of eIF4G in initiation makes it a valid target for modulation of translation.

eIF4G has been isolated and cloned from many different species including the yeasts *S. cerevisiae* and *S. pombe* (Goyer et al., 1993), *Drosophila* (Zapata et al., 1994), wheat (Browning, 1996), and human (Yan et al., 1992; Gradi et al., 1998). In *C. elegans*, two splice-variants of eIF4G, encoded by *ifg-1*, have been identified (Long et al., 2002; Kamath and Ahringer, 2003). The eIF4G proteins of *C. elegans* and human exhibit moderate sequence conservation, yet overall they share similar biochemical functions.

The mammalian eIF4GI can be divided into three regions; an amino-terminal third, which contains the poly(A) binding protein (PABP) and eIF4E binding sites; a middle third, which binds eIF4A and eIF3; and a carboxy-terminal third, which harbors a second site for eIF4A binding and a docking sequence for the Ser/Thr kinase Mnk1 (Figure A1.3) (Morino et al., 2000). The mutation in *ifg-1 (ne4271)* has a substitution at a highly conserved residue at position 745 from an arginine to a cysteine. This point mutation lies in the middle third of the protein, which is the eIF4A and eIF3 binding

domain. It has been previously shown that eIF4A and eIF3 binding domain is important for the cap-dependent translation (Morino et al., 2000).

In earlier studies, mutational analysis was performed to elucidate the roles of some of the conserved residues in the middle third region of human eIF4GI (eIF4A and eIF3 binding domain) (Morino et al., 2000). It was shown that the residues at Q533, K610, and F720 had no effect on eIF4A or eIF3 binding, yet mutations at Y273, F650, and F736 abolished binding to eIF4A and had no effect on eIF3 binding. The role of R745, where *ifg-1 (ne4271)* has a mutation that suppresses the *wnt* phenotype, remains to be uncovered. It would be interesting to see the role of R745C mutation on eIF4A and/or eIF3 binding and observe its ultimate effect on eIF4F, the translation initiation complex function.

Novel regulator of the Wnt signaling pathway

Up to date, a direct relation between the Wnt signaling pathway and the translational machinery has not been reported. Thus, finding eIF4G, a key protein of a novel cellular mechanism, as a suppressor of *mom-2* mutant was unanticipated. Recently, similar unexpected functions of the translational machinery components have been identified in other cellular events. Li *et al* isolated eIF4A, a component of the eIF4F complex, as a suppressor of *dpp*, a member of the superfamily of TGFβ (**T**ransforming **G**rowth **F**actor β) in *Drosohpila* (Li et al., 2005). They showed that eIF4A acts as a specific inhibitor of Dpp signaling and mediates the degradation of Smad homologs for

signal activation (Li and Li, 2006a; Li and Li, 2006b). Moreover, both human and *Drosophila* eIF4A-III are components of the exon-junction complex, which is formed during mRNA splicing (Ferraiuolo et al., 2004; Shibuya et al., 2004). In mammals, the resulting complex is essential for nonsense-mediated mRNA decay. Strikingly, eIF4A-III is also essential for the proper localization of oskar mRNA in the *Drosophila* embryos (Palacios et al., 2004).

Even though more investigations need to be conducted to elucidate the mechanism underlying the connection between eIF4G and the Wnt signaling pathway, we can propose several possibilities to explain their association: First, negative regulators of Wnt signaling may be sensitive to IFG-1 levels. For example, it is possible that *ifg-1(ne4271)* may act to reduce the POP-1 levels, since the heterozygote of hypomorphic *pop-1* allele rescues the *mom-2* phenotype (personal communication with Dr. Soyoung Kim). Second, eIF4G itself may be a negative regulator of the Wnt signaling pathway. Third, the Wnt signaling pathway may directly regulate the translational machinery. For example, the components of translational machinery might be phosphorylated by Wnt regulators. eIF4G could also function completely independent of the Wnt signaling pathway, yet the two pathways may converge on the same targets with opposing effects.

Our suppressor screen has provided brief structural information about Wnt proteins through intragenic suppressors. Through our screen we isolated *ifg-1*, a component of translational machinery, as a suppressor of Wnt signaling pathway in *C. elegans* gut development. Our data suggests an intriguing connection between the Wnt signaling pathway and the translational machinery. Future studies elucidating the

molecular mechanisms underlying this connection may shed light on this complex network of interactions.

EXPERIMENTAL PROCEDURES

*Genetics and Strains***.** All strains were handled and cultured as described previously (Brenner, 1974). *ifg-1(ok1211)* was obtained from CGC (**C**aenorhabditis **G**enetics **C**enter). Mutant strains used were: *mom-2(ne834)* (V), *mom-2(ne874)* (V), *mom-4(ne1539)* (I), *wrm-1(ne1982)* (III), *lit-1(ne1991)* (III), VC778 *ifg-1(ok1211)/mIn1[mIs14 dpy-10(e128)]* (II).

ENU mutagenesis screen for suppressors of mom-2 (ne834, ne874). The Ts alleles of *mom-2 (ne834, ne874)*, in the background of the Hawaiian CB4856-derived *lin-11(ne832)* egg-laying deficient strain (WM59), were used for the suppressor screens. L4 worms were grown at 15°C. Prior to mutagenesis worms were washed with 10 mL M9 buffer. A final concentration of 1.00 mM ENU (N-**E**thyl-N-**N**itroso**u**rea) in 4 mL of M9 was used as mutagen. Worms were M9-ENU incubated on rotating shaker set at 100 rpm for 4 hours at 15°C. After mutagenesis worms were washed with 10 mL M9 buffer. Later, half of the F1 progenies were shifted to 25 °C at the L4 stage to select for the F1 dominant suppressors, and the other half was maintained to produce F2 progeny. In order to screen for the F2 recessive suppressors, L4 stage F2 animals were shifted to 25°C.

RNAi assays. RNAi was performed by injecting dsRNA as described previously (Bei et al., 2002). The *ifg-1* dsRNA was prepared from full length genomic DNA. Embryos were collected 24 hr post injection and were scored for phenotypes at the appropriate temperature.

Appendix II

Characterization of the C-terminally HA tagged KCNE1

Contributors to the work presented in Appendix II:

The author of this thesis, Tuba Bas, conducted all biochemical experiments. Dr Trevor Morin, Dr Jessica Rochelau and Dr Steven Gage conducted the electrophysiological experiments.

ABSTRACT

KCNE1 is the founding member of the KCNE family of proteins, modulatory β-subunit of a number of hereromultimeric K^+ channels, including KCNQ1. KCNE1 and KCNQ1 are coexpressed in the heart and inner ear and mutations in either channel subunit lead to diseases such as Romano-Ward (autosomal dominant long-QT syndrome) and Jervell-Lange-Nielsen Syndrome (autosomal recessive long-QT syndrome accompanied with deafness). KCNE1 has a single pass transmembrane domain with an N-terminus exposed to the exterior side of the membrane, which bears two N-linked glycosylation sides (N5 and N26) and a C-terminus facing the cytoplasm. We wanted to investigate the effects of KCNE1 glycosylation on channel assembly and trafficking. Therefore, we constructed a C-terminally HA-tagged KCNE1 protein, which functions like WT KCNE1. Here, I will present the characterization of the C-terminally HA tagged KCNE1 protein that we used throughout the experiments that are presented in Chapter II, Chapter III and Chapter IV.

INTRODUCTION

KCNQ1 is a voltage-gated K^+ channel identified in a linkage study looking at the genetic causes of sudden death from cardiac arrhythmia (Wang et al., 1996). KCNQ1 proteins form homotetramers and co-assemble with members of KCNE peptides achieving great channel diversity (Melman et al., 2002a; Melman et al., 2002b). KCNE1, the founding member of KCNE gene family, and KCNQ1 are coexpressed in the heart and inner ear. KCNE1 effects channel function by changing channel gating and by modulating ion selectivity, single channel conductance and drug interactions (Abbott and Goldstein, 1998; Trimmer, 1998; Pongs et al., 1999). Mutations in either KCNE1 and/or KCNQ1 lead to chanellopathies such as Romano-Ward and Jervell-Lange-Nielsen Syndrome effecting more than 1 in every 5000 people. Romano-Ward (autosomal dominant long-QT syndrome) is a heart disorder giving rise to cardiac arrhthymia and can be inherited or acquired. Jervell-Lange-Nielsen Syndrome (autosomal recessive long-QT syndrome with deafness) is a form of long-QT syndrome accompanied with congenital deafness. The endolymphatic space of these patients is collapsed due to loss of K^+ homeostasis in the inner ear (Neyroud et al., 1997; Schulze-Bahr et al., 1997; Tyson et al., 1997; Splawski et al., 2000).

KCNE1 is a type I membrane glycoprotein. Type I proteins are integral membrane proteins with a single transmembrane stretch of hydrophobic residues. The N-terminal side of the transmembrane domain is exposed on the exterior side of the plasma

membrane and the C-terminus exposed on the cytoplasmic side of the cell. KCNE1 has 129 amino acids with two consensus N-linked glycosylation sites (sequons) at N5 and N26 on the N-terminal side of the transmembrane domain (Figure A2.1***B***). These two N-linked glycosylation sites are glycosylated in expression systems and native tissues (Chapter II and Chapter III) (Finley et al., 2002).

Glycosylation is an important posttranslational modification. In eukaryotes, N-glycosylation starts with the transfer of a 14-sugar precursor to the asparagine residue of the consensus site on the protein (-NXT/S-, X cannot be proline), mostly cotranslationally and rarely post-tranlationally. N-linked glycans can effect both the physico-chemical and biological functions of the proteins to which they are attached (Apweiler et al., 1999; Walsh, 2006). Previous studies gave a small hint for the possible role of N-linked glycosylation of the two sequons on KCNE1 function; especially the sequon closer to the N-terminus (N5). Deletion studies suggested truncations that remove the N-terminal sequon (N5) effected the electrophsiological properties of the KCNE1/KCNQ1 channel complex. On the contrary the absence of the internal sequon (N26) did not have a significant effect on channel function. These structure-function studies determined the minimal functional KCNE1 protein as being residues 1-9 and 40-94 including the transmembrane domain. Moreover, T7I, a Jervell-Lange-Nielsen Syndrome (JLNS) mutation, eliminates glycosylation at N5 (Takumi et al., 1991; Schulze-Bahr et al., 1997; Abbott and Goldstein, 1998; Freeman et al., 2000).

In order to investigate the two N-linked glycosylation sites, I constructed and characterized a C-terminally HA-tagged KCNE1 protein (E1-HAc). Construction of the

tagged protein involved multiple steps: tagging the protein via PCR techniques; testing the expression of the candidate protein alone and in the presence of the channel partner KCNQ1; analyzing the ER-exit via enzymatic deglycosylation assays; checking the presence of the protein at the plasma membrane using a cell surface biotinylation assay and comparing the results with an established N-terminally HA-tagged KCNE1 construct (E1-HAn). Finally, we performed functional analysis through the co-expression of E1-HAc with Q1 and measuring currents through KCNE1/KCNQ1 channel complex. While characterizing the C-terminally HA-tagged KCNE1 protein, we observed two interesting properties of the KCNE1 protein. First, it has an internal start site at M27. Second, it has a putative proteolytic cleavage site spanning the residues R32, R33, and R36, which requires further investigation.

RESULTS

In order to study the two N-linked glycosylation sites on KCNE1, we constructed a panel of C-terminal tags using 2-Step PCR, gel purification, ligation and transformation techniques. Seven tags were introduced at different locations on the KCNE1 C-terminus (Table A2.1). All tagged KCNE1 derivatives were confirmed by sequencing and went through a series of biochemical and functional tests to ascertain whether they behave like WT KCNE1. Among seven tags studied only the HA tag (-YPYDVPDYA) with a preceding spacer (-SGSG-) attached at the very end of the KCNE1 C-terminus (after P129) met all the WT KCNE1 criteria (Figure A2.1***A***) (*vide infra*).

Epitope tag on KCNE1 C-terminal: Choosing the right tag and testing the protein expression

After the addition of the epitope tag on C-terminus, we first tested the expression of the C-terminally HA-tagged protein (E1-HAc) in CHO cells (CHO cells lack endogenous K^+ channels). We transiently transfected CHO cells with E1-HAc alone or with KCNQ1. The cells were lysed in RIPKA buffer with protease inhibitors and lysates were resolved on SDS-PAGE gel and probed for the HA-tag on E1 (Figure A2.1***B***). When E1 was expressed alone, we observed a doublet around ~15 kDa and a sigle band at ~25 kDa. When E1 was coexpressed with Q1, E1 resolved to a higher molecular weight band above ~37 kDa. These results compared favorably with those of an

Table A2.1: **The different C-terminally tagged versions of KCNE1 protein and their characterization.**

	Expression	Mature Protein	Cell Surface Expression	Function
Flag1	**+**	**None**	**None**	**N/D**
Flag2	**+**	**None**	**None**	**N/D**
Myc	**+**	**None**	**None**	**N/D**
HA-Rep	**+++**	**+**	**+**	**Q1-like**
HA-End	**++**	**++**	**++**	**I_{ks} currents**
HA-Psp	**++**	**+**	**+**	**N/D**
E1-HAc	**+++**	**+++**	**+++**	**I_{ks} currents**

Epitope tags inserted in KCNE1 C-terminus are FLAG: -DYKDDDDK- ; Myc: -EQKLISEEDL- and HA: -YPYDVPDYA-. FLAG1 bears the insert between residues 91 and 92; FLAG2: 125-126; Myc: 118-119; HA-Rep: replaces the 8 residues 103 through 110; HA-End: places the HA-tag at the very end of KCNE1 (after P129); HA-Psp: A linker, -PSP- is placed after P129, followed by the HA-tag; E1-HAc: A linker, -SGSG- is placed after P129, followed by the HA-tag.

+, O.K; ++: good; +++: very good; N/D: Not determined.

Q1-like: KCNQ1 currents; I_{ks} currents: KCNQ1/ KCNE1 currents.

A


1
10
20
30
40
142
hKCNE1 MilsNtTavtpfltklwqetvqqggNMSglaRRspRsgdg kpspsgsgypydvpdya

B

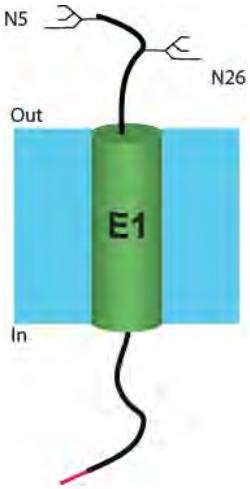
N5
N26
Out
E1
In

C

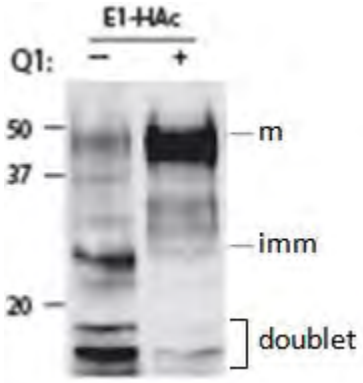
E1-HAc
Q1:
–
+
50
37
20
m
imm
doublet

Figure A2.1: **C-terminally HA-tagged KCNE1 (E1-HAc)**. (**A**) The amino acid sequence of hKCNE1, 1-40 and 126-142. Green cylinder represents the transmembrane domain. First sequon (-NTT-) is underlined red, second sequon blue (-NMS-), arginine cluster (-RRSPR-) purple, linker (-SGSG-) orange, HA-tag (-YPYDVPDYA-) mahogany. (**B**) The diagram of C-terminally HA-tagged KCNE1 with a single pass transmembrane domain. The two consensus N-linked glycosylation sites (N5 and N26) are on N-terminus, facing the exterior side of the plasma membrane. (**C**) Expression of E1-HAc alone and with Q1, 48 hours post-transfection. When E1 was expressed alone the bands resolved to a doublet around ~15 kDa and a single band at ~25 kDa on an SDS-PAGE. When E1 was coexpressed with Q1, E1 resolved to a higher molecular weight band above ~37 kDa. m: mature glycans on E1; imm: immature glycans on E1; doublet: the two bands resolving around ~15 kDa.

established and long used N-terminally HA-tagged KCNE1 protein (E1-HAn) (Figure A2.1***B*** and Figure2.1, Chapter II). However, E1-HAc construct also possessed an extra fast migrating band not observed with the E1-HAn construct.

Determining the glycoforms of E1-HAc through enzymatic deglycosylation assays

KCNE1 has two N-linked glycosylation sites at N5 and N26. KCNE1 glycans allow us to follow trafficking of E1 through the secretory pathway (Chapter II) (Chandrasekhar et al., 2006). ER resident proteins have immature N-linked glycans. The ER uses these high mannose oligosaccharide handles to promote protein folding, oligomerization, quality control, retention and trafficking (Parodi, 2000b; Walsh, 2006). Once the proteins are correctly folded and assembled they are ready to leave the ER and migrate through medial- and trans-Golgi compartments. While trafficking through secretory pathway, glycoproteins acquire complex modifications to their N-linked glycans and this process is known as glycan maturation (High et al., 2000; Parodi, 2000a; Trombetta, 2003; Walsh, 2006). In order to distinguish between E1 glycoforms, we performed an enzymatic deglycosylation assay on E1-HAc to fully characterize the nature of all the bands observd on the western blot (Figure A2.2***A***).

We used two glycosidases to differentiate between the unglycosylated E1 protein and the mature and immature glycoforms. Endo H cleaves only high mannose and some hybrid N-linked glycans, removing immature glycans found in the ER and cis-Golgi forms of KCNE1 proteins. PNGase F removes all N-linked glycans (high mannose, hybrid and complex).

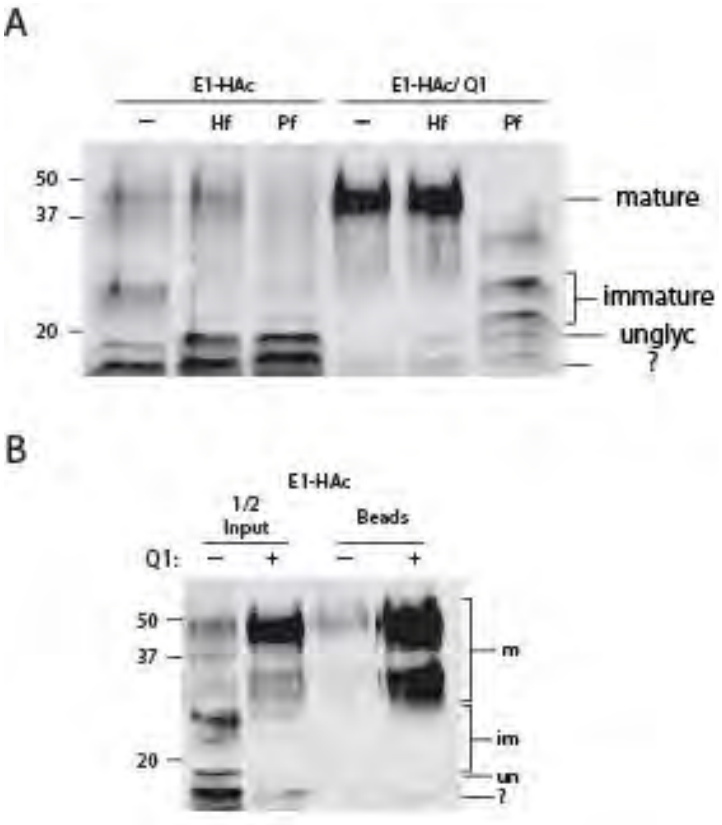
A
E1-HAc
E1-HAc/ Q1
–
Hf
Pf
–
Hf
Pf
50
37
20
mature
immature
unglyc
?
B
E1-HAc
1/2 Input
Beads
Q1:
–
+
–
+
50
37
20
m
im
un
?

Figure A2.2: **Only mature E1-HAc could reach cell membrane**. (***A***) Immuboblot of enzymatic deglycosylation assay of E1-HAc from CHO cells transfected with E1 and E1/Q1 DNA. The samples were left untreated (–), digested with Endo H (Hf) or PNGase F (Pf), and separated by SDS-PAGE (15%). Expression of E1 alone resulted in a doublet at ~15 kDa, a faint 37 kDa band that was Hf resistant and a ~25 kDA band that collapsed to the upper band of the doublet (~17 kDa) upon Hf and Pf treatment. Expression of E1 with Q1 channel subunits resulted in robust expression of a ~37 kDa band that was identified as maturely glycosylated E1 after enzymatic deglycosylation. Mature (*mature*), immature (*immature*), and unglycosylated (*unglyc*) samples are indicated as determined by enzymatic deglycosylation. The "?" denotes the lower, unknown band. PNGase F digestion products that migrated slower than unglycosylated or immature E1 protein are different glycoforms of E1 due to O-linked glycosylation (personal communication with Kshama Chandrasakher). (***B***) Immunoblot of a cell surface biotinylation assay of E1-HAc expressed in CHO cells with and without Q1 channel subunits. Transfected cells were labeled with a membrane-impermeant biotin reagent and subsequently lysed (Experimental Procedures). The isolated biotinylated proteins (Beads) and half of the input (1/2 Input) were separated on an SDS-PAGE (15%). Mature (*m*), immature (*im*), and unglycosylated (*un*) samples are indicated as determined by the enzymatic deglycosylation assay above. The "?" denotes the lower unknown band.

Therefore, cell lysates were treated with PNGase F (Pf) or Endo H (Hf) and resolved by SDS-PAGE (Figure A2.2***A***).

When E1 was expressed alone, both enzymes collapsed the band running at ~25 kDa to the top band resolving at ~17 kDa. This identified the larger ~17 kDa band as unglycosylated E1 and the ~25 kDa species as the immaturely glycosylated E1 protein (Figure A2.2***A***). With Q1 co-expression, we primarily observed a ~37 kDa band, resistant to Endo-H treatment. This band collapsed to lower molecular weight bands upon PNGase-F treatment, indicating that the higher molecular band was maturely glycosylated E1. The identity of the lowest band, which resolved to smaller ~16 kDa and was missing in the N-terminally HA-tagged E1, was analyzed further (*vide infra*).

Measuring membrane protein levels by cell surface biotinylation assay

Previously, cell surface biotinylation assay showed that maturely glycosylated E1-HAn proteins were found at the cell surface. Hence, we tested whether the cell surface expression of E1-HAc was the same as E1-HAn. We expressed E1-HAc alone and with Q1 in CHO cells. We labeled the proteins with a membrane impermeant, amine reactive biotin derivative at 4^{o}C to stop membrane recycling and pulled down biotinylated cell surface proteins using streptavidin beads (Experimental Procedures). The samples were resolved by an SDS-PAGE and probed for the HA tag. Consistent with E1-HAn, our results showed that E1-HAc requires Q1 to reach cell surface and only the mature glycoform is detected at the cell surface (Figure A2.2***B*** and Figure 2.4***A***, Chapter II).

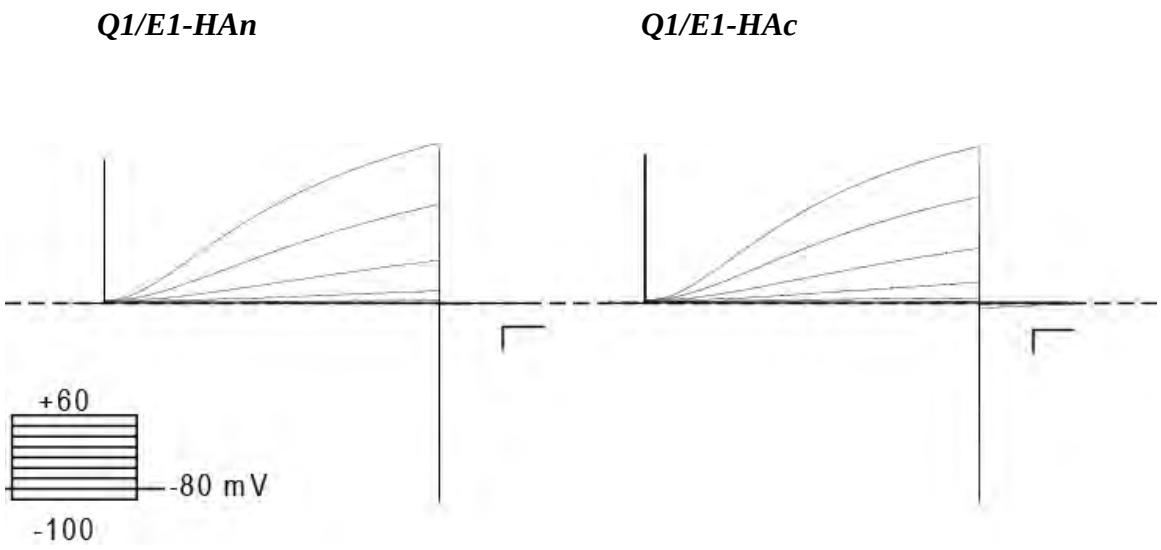

Figure A2.3: **Q1/E1-HAc currents were like Q1/E1-HAn currents**. Representative families of traces were recorded from *Xenopus laevis* oocytes. Oocytes were microinjected with KCNQ1 (Q1) and with KCNE1 (E1-HAn or E1-HAc) RNA (Experimental Procedures). The currents were evoked by holding oocytes at −80 mV and pulsing to a command potential of -100 mV to + 60 mV in 20 mV increments.

Functional analysis of E1-HAc: E1-HAc and KCNQ1 channels give I_{Ks} currents

With the exception of a single, faster migrating band on a western blot, E1-HAc seemed to behave like E1-HAn. Therefore, we wanted to test E1-HAc for native function by analyzing E1-HAc/KCNQ1 channel currents. KCNE1/KCNQ1 channels give rise to cardiac I_{Ks} currents in native tissues. Figure A2.3 shows two electrode voltage clamp recordings from *Xenopus* oocytes injected with Q1/E1-HAn or Q1/E1-HAc. Both E1-HAn/KCNQ1 and E1-HAc/KCNQ1 channels gave rise to slowly activating cardiac I_{Ks} like currents. Therefore, the placement of this HA-tag in KCNE1 C-terminus does not distrupt E1 function.

Investigation of the lower band

Each C-terminally tagged KCNE1 construct possessed an extra band below the unglycosylated band (~17 KDa). Since we were not able to see the truncated protein in the western blots of the N-terminally tagged E1, we wanted to be certain this band was not an artifact of the C-terminal HA-tag. Therefore, we probed E1-HAn immunoblots with native KCNE1 antibody (rabbit α-KCNE1). We observed the presence of the lower, band with E1-HAn (Figure A2.4***A***), demonstrating that this putative post-translational modification was also present in N-terminally HA-tagged KCNE1.

This gave us the biggest clue as to why we were not able to see this truncated protein with E1-HAn. We hypothesized that a proteolytic cleavage was occurring downstream of the HA tag, which was located between the residues 22 and 23. Once the

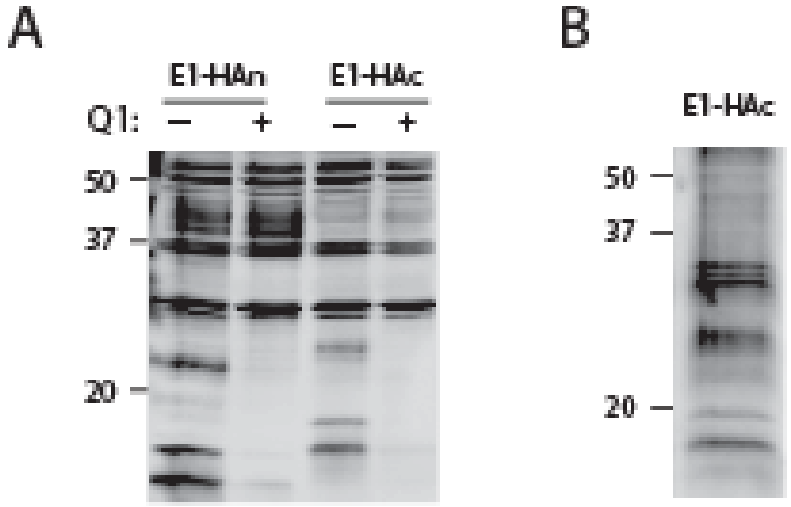
A
E1-HAn
E1-HAc
Q1:
–
+
–
+
50
37
20
B
E1-HAc
50
37
20

Figure A2.4: **The unknown band was membrane associated and also detected wih E1-HAn when probed with native antibody**. (A) Immunoblots of N-terminally HA-tagged KCNE1 (E1-HAn) and C-terminally HA-tagged KCNE1 (E1-HAc) from solubilized CHO cells transfected with E1 and E1/Q1 DNA. The samples were separated by SDS-PAGE (15%). Immuboblots were probed with α-KCNE1 (native antibody). For both constructs expression of E1 alone resulted in a doublet at ~15 kDa (the fast migrating, unknown band was present in E1-HAn and E1-HAc) and a ~25 kDa band. Expression of E1-HAn with Q1 channel subunits resulted in expression of a 37 kDa band, corresponding to the maturely glycosylated E1 protein, and it was not observed with E1-HAc. This was not a surprise since we knew that the native antibody was raised against the C-terminus, and the 9 amino acid HA tag with the 4 amino acid linker might interfere with antibody binding to this segment. (B) Immuboblot from solubilized CHO cells transfected with E1-HAc DNA. CHO cells were hypotonically lysed; membrane was pelleted, washed, and solubilized in 1.5% RIPKA solution. The resuspended membrane proteins were separated by SDS-PAGE (15%) and probed for the HA tag. A doublet at ~15 kDa, a ~25 kDa band and an extra band below 37 kDa band was observed (O-glycosylated E1 glycoform could be membrane associated). The fast migrating - unknown band, which was running below the ~17 kDa band (unglycosylated E1), was membrane associated.

N-terminus was partially cleaved we were losing the tag on N-terminus; whereas with E1-HAc, the tag on the C-terminus stayed intact and allowed us to observe this previously unobserved post-translational modification. Later, autoradiographs of metabolically labeled E1-HAn also showed the presence of the lower band below the unglycosylated E1-HAn protein, consistent with our hypothesis (data not shown).

In order to further analyze this truncated protein, we asked whether (a) it was membrane associated, (b) it was a degradation product, or (c) whether phosphorylation – dephosphorylation had an effect on electrophoretic mobility.

I used different protease inhibitor cocktails to inhibit probable degradation pathways. Phenylmethylsulfonyl fluoride (PMSF) and leupeptin, pepstatin and aprotinin (LPA) are the protease inhibitors regularly used to prevent proteolysis during cell lysis. In addition to these inhibitors, I supplemented the lysates with additional Protease Inhibitor Cocktails (Experimental Procedures).

Deoxymannojirimycin (DMJ) was used to check whether the lower unidentified band was due to ER based degradation. DMJ inhibits the action of ER mannosidases 1 and 2, preventing the removal of the outermost mannose residues on the core oligosaccharides, thereby blocking ER assisted degradation (Helenius and Aebi, 2001). NH_4Cl and chloroquine were used to prevent lysosomal degradation (Experimental Procedures). NH_4Cl and chloroquine are both weak bases that inhibit lysosomal hydrolysis by reducing the acidification of the endosomal/lysosomal compartments. ALLN, lactacystin and MG132 were used to inhibit proteosomal degradation (Experimental Procedures). With the exception of one lysosomal inhibitor, none of the

inhibitors or reagents tested resulted in any observable difference on the expression of the lower band (data not shown). With the lysosomal inhibitor, chloroquine, we saw an increase in the signal of the lower band, which suggested that this cleavage product was degraded in the lysosomal compartments. However, this did not indicate how and where the 15 kDa band was made.

Next, I tested whether the band shift might be due to phoshorylation. Calf intestinal alkaline phosphatase (CIP) is an enzyme that releases the phosphate group from phosphorylated tyrosine (Y), serine (S) and threonine (T) residues. The cell lysates were treated with CIP for 1 hour at 37^{o}C. I used endogenous protein kinase C (PKC, a known phosphorylated protein) as a positive control. Both CIP treated and untreated samples were compared on SDS-PAGE. The western blot was probed with α-HA and α-phospho PKC. CIP treatment had no effect on the intensity or migration pattern of the unknown KCNE1 band (data not shown).

Finally, I asked whether this truncated protein was membrane associated or soluble. To test this, cells were hypotonically lysed to release cytoplasmic proteins. The membrane was pelleted, washed, and then solubilized in 1.5% RIPKA solution. The resuspended membrane proteins were resolved on SDS-PAGE and probed for the HA tag. The western blots showed that the KCNE1 truncated protein was membrane associated (Figure A2.4***B***).

Finding an internal translation start site at M27

Next, we tested the presence of an internal translation start site, since KCNE1 has a methionine at M27. We also knew that the unknown band was not observed with E1-HAn where the N-terminal tag was placed before the 23rd residue, preceding the internal methionine. Therefore, I made a panel of start site mutants, M1L, M27L and M27V, to find out the contribution of the internal start site (M27) on protein expression.

When I mutated the first methionine to a leucine (M1L), we were still able to see the lower band (Figure A2.5***A***). This suggested that in the absence of M1, M27 could act as a translational start site. Yet, it was not clear whether the lower band was solely due to the presence of an internal translational start site. Therefore, I mutated the methionine at 27 to a leucine (M27L). M27L reduced the overall signal for the KCNE1 glycoforms on a western blot, and we still could see the lower band (Figure A2.5***A***). Since M27L did not completely abolish the lower band, this KCNE1 isoform might not be solely due to the presence of an internal translational start site.

This second start site (M27) happens to be the variable amino acid at the center of the internal sequon (-NMS-) and it is conserved in rat, human and pig homologues of E1 protein. Yet, mouse has a valine instead of a methionine (Figure1.4***B***, Chapter I). Since, the point mutation from Met to Leu resulted in reduced protein expression of KCNE1 glycoforms, I decided to mutate the internal translation start site to another conserved residue, valine (M27V). M27V improved overall KCNE1 expression, but still yielded the unknown band (Figure A2.5***A***).

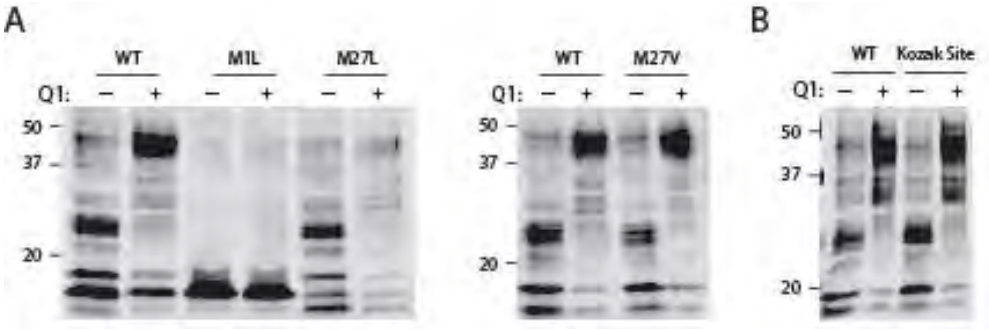

Figure A2.5: **M27 on KCNE1 is an internal translational start site**. Immunoblots of WT (E1-HAc), the start site mutants (M1L, M27L, M27V), and the E1-HAc with the Kozak site. E1-HAc proteins were expressed alone and with Q1. WT (E1-HAc) was used as a positive control. (***A***) M1L abolished the start site and resulted in a robust expression from the internal start site (M27) resolving as the unknown, fast migrating lower band (~15 kDa) on an SDS-PAGE (15%). Both M27L and M27V partially reduced the unknown, fast migrating lower band (~15 kDa). With M27L appeared an extra band below the unknown band. Co-expression of M27V with Q1 resulted in an abundance of the maturely glycosylated proteins (~37 kDa), whereas with M27L the signal was significantly low, suggesting a reduction in glycan maturation in the case of M27L. (***B***) Kozak site (GCC GCC (A/G)CC ATG) partially disrupted the unknown, fast migrating lower band (~15 kDa). Co-expression with Q1 resulted in an abundance of maturely glycosylated proteins (~37 kDa).

In order to prevent the internal start site from complicating the future results, an optimal translation initiation site (Kozak site; -GCC GCC (A/G)CC ATG-) was engineered into all our expression vectors, which has been reported to improve translation initiation in higher eukaryotes (Kozak, 1989). In our expression vectors, the Kozak sites improved overall KCNE1 expression (Figure A2.5***B***). All E1-HAc constructs used in Chapters II, III, and IV possess the optimal translation initiation site.

A probable proprotein convertase site on E1

KCNE1 protein has a potential proprotein convertase recognition site that starts with R32 and ends with S38 (--RRSPRSS--) according to the propeptide cleavage site prediction program, ProPv.1.0b. Therefore we wanted to test whether the lower band observed in our western blots was the proteolytic cleavage product of a proprotein convertase (PC). The proprotein convertases are a family of calcium-dependent, subtisilin-like serine endoproteases that cleave the proprotein substrates at the carboxy terminal side of doublets or clusters of basic amino acids, (-Arg/Lys)- $(X)_n$-(Arg/Lys)- ↓ . Moreover, two arginines within this consensus cleavage site, R32H and R36H, are Long QT mutations (Splawski et al. 2000 and Napolitano et al. 2005). R36 also scored high as PC cleavage site *in silico*.

Furin is the most studied member of PCs. First, I used furin inhibitors to see whether they could prevent formation of the unknown band. Two different furin inhibitors were used: furin Inhibitor I (Decanoyl-Arg-Val-Lys-Arg-CMK) and furin Inhibitor II, (H(D)Arg-Arg-Arg-Arg-Arg-NH_2). Neither of the inhibitors had an effect on

the lower band, indicating that the probable proprotein convertase cleavage site is not a substrate for furin or other known proprotein convertases that are sensitive to furin inhibitors (data not shown).

Next, I introduced point mutations and changed the arginines at the potential proprotein convertase recognition site to alanines: R32A, R33A, R36A. Individual alanine mutants did not result in a significant reduction of the lower band. However, we did observe a better expression of E1 alone and with Q1, especially with the two Long QT mutants: R33A and R36A (Figure A2.6***A***). Then, I designed a double arginine mutant (R33A; R36A), disrupting the entire recognition site (Figure A2.6***B***). With the double arginine mutants, expression of immature E1 increased significantly and unglycosylated glycoform was almost abolished, but the lower band was still present. Finally, the double mutant (R33A; R36A) in the Kozak plasmid resulted in almost complete loss of the lower band (Figure A2.6***B***), suggesting a role for R33 and R36 (R32 and R36 are the residues prone to Long QT mutations) in proteolytic cleavage of KCNE1 proteins.

A

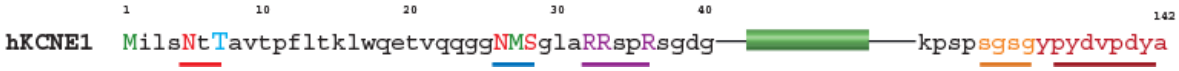
1
10
20
30
40
142
hKCNE1
MilsNtTavtpfltklwqetvqqqgNMSglaRRspRsgdg
kpspsgsgypydvpdya

B

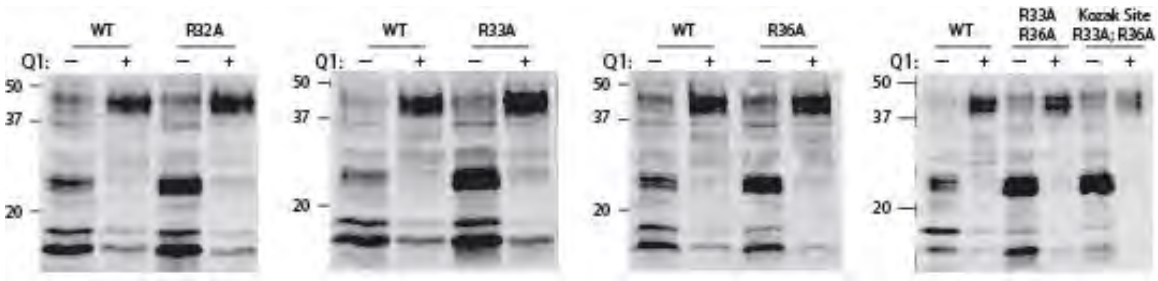
WT
R32A
WT
R33A
WT
R36A
WT
R33A R36A
Kozak Site R33A; R36A
Q1:
50
37
20

Figure A2.6: **The basic residues residing between 32-36 are partially responsible for the unknown band**. (***A***) The amino acid sequence of hKCNE1, 1-40 and 126-142. Green cylinder represents transmembrane domain. First sequon (-NTT-) is underlined in red, second sequon in blue (-NMS-), linker (-SGSG-) in orange, HA-tag (-YPYDVPDYA-) in mahogany, arganine cluster (-RRSPR-) bearing R32, R33 and R36 in purple. (***B***) Immunoblots of WT (E1-HAc) and the arginine mutants (R32A, R33A, R36A, R33A;R36A; R33A;R36A with Kozak site). WT and mutant proteins were expressed alone and with Q1. WT (E1-HAc) was used as a positive control. With single arganine mutants (R32A, R33A, R36A) and R33A;R36A the bands resolved on an 15 % SDS-PAGE were like WT protein: the doublet around ~15 kDa (unglycosylated band and the unknown species); ~25 kDa (immaturely glycosylated protein); ~37 kDa (maturely glycosylated protein in the presence of Q1). Whereas with R33A;R36A with the Kozak site, the unknown band was significantly reduced, almost abolished.

DISCUSSION

KCNE1 has two glycosylation sites at N5 and N26; N5 acquires glycans co-translationally, and N26 acquires glycans post-translationally (Chapter II). KCNE1 also has an O-linked glycosylation site (personal communication with Kshama Chandrasekhar). The need for building a C-terminally tagged KCNE1 protein for studying the two glycosylation sites on N-terminus led to the investigation of two previously unobserved features of this glycoprotein. We now know that KCNE1 has an internal translation start site, a methionine at position 27 that gives rise to a fast migrating band below the unglycosylated E1 protein on a western blot. This lower band was not observed in the long-used N-terminally tagged E1, since the tag was between the residues Q22 and Q23, four amino acids upstream of the M27.

We also found a putative proteolytic cleavage site at the arginine cluster spanning the residues 32 through 38 contributing to the signal of fast migrating band on an SDS-PAGE. This region of KCNE1 bears strong sequence homology to a potential proprotein convertase cleavage site, (-Arg/Lys)- $(X)_n$-(Arg/Lys)- ↓. The potential importance of this putative proteolytic cleavage site may be highlighted by two known Long QT mutations (R32H and R36H) (Splawski et al., 2000; Napolitano et al., 2005). Yet, inhibitors targeting the known proprotein convertases did not have an effect on the expression of the lower band. This leaves the door open for finding the enzyme that is responsible for the cleavage of the KCNE1 protein. More importantly, the functional significance of this

membrane associated post-translationally modified KCNE1 form has to yet be discovered.

EXPERIMENTAL PROCEDURES

Plasmids and cDNAs. Human Q1 and E1 were subcloned into pcDNA3.1(-) (Invitrogen). Two hemagglutinin A (HA)-tagged versions of E1 were used. For comparison purposes, a well established extracellular HA tag (YPYDVPDYA) was incorporated in the E1 N terminus between residues 22 and 23. The C-terminally epitope tagged KCNE1 had an HA tag (YPYDVPDYA) appended to the E1 C terminus via an SGSG linker through PCR techniques. All E1 constructs (wild type and mutants) possessed this C-terminal HA epitope tag. To produce the M1L, M27L, R32A, R33A, R36A, (R33A;R36A) mutants and Kozak site (GCC GCC (A/G)CC ATG) site-directed mutagenesis was performed using the QuikChange system (Stratagene) and the mutations were confirmed by DNA sequencing of the entire gene.

Cell culture and transfections. Chinese Hamster Ovary (CHO-K1) cells were cultured in F-12K nutrient mixture (Gibco – Invitrogen). The media was supplemented with 10% fetal bovine serum (Hyclone) and 10^2 U/mL penicillin/streptomycin (Gibco – Invitrogen). Cells were plated at 60 – 75 % confluency in 35 mm dishes for all experiments. After 24 h, cells were transiently transfected at RT with Lipofectamine (Invitrogen) 8 μl per mL of Opti-MEMI (Gibco - Invitrogen) and returned to fresh media after 6 hr. DNA ratios (in μg): E1/empty pcDNA 3.1 plasmid: 1.25/1.25; Q1/E1 (western blots). Cells were used 48 h post-transfection for western blots.

Cell lysis and Western Blot Analysis. Cells were washed in ice-cold PBS (3 × 2 mL) and lysed at 4°C in RIPKA buffer (in mM): 10 Tris·HCl, pH 7.4, 140 NaCl, 10 KCl,

1 EDTA, and 1% Triton-X, 0.1% SDS, 1% sodium deoxycholate and supplemented with protease-inhibitors: 1 mM phenylmethylsulfonyl fluoride (PMSF) and 1 μg/mL each of leupeptin, pepstatin and aprotinin (LPA). Lysates were diluted with SDS-PAGE loading buffer containing 100 mM DTT, loaded on a 15% SDS-polyacrylamide gel, transferred to a nitrocellulose membrane, and blocked in western blocking buffer (5% nonfat dry milk in Tris-buffered saline containing 0.2% Tween-20 (TBS-T)) for 30 min at RT. Membranes were incubated overnight at 4°C with rat anti-HA (Roche) (1:750) in western blocking buffer and washed in TBS-T next day and incubated with goat anti-rat horseradish peroxidase (HRP)-conjugated antibody (Jackson Immunoresearch Labs, Inc.) (1:2000) in western blocking buffer for 45 min at RT. Membranes were washed with TBS-T and incubated with SuperSignal West Dura Extended Duration Substrate (Pierce) for 5 min. HRP-bound proteins were detected by chemiluminescence using Fujifilm LAS-3000 CCD camera and quantified using the Image Gauge V2.1 software (Fujifilm).

Ezymatic deglycosylation assay. NP-40, BME, and reaction buffer (G5 for Endo H; G7 for PNGase F) were added to the cell lysates (20 μL), which were diluted with water to a final concentration of 1% NP40 and 1% BME. Endo Hf (2 μL) or PNGase F (1 μL) (New England BioLabs, Inc.) were added to the samples and incubated at 37°C for 30 min. The samples were brought to a final concentration of 100 mM DTT and 1.3% SDS and were separated on an SDS-PAGE (15% gel) and analyzed by western blot as described above.

Cell surface biotinylation. Transfected cells were rinsed with ice-cold PBS^{2+} buffer (PBS containing 1 mM $MgCl_2$, 0.1 mM $CaCl_2$), incubated with 1 mg/mL sulfo-

NHS-SS-biotin (Pierce) in PBS^{2+} buffer for 2 × 15 min at 4°C. The biotin reagent was quenched by washing with (3 × 2 mL) with quench solution (PBS^{2+} containing 100 mM glycine) and then incubated with quench solution for 2 × 15 min at 4°C. Cells were lysed in RIPKA buffer and cell debris was removed by centrifugation. For each sample, 75 µg of total protein was quantitated by BCA analysis and incubated with 25 µL of Immunopure® Immobilized streptavidin beads (Pierce) overnight at 4°C. One-half of the input (37.5 µg of total protein) was saved as a control for each sample. Beads were washed 3 X with 0.1% SDS buffer (500 µL) and biotinylated proteins were eluted first with 30 µl 2× SDS-PAGE and 200 µM DTT mix for 15 min at 55°C, then with 30 µl 200 µM DTT for 5 min at 55°C and the two elutions were combined to achieve 60 µl final volume. Half of the input and bead-eluted proteins were separated by SDS-PAGE, analyzed by Western Blot as described above.

cRNA Preparation; Oocyte Preparation and cRNA Injection. KCNE1 and KCNQ1 plasmids were linearized with MluI, and RNA synthesized by run-off transcription using SP6 (Promega). Mature oocytes were surgically extracted from anesthetized *Xenopus laevis*; isolated and prepared for injection as described in (Gage and Kobertz, 2004). Oocytes were microinjected with RNA approximately 24 hours after extraction with 36 nL total volume of cRNA solution. Oocytes were injected with Q1 (10 ng/oocyte) and E1 (5 ng/oocyte) at RT. After 3–6 days, currents were measured using two-electrode voltage clamp, TEVC (OC-725-C; Warner Instrument Corp.) and data acquired with Digidata 1322A (Axon Instruments) using pClamp 8 or 9 (Axon Instruments) at RT. Electrodes were filled with 3 M KCl, 5 mM EGTA, 10 mM HEPES,

pH 7.6, and had resistance between 0.2 and 1 MΩ. For each experiment, oocytes were held at −80 mV in ND96 (in mM): 96 NaCl, 2 KCl, 0.3 $CaCl_2$, 1 $MgCl_2$, 5 HEPES, pH 7.4, and pulsed to a command potential of + 60 mV in 20 mV increments.

Additional Enzyme Assays and Inhibitors used: We used rabbit α-KCNE1 (1:600) from Alomone Labs. The 30 µl of cell lysates were treated with 1 µl of calf intestinal alkaline phosphatase, CIP, (New England BioLabs), 4 µl of 10 X NEBuffer 3 (New England BioLabs) and brought up to a final volume of 40 µl with H_2O and incubated for 1 hour at 37^oC. CIP treated and untreated samples were resolved on a western blot and analyzed as described above. We used endogeneous protein kinase C, PKC, as a positive control and probed the blots with (1:1000) rabbit α-phospho-PKCδ antibody (Cell Signaling Technology) as 1^o antibody and (1:2000) donkey α-rabbit IgG, HRP (Promega) as 2^o antibody. In addition to the protease inhibitor mix LPA and PMSF, we used Roche Complete, EDTA-free protease inhibitor tablets (each tablet was dissolved in 500 µl H_2O to obtain 100X solution) and Protease Inhibitor Cocktail (Sigma). 1 µl of each protease inhibitor was used for 100 µl final volume. To test ER based degradation 1 mM deoxymannojirimycin, DMJ (Toronto Research Chemicals, Inc.) was used. To prevent lysosomal degradation 50 mM NH_4Cl and 50 µM chloroquine (Sigma) were used. To test proteosomal degradation 50 µM ALLN (Calbiochem), 25 µM lactacystin (Calbiochem) and 10 µM MG132 (Calbiochem) were used. To check proteolytic cleavage by furin we used 25 µM furin inhibitor I (Decanoyl-Arg-Val-Lys-Arg-CMK) and 25 µM furin inhibitor II, (H(D)Arg-Arg-Arg-Arg-Arg-NH_2) from Calbiochem. Cells were incubated with the media containing inhibitors for 24 hours to 48 hours.

REFERENCES

Abbott, G.W., and S.A. Goldstein. 1998. A superfamily of small potassium channel subunits: form and function of the MinK-related peptides (MiRPs). *Q Rev Biophys*. 31:357-398.

Abbott, G.W., and S.A. Goldstein. 2001. Potassium channel subunits encoded by the KCNE gene family: physiology and pathophysiology of the MinK-related peptides (MiRPs). *Mol Interv*. 1:95-107.

Abitbol, I., A. Peretz, C. Lerche, A.E. Busch, and B. Attali. 1999. Stilbenes and fenamates rescue the loss of I(KS) channel function induced by an LQT5 mutation and other IsK mutants. *Embo J*. 18:4137-4148.

Ackerman, M.J., and D.E. Clapham. 1997. Ion channels--basic science and clinical disease. *N Engl J Med*. 336:1575-1586.

Adelman, J.P. 1995. Proteins that interact with the pore-forming subunits of voltage-gated ion channels. *Curr Opin Neurobiol*. 5:286-295.

Alberts, B., A. Johnson, J. Lewis, M. Raff, K. Roberts, and P. Walter. 2002. Molecular Biology of the Cell, 4th edition. Garland Science, New York.

Anderson, E.D., J.K. VanSlyke, C.D. Thulin, F. Jean, and G. Thomas. 1997. Activation of the furin endoprotease is a multiple-step process: requirements for acidification and internal propeptide cleavage. *Embo J*. 16:1508-1518.

Angelo, K., T. Jespersen, M. Grunnet, M.S. Nielsen, D.A. Klaerke, and S.P. Olesen. 2002. KCNE5 induces time- and voltage-dependent modulation of the KCNQ1 current. *Biophys J*. 83:1997-2006.

Apweiler, R., H. Hermjakob, and N. Sharon. 1999. On the frequency of protein glycosylation, as deduced from analysis of the SWISS-PROT database. *Biochim Biophys Acta*. 1473:4-8.

Attali, B. 2002. Human congenital long QT syndrome: more than previously thought? *Trends Pharmacol Sci*. 23:249-251.

Barhanin, J., F. Lesage, E. Guillemare, M. Fink, M. Lazdunski, and G. Romey. 1996. K(V)LQT1 and lsK (minK) proteins associate to form the I(Ks) cardiac potassium current. *Nature*. 384:78-80.

Bei, Y., J. Hogan, L.A. Berkowitz, M. Soto, C.E. Rocheleau, K.M. Pang, J. Collins, and C.C. Mello. 2002. SRC-1 and Wnt signaling act together to specify endoderm and to control cleavage orientation in early C. elegans embryos. *Dev Cell*. 3:113-125.

Bendahhou, S., C. Marionneau, K. Haurogne, M.M. Larroque, R. Derand, V. Szuts, D. Escande, S. Demolombe, and J. Barhanin. 2005. In vitro molecular interactions and distribution of KCNE family with KCNQ1 in the human heart. *Cardiovasc Res*. 67:529-538.

Ben-Dor, S., N. Esterman, E. Rubin, and N. Sharon. 2004. Biases and complex patterns in the residues flanking protein N-glycosylation sites. *Glycobiology*. 14:95-101.

Bianchi, L., S.M. Kwok, M. Driscoll, and F. Sesti. 2003. A potassium channel-MiRP complex controls neurosensory function in Caenorhabditis elegans. *J Biol Chem*. 278:12415-12424.

Bolt, G., C. Kristensen, and T.D. Steenstrup. 2005. Posttranslational N-glycosylation takes place during the normal processing of human coagulation factor VII. *Glycobiology*. 15:541-547.

Brenner, S. 1974. The genetics of Caenorhabditis elegans. *Genetics*. 77:71-94.

Browning, K.S. 1996. The plant translational apparatus. *Plant Mol Biol*. 32:107-144.

Burda, P., and M. Aebi. 1999. The dolichol pathway of N-linked glycosylation. *Biochim Biophys Acta*. 1426:239-257.

Busch, A.E., G.L. Busch, E. Ford, H. Suessbrich, H.J. Lang, R. Greger, K. Kunzelmann, B. Attali, and W. Stuhmer. 1997. The role of the IsK protein in the specific pharmacological properties of the IKs channel complex. *Br J Pharmacol*. 122:187-189.

Busch, A.E., M.D. Varnum, R.A. North, and J.P. Adelman. 1992. An amino acid mutation in a potassium channel that prevents inhibition by protein kinase C. *Science*. 255:1705-1707.

Cadigan, K.M., and R. Nusse. 1997. Wnt signaling: a common theme in animal development. *Genes Dev*. 11:3286-3305.

Catterall, W.A. 1995. Structure and function of voltage-gated ion channels. *Annu Rev Biochem*. 64:493-531.

Chandrasekhar, K.D., T. Bas, and W.R. Kobertz. 2006. KCNE1 subunits require co-assembly with K+ channels for efficient trafficking and cell surface expression. *J Biol Chem*. 281:40015-40023.

Chen, H., and S.A. Goldstein. 2007. Serial perturbation of MinK in IKs implies an alpha-helical transmembrane span traversing the channel corpus. *Biophys J*. 93:2332-2340.

Chen, L., J. Kurokawa, and R.S. Kass. 2005. Phosphorylation of the A-kinase-anchoring protein Yotiao contributes to protein kinase A regulation of a heart potassium channel. *J Biol Chem*. 280:31347-31352.

Chen, W., J. Helenius, I. Braakman, and A. Helenius. 1995. Cotranslational folding and calnexin binding during glycoprotein synthesis. *Proc Natl Acad Sci U S A*. 92:6229-6233.

Cheung, J.C., and R.A. Reithmeier. 2007. Scanning N-glycosylation mutagenesis of membrane proteins. *Methods*. 41:451-459.

Chouabe, C., N. Neyroud, P. Guicheney, M. Lazdunski, G. Romey, and J. Barhanin. 1997. Properties of KvLQT1 K+ channel mutations in Romano-Ward and Jervell and Lange-Nielsen inherited cardiac arrhythmias. *Embo J*. 16:5472-5479.

Cohen, P. 2000. The regulation of protein function by multisite phosphorylation--a 25 year update. *Trends Biochem Sci*. 25:596-601.

Cohen, P. 2002. The origins of protein phosphorylation. *Nat Cell Biol*. 4:E127-130.

Cotella, D., S. Radicke, A. Bortoluzzi, U. Ravens, E. Wettwer, C. Santoro, and D. Sblattero. 2010. Impaired glycosylation blocks DPP10 cell surface expression and alters the electrophysiology of I (to) channel complex. *Pflugers Arch*.

Dahimene, S., S. Alcolea, P. Naud, P. Jourdon, D. Escande, R. Brasseur, A. Thomas, I. Baro, and J. Merot. 2006. The N-terminal juxtamembranous domain of KCNQ1 is critical for channel surface expression: implications in the Romano-Ward LQT1 syndrome. *Circ Res*. 99:1076-1083.

Dall'olio, F. 1996. Protein glycosylation in cancer biology: an overview. *Clin Mol Pathol*. 49:M126-M135.

DasGupta, R., A. Kaykas, R.T. Moon, and N. Perrimon. 2005. Functional genomic analysis of the Wnt-wingless signaling pathway. *Science*. 308:826-833.

Demolombe, S., D. Franco, P. de Boer, S. Kuperschmidt, D. Roden, Y. Pereon, A. Jarry, A.F. Moorman, and D. Escande. 2001. Differential expression of KvLQT1 and its regulator IsK in mouse epithelia. *Am J Physiol Cell Physiol*. 280:C359-372.

Deschenes, I., and G.F. Tomaselli. 2002. Modulation of Kv4.3 current by accessory subunits. *FEBS Lett*. 528:183-188.

Deutsch, C. 2002. Potassium channel ontogeny. *Annu Rev Physiol*. 64:19-46.

Do, H., D. Falcone, J. Lin, D.W. Andrews, and A.E. Johnson. 1996. The cotranslational integration of membrane proteins into the phospholipid bilayer is a multistep process. *Cell*. 85:369-378.

Doyle, D.A., J. Morais Cabral, R.A. Pfuetzner, A. Kuo, J.M. Gulbis, S.L. Cohen, B.T. Chait, and R. MacKinnon. 1998. The structure of the potassium channel: molecular basis of K+ conduction and selectivity. *Science*. 280:69-77.

Duvet, S., A. Op De Beeck, L. Cocquerel, C. Wychowski, R. Cacan, and J. Dubuisson. 2002. Glycosylation of the hepatitis C virus envelope protein E1 occurs posttranslationally in a mannosylphosphoryldolichol-deficient CHO mutant cell line. *Glycobiology*. 12:95-101.

Egenberger, B., G. Polleichtner, E. Wischmeyer, and F. Doring. 2010. N-linked glycosylation determines cell surface expression of two-pore-domain K+ channel TRESK. *Biochem Biophys Res Commun*. 391:1262-1267.

Ellgaard, L., and A. Helenius. 2003. Quality control in the endoplasmic reticulum. *Nat Rev Mol Cell Biol*. 4:181-191.

Ferraiuolo, M.A., C.S. Lee, L.W. Ler, J.L. Hsu, M. Costa-Mattioli, M.J. Luo, R. Reed, and N. Sonenberg. 2004. A nuclear translation-like factor eIF4AIII is recruited to the mRNA during splicing and functions in nonsense-mediated decay. *Proc Natl Acad Sci U S A*. 101:4118-4123.

Finley, M.R., Y. Li, F. Hua, J. Lillich, K.E. Mitchell, S. Ganta, R.F. Gilmour, Jr., and L.C. Freeman. 2002. Expression and coassociation of ERG1, KCNQ1, and KCNE1 potassium channel proteins in horse heart. *Am J Physiol Heart Circ Physiol*. 283:H126-138.

Folander, K., J.S. Smith, J. Antanavage, C. Bennett, R.B. Stein, and R. Swanson. 1990. Cloning and expression of the delayed-rectifier IsK channel from neonatal rat heart and diethylstilbestrol-primed rat uterus. *Proc Natl Acad Sci U S A*. 87:2975-2979.

Freeman, L.C., J.J. Lippold, and K.E. Mitchell. 2000. Glycosylation influences gating and pH sensitivity of I(sK). *J Membr Biol*. 177:65-79.

Furmanek, A., and J. Hofsteenge. 2000. Protein C-mannosylation: facts and questions. *Acta Biochim Pol*. 47:781-789.
Gage, S.D., and W.R. Kobertz. 2004. KCNE3 Truncation Mutants Reveal a Bipartite Modulation of KCNQ1 K+ Channels. ***J. Gen. Physiol.*** 124:759-771.
Gandhi, C.S., and E.Y. Isacoff. 2002. Molecular models of voltage sensing. *J Gen Physiol*. 120:455-463.
Gavel, Y., and G. von Heijne. 1990. Sequence differences between glycosylated and non-glycosylated Asn-X-Thr/Ser acceptor sites: implications for protein engineering. *Protein Eng*. 3:433-442.
Gingras, A.C., B. Raught, and N. Sonenberg. 1999. eIF4 initiation factors: effectors of mRNA recruitment to ribosomes and regulators of translation. *Annu Rev Biochem*. 68:913-963.
Gomez, M., S.J. Scales, T.E. Kreis, and F. Perez. 2000. Membrane recruitment of coatomer and binding to dilysine signals are separate events. *J Biol Chem*. 275:29162-29169.
Gordon, E., T.K. Roepke, and G.W. Abbott. 2006. Endogenous KCNE subunits govern Kv2.1 K+ channel activation kinetics in Xenopus oocyte studies. *Biophys J*. 90:1223-1231.
Goyer, C., M. Altmann, H.S. Lee, A. Blanc, M. Deshmukh, J.L. Woolford, Jr., H. Trachsel, and N. Sonenberg. 1993. TIF4631 and TIF4632: two yeast genes encoding the high-molecular-weight subunits of the cap-binding protein complex (eukaryotic initiation factor 4F) contain an RNA recognition motif-like sequence and carry out an essential function. *Mol Cell Biol*. 13:4860-4874.
Gradi, A., H. Imataka, Y.V. Svitkin, E. Rom, B. Raught, S. Morino, and N. Sonenberg. 1998. A novel functional human eukaryotic translation initiation factor 4G. *Mol Cell Biol*. 18:334-342.
Grahammer, F., R. Warth, J. Barhanin, M. Bleich, and M.J. Hug. 2001. The small conductance K+ channel, KCNQ1: expression, function, and subunit composition in murine trachea. *J Biol Chem*. 276:42268-42275.
Grunnet, M., T. Jespersen, H.B. Rasmussen, T. Ljungstrom, N.K. Jorgensen, S.P. Olesen, and D.A. Klaerke. 2002. KCNE4 is an inhibitory subunit to the KCNQ1 channel. *J Physiol*. 542:119-130.
Gutman, G.A., K.G. Chandy, S. Grissmer, M. Lazdunski, D. McKinnon, L.A. Pardo, G.A. Robertson, B. Rudy, M.C. Sanguinetti, W. Stuhmer, and X. Wang. 2005. International Union of Pharmacology. LIII. Nomenclature and molecular relationships of voltage-gated potassium channels. *Pharmacol Rev*. 57:473-508.
Hanlon, M.R., and B.A. Wallace. 2002. Structure and function of voltage-dependent ion channel regulatory beta subunits. *Biochemistry*. 41:2886-2894.
Hao, B., W. Gong, T.K. Ferguson, C.M. James, J.A. Krzycki, and M.K. Chan. 2002. A new UAG-encoded residue in the structure of a methanogen methyltransferase. *Science*. 296:1462-1466.
Hegle, A.P., H. Nazzari, A. Roth, D. Angoli, and E.A. Accili. 2010. Evolutionary Emergence of N-Glycosylation as a Variable Promoter of HCN Channel Surface Expression. *Am J Physiol Cell Physiol*.

Heinrich, S.U., W. Mothes, J. Brunner, and T.A. Rapoport. 2000. The Sec61p complex mediates the integration of a membrane protein by allowing lipid partitioning of the transmembrane domain. *Cell*. 102:233-244.
Helenius, A., and M. Aebi. 2001. Intracellular functions of N-linked glycans. *Science*. 291:2364-2369.
Helenius, A., and M. Aebi. 2004. Roles of N-linked glycans in the endoplasmic reticulum. *Annu Rev Biochem*. 73:1019-1049.
Helenius, J., D.T. Ng, C.L. Marolda, P. Walter, M.A. Valvano, and M. Aebi. 2002. Translocation of lipid-linked oligosaccharides across the ER membrane requires Rft1 protein. *Nature*. 415:447-450.
Hershey, J.W. 1991. Translational control in mammalian cells. *Annu Rev Biochem*. 60:717-755.
High, S., F.J. Lecomte, S.J. Russell, B.M. Abell, and J.D. Oliver. 2000. Glycoprotein folding in the endoplasmic reticulum: a tale of three chaperones? *FEBS Lett*. 476:38-41.
Hille, B. 2001. Ion Channels of Excitable Membranes, 3rd edition. Sinauer Associates, Inc., Sunderland, MA.
Hobmayer, B., F. Rentzsch, K. Kuhn, C.M. Happel, C.C. von Laue, P. Snyder, U. Rothbacher, and T.W. Holstein. 2000. WNT signalling molecules act in axis formation in the diploblastic metazoan Hydra. *Nature*. 407:186-189.
Hubner, C.A., and T.J. Jentsch. 2002. Ion channel diseases. *Hum Mol Genet*. 11:2435-2445.
Hunte, C., and S. Richers. 2008. Lipids and membrane protein structures. *Curr Opin Struct Biol*. 18:406-411.
Ishitani, T., J. Ninomiya-Tsuji, S. Nagai, M. Nishita, M. Meneghini, N. Barker, M. Waterman, B. Bowerman, H. Clevers, H. Shibuya, and K. Matsumoto. 1999. The TAK1-NLK-MAPK-related pathway antagonizes signalling between beta-catenin and transcription factor TCF. *Nature*. 399:798-802.
Isom, L.L., K.S. De Jongh, and W.A. Catterall. 1994. Auxiliary subunits of voltage-gated ion channels. *Neuron*. 12:1183-1194.
Jaeken, J., and H. Carchon. 2000. What's new in congenital disorders of glycosylation? *Eur J Paediatr Neurol*. 4:163-167.
Jaeken, J., and G. Matthijs. 2001. Congenital disorders of glycosylation. *Annu Rev Genomics Hum Genet*. 2:129-151.
Jentsch, T.J. 2000. Neuronal KCNQ potassium channels: physiology and role in disease. *Nat Rev Neurosci*. 1:21-30.
Jespersen, T., M. Grunnet, and S.P. Olesen. 2005. The KCNQ1 potassium channel: from gene to physiological function. *Physiology (Bethesda)*. 20:408-416.
Jiang, B., X. Sun, K. Cao, and R. Wang. 2002a. Endogenous Kv channels in human embryonic kidney (HEK-293) cells. *Mol Cell Biochem*. 238:69-79.
Jiang, Y., A. Lee, J. Chen, M. Cadene, B.T. Chait, and R. MacKinnon. 2002b. The open pore conformation of potassium channels. *Nature*. 417:523-526.
Johnson, L.N., and R.J. Lewis. 2001. Structural basis for control by phosphorylation. *Chem Rev*. 101:2209-2242.

Kamath, R.S., and J. Ahringer. 2003. Genome-wide RNAi screening in Caenorhabditis elegans. *Methods*. 30:313-321.
Kasturi, L., H. Chen, and S.H. Shakin-Eshleman. 1997. Regulation of N-linked core glycosylation: use of a site-directed mutagenesis approach to identify Asn-Xaa-Ser/Thr sequons that are poor oligosaccharide acceptors. *Biochem J*. 323 (Pt 2):415-419.
Keating, M.T., and M.C. Sanguinetti. 2001. Molecular and cellular mechanisms of cardiac arrhythmias. *Cell*. 104:569-580.
Kelleher, D.J., and R. Gilmore. 2006. An evolving view of the eukaryotic oligosaccharyltransferase. *Glycobiology*. 16:47R-62R.
Kelleher, D.J., D. Karaoglu, E.C. Mandon, and R. Gilmore. 2003. Oligosaccharyltransferase isoforms that contain different catalytic STT3 subunits have distinct enzymatic properties. *Mol Cell*. 12:101-111.
Khanna, R., E.J. Lee, and D.M. Papazian. 2004. Transient calnexin interaction confers long-term stability on folded K+ channel protein in the ER. *J Cell Sci*. 117:2897-2908.
Khanna, R., M.P. Myers, M. Laine, and D.M. Papazian. 2001. Glycosylation increases potassium channel stability and surface expression in mammalian cells. *J Biol Chem*. 276:34028-34034.
Kikuchi, N., and H. Narimatsu. 2006. Bioinformatics for comprehensive finding and analysis of glycosyltransferases. *Biochim Biophys Acta*. 1760:578-583.
Kleber, A.G., and Y. Rudy. 2004. Basic mechanisms of cardiac impulse propagation and associated arrhythmias. *Physiol Rev*. 84:431-488.
Kolhekar, A.S., A.S. Quon, C.A. Berard, R.E. Mains, and B.A. Eipper. 1998. Post-translational N-glycosylation of a truncated form of a peptide processing enzyme. *J Biol Chem*. 273:23012-23018.
Korneeva, N.L., B.J. Lamphear, F.L. Hennigan, W.C. Merrick, and R.E. Rhoads. 2001. Characterization of the two eIF4A-binding sites on human eIF4G-1. *J Biol Chem*. 276:2872-2879.
Kozak, M. 1989. The scanning model for translation: an update. *J Cell Biol*. 108:229-241.
Krieg, J., S. Hartmann, A. Vicentini, W. Glasner, D. Hess, and J. Hofsteenge. 1998. Recognition signal for C-mannosylation of Trp-7 in RNase 2 consists of sequence Trp-x-x-Trp. *Mol Biol Cell*. 9:301-309.
Krumerman, A., X. Gao, J.S. Bian, Y.F. Melman, A. Kagan, and T.V. McDonald. 2004. An LQT mutant minK alters KvLQT1 trafficking. *Am J Physiol Cell Physiol*. 286:C1453-1463.
Kurokawa, J., L. Chen, and R.S. Kass. 2003. Requirement of subunit expression for cAMP-mediated regulation of a heart potassium channel. *Proc Natl Acad Sci U S A*. 100:2122-2127.
Lehmann-Horn, F., and K. Jurkat-Rott. 1999. Voltage-gated ion channels and hereditary disease. *Physiol Rev*. 79:1317-1372.

Lemp, D., A. Haselbeck, and F. Klebl. 1990. Molecular cloning and heterologous expression of N-glycosidase F from Flavobacterium meningosepticum. *J Biol Chem*. 265:15606-15610.

Lerche, C., I. Bruhova, H. Lerche, K. Steinmeyer, A.D. Wei, N. Strutz-Seebohm, F. Lang, A.E. Busch, B.S. Zhorov, and G. Seebohm. 2007. Chromanol 293B binding in KCNQ1 (Kv7.1) channels involves electrostatic interactions with a potassium ion in the selectivity filter. *Mol Pharmacol*. 71:1503-1511.

Lesage, F., B. Attali, J. Lakey, E. Honore, G. Romey, E. Faurobert, M. Lazdunski, and J. Barhanin. 1993. Are Xenopus oocytes unique in displaying functional IsK channel heterologous expression? *Receptors Channels*. 1:143-152.

Levitan, I.B., and L.K. Kaczmarek. 2002. The Neuron Cell and Molecular Biology, 3rd edition. Oxford University Press, Inc., New York.

Lewis, A., Z.A. McCrossan, and G.W. Abbott. 2004. MinK, MiRP1, and MiRP2 diversify Kv3.1 and Kv3.2 potassium channel gating. *J Biol Chem*. 279:7884-7892.

Li, J., and W.X. Li. 2006a. A novel function of Drosophila eIF4A as a negative regulator of Dpp/BMP signalling that mediates SMAD degradation. *Nat Cell Biol*. 8:1407-1414.

Li, J., W.X. Li, and W.M. Gelbart. 2005. A genetic screen for maternal-effect suppressors of decapentaplegic identifies the eukaryotic translation initiation factor 4A in Drosophila. *Genetics*. 171:1629-1641.

Li, Z., and J. Li. 2006b. Local expressions of TGF-beta1, TGF-beta1RI, CTGF, and Smad-7 in Helicobacter pylori-associated gastritis. *Scand J Gastroenterol*. 41:1007-1012.

Lin, R., S. Thompson, and J.R. Priess. 1995. pop-1 encodes an HMG box protein required for the specification of a mesoderm precursor in early C. elegans embryos. *Cell*. 83:599-609.

Lis, H., and N. Sharon. 1993. Protein glycosylation. Structural and functional aspects. *Eur J Biochem*. 218:1-27.

Liu, X.S., M. Zhang, M. Jiang, D.M. Wu, and G.N. Tseng. 2007. Probing the interaction between KCNE2 and KCNQ1 in their transmembrane regions. *J Membr Biol*. 216:117-127.

Lo, C.F., and R. Numann. 1998. Independent and exclusive modulation of cardiac delayed rectifying K+ current by protein kinase C and protein kinase A. *Circ Res*. 83:995-1002.

Logan, C.Y., and R. Nusse. 2004. The Wnt signaling pathway in development and disease. *Annu Rev Cell Dev Biol*. 20:781-810.

Lomakin, I.B., C.U. Hellen, and T.V. Pestova. 2000. Physical association of eukaryotic initiation factor 4G (eIF4G) with eIF4A strongly enhances binding of eIF4G to the internal ribosomal entry site of encephalomyocarditis virus and is required for internal initiation of translation. *Mol Cell Biol*. 20:6019-6029.

Long, S.B., E.B. Campbell, and R. Mackinnon. 2005. Crystal structure of a mammalian voltage-dependent Shaker family K+ channel. *Science*. 309:897-903.

Long, X., C. Spycher, Z.S. Han, A.M. Rose, F. Muller, and J. Avruch. 2002. TOR deficiency in C. elegans causes developmental arrest and intestinal atrophy by inhibition of mRNA translation. *Curr Biol*. 12:1448-1461.

Lundquist, A.L., L.J. Manderfield, C.G. Vanoye, C.S. Rogers, B.S. Donahue, P.A. Chang, D.C. Drinkwater, K.T. Murray, and A.L. George, Jr. 2005. Expression of multiple KCNE genes in human heart may enable variable modulation of I(Ks). *J Mol Cell Cardiol*. 38:277-287.

MacKinnon, R., S.L. Cohen, A. Kuo, A. Lee, and B.T. Chait. 1998. Structural conservation in prokaryotic and eukaryotic potassium channels. *Science*. 280:106-109.

Manning, G., D.B. Whyte, R. Martinez, T. Hunter, and S. Sudarsanam. 2002. The protein kinase complement of the human genome. *Science*. 298:1912-1934.

Marban, E. 2002. Cardiac channelopathies. *Nature*. 415:213-218.

Marshall, R.D. 1972. Glycoproteins. *Annu Rev Biochem*. 41:673-702.

McCormick, P.J., Y. Miao, Y. Shao, J. Lin, and A.E. Johnson. 2003. Cotranslational protein integration into the ER membrane is mediated by the binding of nascent chains to translocon proteins. *Mol Cell*. 12:329-341.

McCrossan, Z.A., and G.W. Abbott. 2004. The MinK-related peptides. *Neuropharmacology*. 47:787-821.

McDonald, T.V., Z. Yu, Z. Ming, E. Palma, M.B. Meyers, K.W. Wang, S.A. Goldstein, and G.I. Fishman. 1997. A minK-HERG complex regulates the cardiac potassium current I(Kr). *Nature*. 388:289-292.

Melman, Y.F., A. Domenech, S. de la Luna, and T.V. McDonald. 2001. Structural determinants of KvLQT1 control by the KCNE family of proteins. *J Biol Chem*. 276:6439-6444.

Melman, Y.F., A. Krumerman, and T.V. McDonald. 2002a. A single transmembrane site in the KCNE-encoded proteins controls the specificity of KvLQT1 channel gating. *J Biol Chem*. 277:25187-25194.

Melman, Y.F., A. Krummerman, and T.V. McDonald. 2002b. KCNE regulation of KvLQT1 channels: structure-function correlates. *Trends Cardiovasc Med*. 12:182-187.

Melman, Y.F., S.Y. Um, A. Krumerman, A. Kagan, and T.V. McDonald. 2004. KCNE1 Binds to the KCNQ1 Pore to Regulate Potassium Channel Activity. *Neuron*. 42:927-937.

Meneghini, M.D., T. Ishitani, J.C. Carter, N. Hisamoto, J. Ninomiya-Tsuji, C.J. Thorpe, D.R. Hamill, K. Matsumoto, and B. Bowerman. 1999. MAP kinase and Wnt pathways converge to downregulate an HMG-domain repressor in Caenorhabditis elegans. *Nature*. 399:793-797.

Mercer, E.A., G.W. Abbott, S.P. Brazier, B. Ramesh, P.I. Haris, and S.K. Srai. 1997. Synthetic putative transmembrane region of minimal potassium channel protein (minK) adopts an alpha-helical conformation in phospholipid membranes. *Biochem J*. 325 (Pt 2):475-479.

Miloshevsky, G.V., and P.C. Jordan. 2008. Conformational changes in the selectivity filter of the open-state KcsA channel: an energy minimization study. *Biophys J*. 95:3239-3251.
Moon, R.T., B. Bowerman, M. Boutros, and N. Perrimon. 2002. The promise and perils of Wnt signaling through beta-catenin. *Science*. 296:1644-1646.
Morais Cabral, J.H., A. Lee, S.L. Cohen, B.T. Chait, M. Li, and R. Mackinnon. 1998. Crystal structure and functional analysis of the HERG potassium channel N terminus: a eukaryotic PAS domain. *Cell*. 95:649-655.
Morais-Cabral, J.H., Y. Zhou, and R. MacKinnon. 2001. Energetic optimization of ion conduction rate by the K+ selectivity filter. *Nature*. 414:37-42.
Morin, T.J., and W.R. Kobertz. 2008a. Counting membrane-embedded KCNE beta-subunits in functioning K+ channel complexes. *Proc Natl Acad Sci U S A*. 105:1478-1482.
Morin, T.J., and W.R. Kobertz. 2008b. Tethering chemistry and K+ channels. *J Biol Chem*. 283:25105-25109.
Morino, S., H. Imataka, Y.V. Svitkin, T.V. Pestova, and N. Sonenberg. 2000. Eukaryotic translation initiation factor 4E (eIF4E) binding site and the middle one-third of eIF4GI constitute the core domain for cap-dependent translation, and the C-terminal one-third functions as a modulatory region. *Mol Cell Biol*. 20:468-477.
Nakamura, K., S. Kim, T. Ishidate, Y. Bei, K. Pang, M. Shirayama, C. Trzepacz, D.R. Brownell, and C.C. Mello. 2005. Wnt signaling drives WRM-1/beta-catenin asymmetries in early C. elegans embryos. *Genes Dev*. 19:1749-1754.
Nakayama, K. 1997. Furin: a mammalian subtilisin/Kex2p-like endoprotease involved in processing of a wide variety of precursor proteins. *Biochem J*. 327 (Pt 3):625-635.
Napolitano, C., S.G. Priori, P.J. Schwartz, R. Bloise, E. Ronchetti, J. Nastoli, G. Bottelli, M. Cerrone, and S. Leonardi. 2005. Genetic testing in the long QT syndrome: development and validation of an efficient approach to genotyping in clinical practice. *Jama*. 294:2975-2980.
Narimatsu, H. 2006. Human glycogene cloning: focus on beta 3-glycosyltransferase and beta 4-glycosyltransferase families. *Curr Opin Struct Biol*. 16:567-575.
Nelson, W.J., and R. Nusse. 2004. Convergence of Wnt, beta-catenin, and cadherin pathways. *Science*. 303:1483-1487.
Neyroud, N., F. Tesson, I. Denjoy, M. Leibovici, C. Donger, J. Barhanin, S. Faure, F. Gary, P. Coumel, C. Petit, K. Schwartz, and P. Guicheney. 1997. A novel mutation in the potassium channel gene KVLQT1 causes the Jervell and Lange-Nielsen cardioauditory syndrome. *Nat Genet*. 15:186-189.
Nicolas, M., D. Dememes, A. Martin, S. Kupershmidt, and J. Barhanin. 2001. KCNQ1/KCNE1 potassium channels in mammalian vestibular dark cells. *Hear Res*. 153:132-145.
Nilsson, I., and G. von Heijne. 2000. Glycosylation efficiency of Asn-Xaa-Thr sequons depends both on the distance from the C terminus and on the presence of a downstream transmembrane segment. *J Biol Chem*. 275:17338-17343.

Nilsson, I.M., and G. von Heijne. 1993. Determination of the distance between the oligosaccharyltransferase active site and the endoplasmic reticulum membrane. *J Biol Chem*. 268:5798-5801.

Ohya, S., K. Asakura, K. Muraki, M. Watanabe, and Y. Imaizumi. 2002a. Molecular and functional characterization of ERG, KCNQ, and KCNE subtypes in rat stomach smooth muscle. *Am J Physiol Gastrointest Liver Physiol*. 282:G277-287.

Ohya, S., B. Horowitz, and I.A. Greenwood. 2002b. Functional and molecular identification of ERG channels in murine portal vein myocytes. *Am J Physiol Cell Physiol*. 283:C866-877.

Palacios, I.M., D. Gatfield, D. St Johnston, and E. Izaurralde. 2004. An eIF4AIII-containing complex required for mRNA localization and nonsense-mediated mRNA decay. *Nature*. 427:753-757.

Palmer, D.J., J.B. Helms, C.J. Beckers, L. Orci, and J.E. Rothman. 1993. Binding of coatomer to Golgi membranes requires ADP-ribosylation factor. *J Biol Chem*. 268:12083-12089.

Panaghie, G., K.K. Tai, and G.W. Abbott. 2006. Interaction of KCNE subunits with the KCNQ1 K+ channel pore. *J Physiol*. 570:455-467.

Park, K.H., S.M. Kwok, C. Sharon, R. Baerga, and F. Sesti. 2003. N-Glycosylation-dependent block is a novel mechanism for drug-induced cardiac arrhythmia. *Faseb J*. 17:2308-2309.

Parodi, A.J. 2000a. Protein glucosylation and its role in protein folding. *Annu Rev Biochem*. 69:69-93.

Parodi, A.J. 2000b. Role of N-oligosaccharide endoplasmic reticulum processing reactions in glycoprotein folding and degradation. *Biochem J*. 348 Pt 1:1-13.

Peifer, M., and P. Polakis. 2000. Wnt signaling in oncogenesis and embryogenesis--a look outside the nucleus. *Science*. 287:1606-1609.

Polakis, P. 2000. Wnt signaling and cancer. *Genes Dev*. 14:1837-1851.

Pongs, O., T. Leicher, M. Berger, J. Roeper, R. Bahring, D. Wray, K.P. Giese, A.J. Silva, and J.F. Storm. 1999. Functional and molecular aspects of voltage-gated K+ channel beta subunits. *Ann N Y Acad Sci*. 868:344-355.

Puente, X.S., L.M. Sanchez, C.M. Overall, and C. Lopez-Otin. 2003. Human and mouse proteases: a comparative genomic approach. *Nat Rev Genet*. 4:544-558.

Pusch, M., R. Magrassi, B. Wollnik, and F. Conti. 1998. Activation and inactivation of homomeric KvLQT1 potassium channels. *Biophys J*. 75:785-792.

Robbins, J. 2001. KCNQ potassium channels: physiology, pathophysiology, and pharmacology. *Pharmacol Ther*. 90:1-19.

Rocheleau, C.E., W.D. Downs, R. Lin, C. Wittmann, Y. Bei, Y.H. Cha, M. Ali, J.R. Priess, and C.C. Mello. 1997. Wnt signaling and an APC-related gene specify endoderm in early C. elegans embryos. *Cell*. 90:707-716.

Rocheleau, C.E., J. Yasuda, T.H. Shin, R. Lin, H. Sawa, H. Okano, J.R. Priess, R.J. Davis, and C.C. Mello. 1999. WRM-1 activates the LIT-1 protein kinase to transduce anterior/posterior polarity signals in C. elegans. *Cell*. 97:717-726.

Rocheleau, J.M., S.D. Gage, and W.R. Kobertz. 2006. Secondary structure of a KCNE cytoplasmic domain. *J Gen Physiol*. 128:721-729.

Romey, G., B. Attali, C. Chouabe, I. Abitbol, E. Guillemare, J. Barhanin, and M. Lazdunski. 1997. Molecular mechanism and functional significance of the MinK control of the KvLQT1 channel activity. *J Biol Chem*. 272:16713-16716.

Rossmann, M.G., and P. Argos. 1981. Protein folding. *Annu Rev Biochem*. 50:497-532.

Roth, J. 2002. Protein N-glycosylation along the secretory pathway: relationship to organelle topography and function, protein quality control, and cell interactions. *Chem Rev*. 102:285-303.

Ruiz-Canada, C., D.J. Kelleher, and R. Gilmore. 2009. Cotranslational and posttranslational N-glycosylation of polypeptides by distinct mammalian OST isoforms. *Cell*. 136:272-283.

Sakagami, M., K. Fukazawa, T. Matsunaga, H. Fujita, N. Mori, T. Takumi, H. Ohkubo, and S. Nakanishi. 1991. Cellular localization of rat Isk protein in the stria vascularis by immunohistochemical observation. *Hear Res*. 56:168-172.

Sanguinetti, M.C., M.E. Curran, A. Zou, J. Shen, P.S. Spector, D.L. Atkinson, and M.T. Keating. 1996. Coassembly of K(V)LQT1 and minK (IsK) proteins to form cardiac I(Ks) potassium channel. *Nature*. 384:80-83.

Scamuffa, N., F. Calvo, M. Chretien, N.G. Seidah, and A.M. Khatib. 2006. Proprotein convertases: lessons from knockouts. *Faseb J*. 20:1954-1963.

Schachter, H., and H.H. Freeze. 2009. Glycosylation diseases: quo vadis? *Biochim Biophys Acta*. 1792:925-930.

Schroeder, B.C., S. Waldegger, S. Fehr, M. Bleich, R. Warth, R. Greger, and T.J. Jentsch. 2000. A constitutively open potassium channel formed by KCNQ1 and KCNE3. *Nature*. 403:196-199.

Schulze-Bahr, E., Q. Wang, H. Wedekind, W. Haverkamp, Q. Chen, Y. Sun, C. Rubie, M. Hordt, J.A. Towbin, M. Borggrefe, G. Assmann, X. Qu, J.C. Somberg, G. Breithardt, C. Oberti, and H. Funke. 1997. KCNE1 mutations cause jervell and Lange-Nielsen syndrome. *Nat Genet*. 17:267-268.

Seidah, N.G., and M. Chretien. 1999. Proprotein and prohormone convertases: a family of subtilases generating diverse bioactive polypeptides. *Brain Res*. 848:45-62.

Sesti, F., G.W. Abbott, J. Wei, K.T. Murray, S. Saksena, P.J. Schwartz, S.G. Priori, D.M. Roden, A.L. George, Jr., and S.A. Goldstein. 2000a. A common polymorphism associated with antibiotic-induced cardiac arrhythmia. *Proc Natl Acad Sci U S A*. 97:10613-10618.

Sesti, F., and S.A. Goldstein. 1998. Single-channel characteristics of wild-type IKs channels and channels formed with two minK mutants that cause long QT syndrome. *J Gen Physiol*. 112:651-663.

Sesti, F., K.K. Tai, and S.A. Goldstein. 2000b. MinK endows the I(Ks) potassium channel pore with sensitivity to internal tetraethylammonium. *Biophys J*. 79:1369-1378.

Shakin-Eshleman, S.H., S.L. Spitalnik, and L. Kasturi. 1996. The amino acid at the X position of an Asn-X-Ser sequon is an important determinant of N-linked core-glycosylation efficiency. *J Biol Chem*. 271:6363-6366.

Shental-Bechor, D., and Y. Levy. 2009. Folding of glycoproteins: toward understanding the biophysics of the glycosylation code. *Curr Opin Struct Biol*. 19:524-533.

Shibuya, T., T.O. Tange, N. Sonenberg, and M.J. Moore. 2004. eIF4AIII binds spliced mRNA in the exon junction complex and is essential for nonsense-mediated decay. *Nat Struct Mol Biol*. 11:346-351.

Shikano, S., and M. Li. 2003. Membrane receptor trafficking: evidence of proximal and distal zones conferred by two independent endoplasmic reticulum localization signals. *Proc Natl Acad Sci U S A*. 100:5783-5788.

Shin, T.H., J. Yasuda, C.E. Rocheleau, R. Lin, M. Soto, Y. Bei, R.J. Davis, and C.C. Mello. 1999. MOM-4, a MAP kinase kinase kinase-related protein, activates WRM-1/LIT-1 kinase to transduce anterior/posterior polarity signals in C. elegans. *Mol Cell*. 4:275-280.

Silberstein, S., and R. Gilmore. 1996. Biochemistry, molecular biology, and genetics of the oligosaccharyltransferase. *Faseb J*. 10:849-858.

Sole, L., and A. Felipe. 2010. Does a physiological role for KCNE subunits exist in the immune system? *Communicative & Integrative Biology*. 3:1-3.

Splawski, I., J. Shen, K.W. Timothy, M.H. Lehmann, S. Priori, J.L. Robinson, A.J. Moss, P.J. Schwartz, J.A. Towbin, G.M. Vincent, and M.T. Keating. 2000. Spectrum of mutations in long-QT syndrome genes. KVLQT1, HERG, SCN5A, KCNE1, and KCNE2. *Circulation*. 102:1178-1185.

Sugimoto, T., Y. Tanabe, R. Shigemoto, M. Iwai, T. Takumi, H. Ohkubo, and S. Nakanishi. 1990. Immunohistochemical study of a rat membrane protein which induces a selective potassium permeation: its localization in the apical membrane portion of epithelial cells. *J Membr Biol*. 113:39-47.

Takumi, T., K. Moriyoshi, I. Aramori, T. Ishii, S. Oiki, Y. Okada, H. Ohkubo, and S. Nakanishi. 1991. Alteration of channel activities and gating by mutations of slow ISK potassium channel. *J Biol Chem*. 266:22192-22198.

Takumi, T., H. Ohkubo, and S. Nakanishi. 1988. Cloning of a membrane protein that induces a slow voltage-gated potassium current. *Science*. 242:1042-1045.

Tapper, A.R., and A.L. George, Jr. 2000. MinK subdomains that mediate modulation of and association with KvLQT1. *J Gen Physiol*. 116:379-390.

Taylor, M.E., and K. Drickamer. 2006. Introduction to Glycobiology, 2nd edition. Oxford University Press, Oxford.

Teixeira, M., S. Viengchareun, D. Butlen, C. Ferreira, F. Cluzeaud, M. Blot-Chabaud, M. Lombes, and E. Ferrary. 2006. Functional IsK/KvLQT1 potassium channel in a new corticosteroid-sensitive cell line derived from the inner ear. *J Biol Chem*. 281:10496-10507.

Ten Hagen, K.G., T.A. Fritz, and L.A. Tabak. 2003. All in the family: the UDP-GalNAc:polypeptide N-acetylgalactosaminyltransferases. *Glycobiology*. 13:1R-16R.

Thomas, G. 2002. Furin at the cutting edge: from protein traffic to embryogenesis and disease. *Nat Rev Mol Cell Biol*. 3:753-766.

Thornberry, N.A., and Y. Lazebnik. 1998. Caspases: enemies within. *Science*. 281:1312-1316.

Thorpe, C.J., A. Schlesinger, J.C. Carter, and B. Bowerman. 1997. Wnt signaling polarizes an early C. elegans blastomere to distinguish endoderm from mesoderm. *Cell*. 90:695-705.

Tinel, N., S. Diochot, M. Borsotto, M. Lazdunski, and J. Barhanin. 2000. KCNE2 confers background current characteristics to the cardiac KCNQ1 potassium channel. *Embo J*. 19:6326-6330.

Trimmer, J.S. 1998. Regulation of ion channel expression by cytoplasmic subunits. *Curr Opin Neurobiol*. 8:370-374.

Trombetta, E.S. 2003. The contribution of N-glycans and their processing in the endoplasmic reticulum to glycoprotein biosynthesis. *Glycobiology*. 13:77R-91R.

Trombetta, E.S., and A.J. Parodi. 2003. Quality control and protein folding in the secretory pathway. *Annu Rev Cell Dev Biol*. 19:649-676.

Tyson, J., L. Tranebjaerg, S. Bellman, C. Wren, J.F. Taylor, J. Bathen, B. Aslaksen, S.J. Sorland, O. Lund, S. Malcolm, M. Pembrey, S. Bhattacharya, and M. Bitner-Glindzicz. 1997. IsK and KvLQT1: mutation in either of the two subunits of the slow component of the delayed rectifier potassium channel can cause Jervell and Lange-Nielsen syndrome. *Hum Mol Genet*. 6:2179-2185.

Tyson, J., L. Tranebjaerg, M. McEntagart, L.A. Larsen, M. Christiansen, M.L. Whiteford, J. Bathen, B. Aslaksen, S.J. Sorland, O. Lund, M.E. Pembrey, S. Malcolm, and M. Bitner-Glindzicz. 2000. Mutational spectrum in the cardioauditory syndrome of Jervell and Lange-Nielsen. *Hum Genet*. 107:499-503.

Um, S.Y., and T.V. McDonald. 2007. Differential association between HERG and KCNE1 or KCNE2. *PLoS One*. 2:e933.

Vallon, V., F. Grahammer, K. Richter, M. Bleich, F. Lang, J. Barhanin, H. Volkl, and R. Warth. 2001. Role of KCNE1-dependent K+ fluxes in mouse proximal tubule. *J Am Soc Nephrol*. 12:2003-2011.

Varki, A., R.D. Cummings, J.D. Esko, H.H. Freeze, P. Stanley, C.R. Bertozzi, G.W. Hart, and M.E. Etzler. 2009. Essentials of Glycobiology, 2nd edition. Cold Spring Harbor Laboratory Press, Cold Spring Harbor, New York.

Vetter, D.E., J.R. Mann, P. Wangemann, J. Liu, K.J. McLaughlin, F. Lesage, D.C. Marcus, M. Lazdunski, S.F. Heinemann, and J. Barhanin. 1996. Inner ear defects induced by null mutation of the isk gene. *Neuron*. 17:1251-1264.

Walsh, C.T. 2006. Posttranslational Modifications of Proteins. Roberts and Company Publishers, Colorado.

Wang, K.W., and S.A. Goldstein. 1995. Subunit composition of minK potassium channels. *Neuron*. 14:1303-1309.

Wang, Q., M.E. Curran, I. Splawski, T.C. Burn, J.M. Millholland, T.J. VanRaay, J. Shen, K.W. Timothy, G.M. Vincent, T. de Jager, P.J. Schwartz, J.A. Toubin, A.J. Moss, D.L. Atkinson, G.M. Landes, T.D. Connors, and M.T. Keating. 1996. Positional cloning of a novel potassium channel gene: KVLQT1 mutations cause cardiac arrhythmias. *Nat Genet*. 12:17-23.

Wangemann, P. 2002. K+ cycling and the endocochlear potential. *Hear Res*. 165:1-9.

Watanabe, I., H.G. Wang, J.J. Sutachan, J. Zhu, E. Recio-Pinto, and W.B. Thornhill. 2003. Glycosylation affects rat Kv1.1 potassium channel gating by a combined

surface potential and cooperative subunit interaction mechanism. *J Physiol*. 550:51-66.
Weerapana, E., and B. Imperiali. 2006. Asparagine-linked protein glycosylation: from eukaryotic to prokaryotic systems. *Glycobiology*. 16:91R-101R.
Whitley, P., I.M. Nilsson, and G. von Heijne. 1996. A nascent secretory protein may traverse the ribosome/endoplasmic reticulum translocase complex as an extended chain. *J Biol Chem*. 271:6241-6244.
Williamson, I.M., S.J. Alvis, J.M. East, and A.G. Lee. 2003. The potassium channel KcsA and its interaction with the lipid bilayer. *Cell Mol Life Sci*. 60:1581-1590.
Wodarz, A., and R. Nusse. 1998. Mechanisms of Wnt signaling in development. *Annu Rev Cell Dev Biol*. 14:59-88.
Wold, F. 1981. In vivo chemical modification of proteins (post-translational modification). *Annu Rev Biochem*. 50:783-814.
Wu, D.M., M. Jiang, M. Zhang, X.S. Liu, Y.V. Korolkova, and G.N. Tseng. 2006. KCNE2 is colocalized with KCNQ1 and KCNE1 in cardiac myocytes and may function as a negative modulator of I(Ks) current amplitude in the heart. *Heart Rhythm*. 3:1469-1480.
Wulff, H., N.A. Castle, and L.A. Pardo. 2009. Voltage-gated potassium channels as therapeutic targets. *Nat Rev Drug Discov*. 8:982-1001.
Yan, Q., and W.J. Lennarz. 2002. Studies on the function of oligosaccharyl transferase subunits. Stt3p is directly involved in the glycosylation process. *J Biol Chem*. 277:47692-47700.
Yan, R., W. Rychlik, D. Etchison, and R.E. Rhoads. 1992. Amino acid sequence of the human protein synthesis initiation factor eIF-4 gamma. *J Biol Chem*. 267:23226-23231.
Ye, Y., and M.E. Fortini. 2000. Proteolysis and developmental signal transduction. *Semin Cell Dev Biol*. 11:211-221.
Yellen, G. 2002. The voltage-gated potassium channels and their relatives. *Nature*. 419:35-42.
Zaika, O., C.C. Hernandez, M. Bal, G.P. Tolstykh, and M.S. Shapiro. 2008. Determinants within the turret and pore-loop domains of KCNQ3 K+ channels governing functional activity. *Biophys J*. 95:5121-5137.
Zapata, J.M., M.A. Martinez, and J.M. Sierra. 1994. Purification and characterization of eukaryotic polypeptide chain initiation factor 4F from Drosophila melanogaster embryos. *J Biol Chem*. 269:18047-18052.
Zerangue, N., B. Schwappach, Y.N. Jan, and L.Y. Jan. 1999. A new ER trafficking signal regulates the subunit stoichiometry of plasma membrane K(ATP) channels. *Neuron*. 22:537-548.
Zhang, M., M. Jiang, and G.N. Tseng. 2001. minK-related peptide 1 associates with Kv4.2 and modulates its gating function: potential role as beta subunit of cardiac transient outward channel? *Circ Res*. 88:1012-1019.
Zhou, A., G. Webb, X. Zhu, and D.F. Steiner. 1999. Proteolytic processing in the secretory pathway. *J Biol Chem*. 274:20745-20748.

Zhou, Y., J.H. Morais-Cabral, A. Kaufman, and R. MacKinnon. 2001. Chemistry of ion coordination and hydration revealed by a K+ channel-Fab complex at 2.0 A resolution. *Nature*. 414:43-48.